Beatriz Zapico Blanco
(coord.)

SCHOOLS, SEISMICITY AND RETROFITTING

PERSISTAH Project (Projetos de Escolas Resilientes aos SISmos no Território do Algarve e de Huelva)

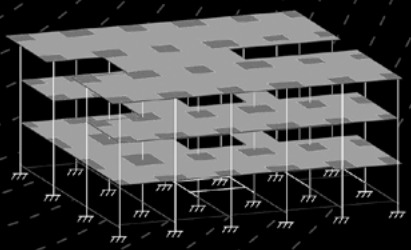

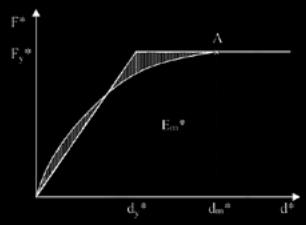

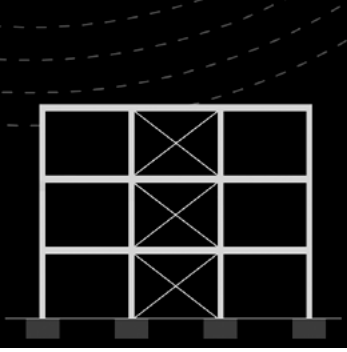

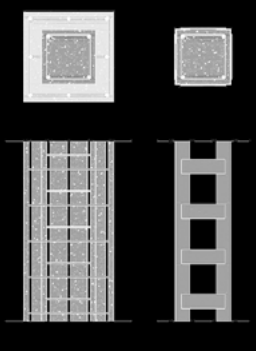

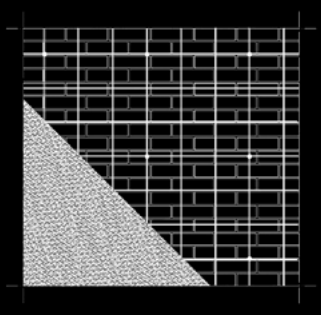

BOOK REVIEW

Editorial Universidad de Sevilla

SUMARY

SUMARY

Beatriz Zapico Blanco (coord.)

SCHOOLS, SEISMICITY AND RETROFITTING

SUMARY

SCHOOLS, SEISMICITY AND RETROFITTING

SUMARY

Beatriz Zapico Blanco (coord.)

Beatriz Zapico Blanco (coord.)

SCHOOLS, SEISMICITY AND RETROFITTING

PERSISTAH Project
(Projetos de Escolas Resilientes aos SISmos no Território do Algarve e de Huelva)

Antonio Morales Esteban, Emilio Romero Sánchez,
Beatriz Zapico Blanco, María Victoria Requena García de la Cruz,
Jaime de Miguel Rodríguez and João Estêvão

Editorial Universidad de Sevilla

Sevilla 2021

SCHOOLS, SEISMICITY AND RETROFITTING

Collection Ediciones especiales

This work has been developed within the framework of the PERSISTAH project, *Projetos de Escolas Resilientes aos Seismos no Território do Algarve e de Huelva* (0313_PERSISTAH_5_P), developed jointly by the universities of the Algarve and Seville and funded by the European Commission through the call EP – INTERREG VA Spain Portugal (POCTEP).

Cover design: Emilio Romero Sánchez

c/ Porvenir, 27 - 41013 Sevilla
Tlf. 954 487 447; 954 487 451 - Fax 954 487 443
Correo electrónico: eus4@us.es
Web: <https://editorial.us.es>

ISBN-e: 978-84-472-3122-5
DOI: http://dx.doi.org/10.12795/9788447231225

Layout and digital edition: Dosgraphic, S.L. (dosgraphic@dosgraphic.es)

SUMARY

Summary

SUMARY

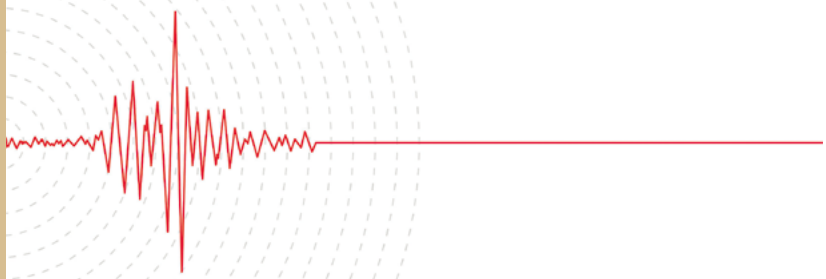

Symbols

A	Thermal expansion Coefficient
A_I	Architectural impact
a_b	Base ground acceleration
a_{gR}	Reference peak acceleration
a_g	Ground acceleration for a type A soil
a_r	Reference PGA ($T_R = 475$).
C	Soil factor
C_I	Cost index
d	MDOF system equivalent displacement
d*	SDOF system equivalent displacement
d_{Di}	Average displacement associated to a damage limit state
d_{et}*	SDOF elastic displacement
d^*_m	Displacement at plastic hinge formation
d_t	MDOF target inelastic displacement
d_t*	SDOF target inelastic displacement
$d^*_{t,D}$	Displacement associated to a damage limit state
d_u*	SDOF ultimate deformation
d_y*	SDOF deformation at yield point
E	Modulus of elasticity (Young's modulus)
E_b	Brick modulus of elasticity
E_m*	Plastic hinge formation energy
E_I	Efficiency index
F*	SDOF system equivalent force
f_b	Brick Compressive strength
f'$_c$	Concrete characteristic compressive strength
Fi	Set of MDOF applied forces
f_k	Masonry characteristic compressive strength
f_m	Mortar strength
F_y	Yield strength
F_u	Ultimate strength
F_y*	SDOF Yield strength

SUMARY

G	Shear modulus
K	Contribution factor
K_f	Constant depending on the brick and mortar combination (EC-6)
k_m*	Bilinear curve stiffness factor
κ_ξ	Damping modification factor
m*	SDOF equivalent mass
m_i	MDOF standardised masses of each floor
M_w	Seismic moment magnitude
N	MDOF node of freedom
q	Behaviour factor, considering structural system and ductility
q_c	Point resistance of the static penetrometer
q_u	Unconfined compressive strength
R_I	Reinforcement index
S	Soil amplification factor
$S_e(T)$	Elastic response spectrum
T	Vibration period of a linear SDOF system
T*	SDOF equivalent system period
T_A, T_B	Characteristic parameters of the response spectrum (NCSE02)
T_B	Lower limit of the period of the constant spectral acceleration branch (EC8-1)
T_C	Upper limit of the period of the constant spectral acceleration branch (EC8-1)
T_D	Value defining the beginning of the constant displacement response range of the spectrum (EC8-1)
T_r	Return period
t_0	Shear resistance
U	Poisson Coefficient
V	MDOF system base shear
v_s	Transverse elastic waves or shear waves propagation speed
v_l	Longitudinal elastic waves propagation speed
W	Density
α_1, α_2 y α_3	Reinforcement index importance factors.¡
$\alpha(T)$	Value of the normalised elastic response spectrum
β_{Di}	Standard deviation of the displacement logarithm d_{Di}
Γ	MDOF-SDOF transformation factor
η	Damping correction factor with reference value
λ	MDOF Lateral load parameter
μ	Ductility coefficient
ξ_i	Equivalent damping
ρ	Dimensionless risk factor
Φ	Cumulative distribution function for the normal distribution
ϕ_i	MDOF Displacement at each floor
$\%S_e$	Spectral acceleration percentage

SUMARY

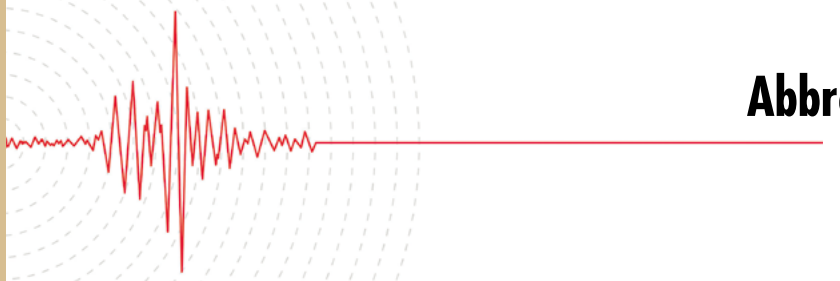

Abbreviations

CFRP	Carbon fibre reinforced polymer
DL	Damage limitation damage state
EC8	Eurocode 8
EC6	Eurocode 6
EC8-1	Eurocode 8, part 1
EC8-3	Eurocode 8, part 3
EMS	European Macroseismic Scale
ERSTA	Algarve Seismic Risk and Tsunami Study *Estudio do Risco Sísmico e de Tsunamis do Algarve*
FRP	Fibre reinforced polymers
IGN	Spanish National Geographic Institute
IGM	Geological and Mining Institute of Spain
LNEG	Portugal's National Laboratory of Energy and Geology
MDOF	Multi-degree of freedom system
NC	Near collapse damage state
NCSE02	Normativa de Construcción Sismorresistente Española de 2002
OP	Operacional damage limit state
PERSISTAH	Projetos de Escolas Resilientes aos SISmos no Território do Algarve e de Huelva
PNRRC	Plataformas Nacionales para la Reducción de Riesgo de Catástrofes
PGA	Peak ground acceleration
PSHA	Probabilistic seismic hazard analysis
RC	Reinforced concrete
RSAEEP	Reglamento de Segurança e Acçoes para Estructuras de Edifícios e Pontes
SD	Significant damage limit state
SIRCO	Seismic Risk Simulator *Simulador de Risco sísmiCO*
SDOF	Single-degree of freedom system

SUMARY

SUMARY

Chapter 1. Introduction

This document presents the work carried out within the European research project PERSISTAH (*Projetos de Escolas Resilientes aos SISmos no Território do Algarve e de Huelva*, in Portuguese), which has been developed jointly by the University of Seville (Spain) and the University of Algarve (Portugal). This research project focuses on the study and assessment of the seismic risk of primary school buildings in the Algarve (Portugal) and Huelva (Spain) regions. To this end, the objectives established by the National Platforms for Disaster Risk Reduction (PNRRC) of the National Civil Protection Commissions of Portugal and Spain have been considered.

Earthquakes are among the natural disasters that cause the greatest number of casualties and economic losses worldwide. Numerous studies establish the importance of studying the seismic risk of buildings in order to estimate and evaluate the possible damage that can be caused by a seismic action, with the aim of minimising human losses and impacts on material and economic assets. The destructive potential of an earthquake depends on its magnitude, but also on the seismic resilience of the affected area.

In Europe, Earthquakes have historically caused significant damage and loss of life. The earthquakes that occurred in this continent at the beginning of the 20th century cost around 29 billion euros and caused 19 000 casualties (Battarra *et al.*, 2018).

The Iberian Peninsula has moderate seismic activity (Morales-Esteban *et al.*, 2014). However, most activity is concentrated in the south, which is characterised by large earthquakes ($Mw \geq 6$), with long return periods (Morales-Esteban *et al.*, 2014), making the population unaware of the danger. This activity is due to the convergence between the Eurasian and African tectonic plates and the proximity of the Azores-Gibraltar fault (Morales-Esteban *et al.*, 2014). The Algarve-Huelva region is located in the south-west of the Iberian Peninsula. This area is close to the Marques de Pombal, Saint Vicente and Horseshoe faults, which have caused some of the most significant earthquakes that have affected the Iberian Peninsula, such as the 1755 Lisbon earthquake-tsunami

SUMARY

(Mw = 8.7 – 9.0) and the 1969 earthquake (Mw = 8). The first is also the largest documented seismic event to have affected Europe, killing 100 000 people. The maximum seismic intensity of this region, based on past earthquakes, is high in the Algarve (IX-X) and Huelva (VII-VIII) (Teves-Costa *et al.*, 2019). Although there is significant seismic risk, few seismic studies of the area have been carried out, as most seismic studies of the Iberian Peninsula focus on the east and south-east.

The seismic vulnerability of the region's buildings was evaluated using estimation methods such as SIRCO (Seismic Risk Simulator) (Fazendeiro Sá *et al.*, 2016) or ERSTA (Algarve Seismic Risk and Tsunami Study) (Autoridade Nacional de Protecção Civi [ANPC], 2010). They conclude that it is possible to reduce seismic risk by improving prevention and emergency plans. In this sense, rigorous vulnerability analyses of existing buildings and the implementation of appropriate retrofitting solutions can contribute to the reduction of the levels of physical damage, human losses and the economic impact of future seismic events.

The seismic behaviour of buildings plays a key role in the destructive potential of an earthquake. The vulnerability of existing buildings has been the focus of European interest in recent years. This is due to the damage caused by recent earthquakes, such as the L'Aquila earthquake in 2019 (Italy), the Lorca earthquake in 2011 (Spain) and the Amatrice earthquake in 2016 (Italy) (Ruiz-Pinilla *et al.*, 2016; Del Gaudio *et al.*, 2017; Fiorentino *et al.*, 2018). A large part of the buildings of these cities were severely damaged during these earthquakes. Therefore, enhancing the seismic performance of buildings has become a major concern (Mazzoni *et al.*, 2018) , which can be achieved through the implementation of seismic retrofitting techniques.

The school buildings in the PERSISTAH project have been chosen as the object of study because of their relevance in case of an earthquake. On the one hand, their community present a high vulnerability, due to their low adult/child ratio and high occupation, making the evacuation of the building during an emergency complicated. Moreover, in the event of an earthquake, not only physical damage and injuries are expected: children would also be emotionally affected in a significant way. In this regard, several studies have shown that serious psychological problems can arise on children who have suffered the effects of an earthquake and the benefits of preparedness (UNICEF, 2011). On the other hand, school building structures also present high seismic vulnerability. Their typically simple and repetitive layouts were designed and calculated based on old regulations that did not take into account the seismic action. Approximately 50% of the buildings were designed with reinforced concrete and have two or three floors, and they have seismically weak elements such as short columns. This type of buildings were significantly damaged during the 2011 Lorca

SUMARY

earthquake (Ruiz-Pinilla *et al.*, 2016). Furthermore, the area is characterised by the presence of superficail soft soil layers, which can amplify the effects of earthquakes.

In addition to this, due to their public nature, schools can also be used as shelters after a disaster. All this makes it essential to assess and guarantee their structural stability in the event of an earthquake.

It is important to note that in the event of an earthquake, both regions (Algarve and Huelva) would be equally affected. One of the objectives of the project is to improve the knowledge related to the current situation of each country, particularly on seismic standards and construction practices. In this sense, the seismic regulations, construction techniques, civil protection policies and seismic risk reduction strategies of both countries have been compared. In addition, a database has been developed with information sheets from each primary school (142 in Algarve and 138 in Huelva), taking into account the specifications of each region.

The main types of primary schools have been identified in this project. Subsequently, an inventory of the constructive and structural characteristics of each building has been created. With this information, the vulnerability of each school has been analysed through a non-linear static (pushover) analysis for obtaining the capacity curve. Finally, the ranking of the seismic behaviour of each school has been made through the *School-Score* system (a system of prioritisation of the seismic risk of school buildings). Seismic behaviour has been evaluated according to the hazard, vulnerability and exposure of each building.

1.1. PROJECT OBJECTIVE AND JUSTIFICATION

The PERSISTAH project was conceived based on a number of key points regarding the seismic resilience of the Algarve and Huelva regions:

- A significant part of the known seismic sources around the Algarve and Huelva areas would have a transboundary impact.
- Knowledge of existing hazards and the seismic vulnerability of buildings is essential for effective emergency response.
- It is important to study the application of mitigation measures in schools in the face of a possible seismic event.
- The development of educational material and the communication of seismic risk to students and teachers would reduce the vulnerability of the community.
- Making recommendations for rehabilitation aimed at technicians involved in construction will have a positive effect on the risk reduction.

SUMARY

— The creation of cooperative links in risk mitigation efforts between these two neighbouring regions will enhance the regions seismic resilience.

Based on these points, the main objective of the European project PERSISTAH is the assessment of the seismic vulnerability of primary schools in the Algarve (Portugal) and Huelva (Spain) regions cooperatively. To this end, the objectives established by the National Platforms for Disaster Risk Reduction (PNRRC) of the National Civil Protection Commissions of Portugal and Spain have been considered.

This objective can be subdivided into the following goals:

— the classification of the school buildings of the area,
— the assessment of their vulnerability,
— the definition of a vulnerability index that allows to compare them,
— the definition of rehabilitation measures for those buildings which may need them,
— the application of those measures to one Portuguese and one Spanish school pilot building,
— the creation of educational guides to create awareness of the seismic risks in the school community, and
— the dissemination of the project results, where the present document is to be found.

1.2. MAIN OUTCOMES OF THE PROJECT

The PERSISTAH research project was conceived for having an impact on the Portuguese and Spanish society. This impact is maximised by the singularities of the seismicity of this geographical area, the international cooperation for risk reduction, and the relevance of the buildings under study.

Accordingly, the PERSISTAH research project has contributed to shaping a society that is more resilient to earthquakes.

The first contribution is the analysis of the seismic vulnerability of school buildings, which are very vulnerable to earthquakes. They play a fundamental role in the lives of children, who are the most vulnerable people in this type of event. After a disaster, the children should feel safe when returning to school, which means a return to normality. Moreover, because of their design and their public nature, they can be adapted as shelters after a disaster.

The **analysis of the schools seismic vulnerability** has been carried out through an integrated assessment methodology. This methodology is based on

SUMARY

a vulnerability analysis through the building capacity curve, used to obtain the structural performance point of the building. With this information, the damage probability of the school building is calculated.

This methodology has been implemented in a new software (Estêvão, 2019; Estêvão, 2020), where was implemented the adaptation of a set of computer programming routines previously developed in the applications *EC8spec* (Estêvão, 2016) and *SIMULSIS* (Estêvão and Oliveira, 2012). The purpose of this software is to obtain the *School-score*, which is based on the damage probability and other parameters, such as the vulnerability of non-structural elements, number of students, aspects affecting evacuation, etc. These are essential elements to take into account when studying the seismic vulnerability of a school building. Obtaining a high value for this parameter indicates that the school is more vulnerable to earthquakes. In this context, a new school database was created with the collaboration of all team members. A list with the classification of the schools has been drawn up based on their *School-score*, and it will be taken into consideration for future seismic retrofitting interventions in the buildings. Furthermore, a series of training activities for technicians on the aspects of the methodology applied and the particularities of the seismic retrofitting design have been carried out, in order to reduce the structural and non-structural risk of the buildings.

Another fundamental factor in this project is the significance of and need for **international cooperation** between countries when it comes to the reduction of seismic risk, since both regions, which present very similar geographical conditions, would be affected equally in the event of an earthquake.

Finally, another key point of the project is **the creation of seismic risk awareness among the educational community** and their training in this subject. Children are the future of our society and play a vital role in it. They learn at school, and bring their knowledge home to their families, which makes of the schools a powerful motor for change. A seismic event causes a great psychological impact on them, and therefore, education and communication of existing risks is essential. A series of trainings have been carried out through a number of activities and seminars in schools for both teachers and students. These dealt with issues related to identifying risks both inside and outside the school building. In addition, earthquake drills were carried out. This action is key to increasing awareness of seismic risk and learning how to act in the event of an earthquake. A number of pedagogical resources for teachers have also been developed. These materials include practical activities for children to learn about these subjects in a fun way, together with easy self-protection actions to be carried out before and after a seismic event[1].

1. *Why does the ground shake?* (https://dx.doi.org/10.12795/9788447230471).
Practical guide for Earthquake resilient schools (https://dx.doi.org/10.12795/9788447230532).

SUMARY

1.3. DOCUMENT STRUCTURE

In the present document, the methodology and seismic regulations applied in the vulnerability analysis and subsequent seismic retrofitting of school buildings will be presented. This methodology responds to the objectives and main ideas of the project. Later on, the seismic hazard of the Algarve and Huelva area is discussed, as well as the seismic action used in each region for seismic analysis. In addition, the characterisation and typological classification of school buildings carried out for their subsequent seismic analysis is shown. Finally, several seismic retrofitting techniques proposed by the different regulations are outlined, as well as the different techniques studied in the project.

SUMARY

Chapter 2. Seismic hazard in the Algarve-Huelva Region

In this chapter, the seismic hazard of the Algarve-Huelva region is shown. In 2.1, the configuration of the region is analysed; in section 2.2, the influence of soil on seismic hazard is shown by analysing the geotechnical characteristics of both areas; in sections 2.3 and 2.4, the requirements set out in the applicable and recommended seismic building codes in Spain and Portugal, respectively, are outlined; lastly, in section 2.5, a comparison of the seismic action determined according to each seismic regulation is carried out, underscoring the fact that in the case of an earthquake, both areas would be equally affected.

2.1. THE ALGARVE-HUELVA REGION

The Iberian Peninsula is characterised by having a moderate level of seismic activity in comparison with other areas of the world (Carre and Zornoza, 2011). However, in the south of the peninsula, there is a significant level of seismic activity. This is due to the convergence of the Eurasian and African tectonic plates, which extend throughout the Mediterranean region and the Strait of Gibraltar, reaching the Azores islands (figure 1).

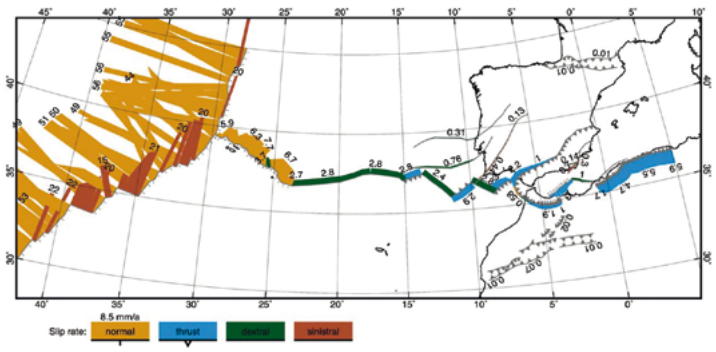

Figure 1. Convergence of the Eurasian and African tectonic plates.

SUMARY

Because of this convergence, the Iberian Peninsula has experienced numerous high-magnitude earthquakes that had disastrous consequences (table 1). Among these, the 1356 (Cape St.Vincent. Intensity VIII), 1722 (Gulf of Cadiz. $M_w = 6.5$), 1755 ($M_w = 8.5-9.0$) and the 1969 ($M_w = 8$) earthquakes stand out (Sá *et al.*, 2018). The 1755 earthquake is known as the famous earthquake and tsunami of Lisbon, considered to be one of the most devastating historical seismic events in the world. At European level, it is the most catastrophic natural disaster ever documented.

Table 1. Historical earthquakes felt in the Iberian Peninsula (Silva and Rodriguez Pascua, 2014).

Year	Place	Mag.	Consequences
1356	Cape St.Vincent	I.VIII	Serious damage in Western Andalusia and the South of Portugal. Serious damage in Lisbon.
1522	Alboran Sea	6.5	Total destruction of Almería and towns in Granada.
1531	Lisbon	7.0	Around 30000 deaths in the city of Lisbon.
1680	Alahaurín el Grande (Málaga)	6.8	Various towns affected causing minor damage.
1722	Gulf of Cadiz	6.5	Serious human and material damage from Cape St.Vincent to Castro Marim. It caused a local tsunami in Tavira.
1755	SW of Cape St.Vincent	8.5	Destruction of most of Lisbon. Tsunami of almost 15 m in height. Between 10000 and 90000 deaths caused by both disasters.
1804	Alboran Sea	6.7	Serious damage in Motril (Spain).
1829	Torrevieja (Alicante)	6.6	Destruction of a large number of houses in various towns in the district. Around 400 deaths.
1884	Arenas del Rey (Granada)	6.7	Almost one thousand deaths.
1969	Cape St.Vincent	8.0	Several deaths and minor damage.
2007	SW of Cape St.Vincent	6.1	Minor damage.
2009	Isla Cristina (Huelva)	6.3	Minor damage. Cracks in buildings. Factory walls collapsed.
2011	Lorca (Murcia)	5.1	Significant damage and victims. Collapses of highly important buildings.
2016	Alboran Sea	6.3	Detachment of façades, cracks and minor injuries. Small tsunami in the Balearic Islands (Spain).

SUMARY

The region with the greatest seismic hazard on the peninsula is located in the southeast and comprises the Alboran Sea and Murcia. This region is characterised by frequent occurrence of moderate- and low-magnitude earthquakes. For this reason, the majority of studies and analyses of seismic hazard and vulnerability are focused on this area. The most devastating seismic event that was most recently felt on the Peninsula was the 2011 Lorca earthquake (Murcia). Despite its moderate magnitude, its hypocentre was located at very little depth, at approximately 1 km from the surface and accelerations of 0.36 g were recorded. This resulted in devastating effects, causing more than 300 injuries, several casualties, and the relocation of more than 10 000 people (Salgado-Gálvez *et al.*, 2016).

However, the Algarve-Huelva region, in the southwest of the peninsula, is characterised by high-magnitude earthquakes ($M_w \geq 6$) and long return periods (Morales-Esteban *et al.*, 2014). This is due to the convergence of the tectonic plates and its closeness to the Azores–Gibraltar fault zone. Recent studies (Gràcia *et al.*, 2010) have also identified fault zones in the southwest region of the Algarve, such as the Marqués de Pombal fault (figure 2) or the San Vicente fault. These faults caused some of the most damaging earthquakes in the Iberian Peninsula. Furthermore, the properties of the region's soil increase the seismic hazard values. However, due to the long return periods of these events, the population inhabiting the region is not aware of the seismic hazard of the area.

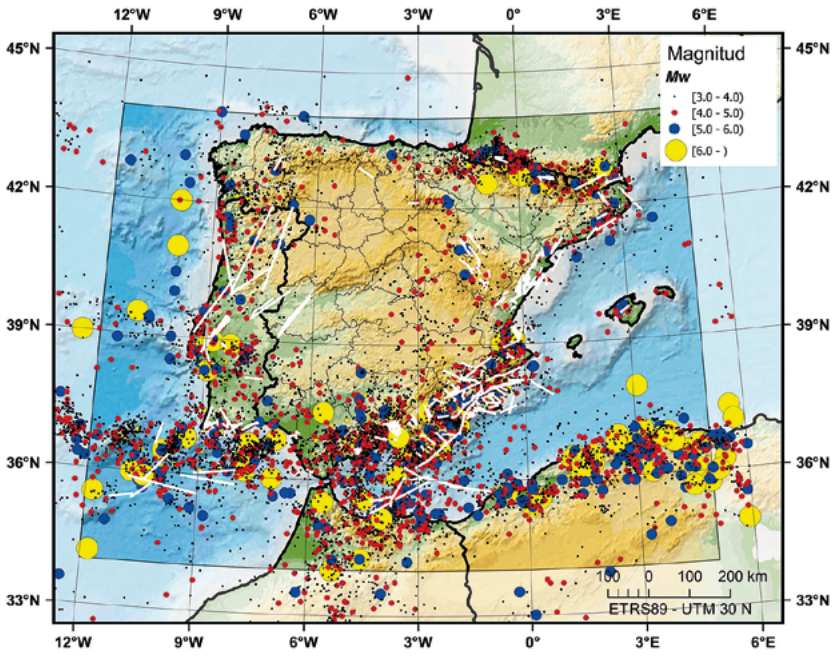

Figure 2. Map of active quaternary faults in the Iberian Peninsula with the magnitude of the earthquakes (created by the author).

SUMARY

2.2. THE IMPACT OF SOIL TYPE ON SEISMIC HAZARD

The territory of the Algarve and Huelva is characterised by having a similar geological profile, although with certain nuances, as can be observed in the geological map of Spain and Portugal by the Geological and Mining Institute of Spain (IGM) and Portugal's National Laboratory of Energy and Geology (LNEG) (<http://info.igme.es/cartografiadigital/portada/>). Huelva is located above tertiary and quaternary materials of the Guadalquivir basin, with evident maritime influences and significant tidal floodplains which make up, in some provincial areas, extensive marshland areas (Meijninger, 2006). The main geological materials that can be found, from the shallowest to the deepest, are fluvial deposits, fluvial terraces, basal sandstones and sandy marlstones, to a greater or lesser degree. The bay of the Algarve is also essentially made of tertiary materials, particularly calcareous materials, clays and sands with some magmatic material (Terrinha *et al.*, 2013).

The presence of soft soil has an amplifying effect on seismic action. This is due to the fact that during a seismic event, soft ground does not have the capacity to dissipate seismic waves. Rocky ground, on the other hand, due to its inertia, has the capacity to absorb the energy that is released (Udías and Mézcua, 1986). In the Algarve, soft soils are to be found on the coast (where the majority of the population lives and where school buildings are located), in some valleys and near some rivers. In the province of Huelva, soft soils are very much abundant, particularly in the South, in estuaries, marshland and near to the coast. In comparison, the south-eastern area of Andalusia, with a geological profile mainly made of rock, is not affected by this amplification.

The effects of the soil type are taken into account in seismic codes through a soil behaviour factor. This factor is tabulated for each type of soil, varying from rock to very soft soils such as slurries or sludge.

2.3. SEISMIC HAZARD IN SPAIN

In this section, the temporal evolution of seismic codes in Spain, the requirements of seismic codes that are currently in place and the updates proposed in the document drawn up by the Spanish National Geographic Institute (IGN) on seismic hazard values will be analysed. Then, the requirements set out in the European code, of recommended application, related to the determination of seismic actions, will be described.

SUMARY

2.3.1. Chronological evolution of seismic building codes in Spain

The first Spanish seismic building code (PGS-1) was passed in 1969 (Ministerio de Planificación del Desarrollo, 1968). This code classified buildings according to their degree of importance. Schools were included in group I, "ordinary buildings". Groups II and III encompassed buildings of high importance such as hydraulic constructions or energy plants. For buildings in group I, the application of this code was optional. In any case, the document proposed different seismic areas, values of seismic action and a design method.

The following seismic building code was the PDS-1 which was passed in 1974 (Ministerio de Planificación del Desarrollo, 1974). This code established an initial classification of buildings according to their structural type to estimate damage, several seismic zones and a similar design method for the buildings to the one set out in the previous code.

In 1994 a new seismic building code was passed called the *Norma de Construcción Sismorresistente* (Seismic Building Code) (NCSE94) (Ministerio de Obras Públicas Transportes y Medio Ambiente, 1994). This document set out new seismic hazard maps and introduced more complex design methods and more restrictive requirements.

The seismic building code that is currently in force in Spain is the *Normativa de Construcción Sismorresistente* Española de 2002 (Spanish Seismic Building Code of 2002) (NCSE02) (Ministerio de Fomento, 2002). In this code, the criteria related to the seismic action to be considered in any building project, reform or retrofitting in Spain are established. Besides, since 2007 the NCSP-07, the eponymous applicable document for the seismic design and analysis of bridges, has been in force. In 2012, an *Update of the seismic hazard maps in Spain* was published, drawn up by the IGN and of recommended use (Ministerio de Fomento de España, 2012).

Lastly, Eurocode 8 (EC8) (AENOR, 1998) is a European code drawn up by the European Committee for Standardization (CEN), the use of which is recommended within Spanish territory. The aim of this document is to standardise criteria related to the seismic design of buildings. The code is complemented by a National Annex drawn up by each country, in which the specific national parameters that should be considered when applying the code in each country are included.

Below, the different criteria established by the NCSE02 code, the update of the seismic hazard maps and the EC8 for the case of Spain, as well as the considerations set out in its National Annex, are analysed.

SUMARY

2.3.2. Mandatory code in Spain

2.3.2.1. The Seismic Building Code (NCSE02)

2.3.2.1.a. Design ground acceleration

Seismic hazard in Spain is defined through the NCSE02 seismic hazard map or the list of municipalities in Annex 1 of said document. It is important to note that the NCSE02 only allows for the elastic behaviour of buildings. Therefore, it does not consider the non-linear behaviour of buildings when analysing potential seismic damage.

The design ground acceleration (a_c) is obtained through equation (1) and is used to determine the elastic response spectrum.

$$a_c = S \cdot \rho \cdot a_b \qquad \text{Eq. (1)}$$

Where:

- a_b *is the base ground acceleration established in the seismic hazard map in Annex 1.*
- ρ *is a dimensionless risk factor with the value 1 for buildings of normal importance and 1.3 for buildings of special importance.*
- S *is the soil amplification factor that takes into account the difference between the ground acceleration at the surface and at bedrock level. It is important to note that the values of a_b correspond to hard soil, approximately, type II.*

For $\rho \cdot a_b \leq 0.1$ g $\quad S = \dfrac{C}{1.25}$

For $0.1\ g < \rho \cdot a_b < 0.4\ g$ $\quad S = \dfrac{C}{1.25} + 3.33 \cdot (\rho \cdot \dfrac{a_b}{1.25} - 0.1)(1 - \dfrac{C}{1.25})$

For $0.4\ g \leq \rho \cdot a_b$ $\quad S = 1.0$

Being:

C soil factor, dependent on the geotechnical properties of the foundation soil. Its value is shown in table 2.

SUMARY

Table 2. Soil classification and factor.

Soil type	v_s (m/s)	Factor C	Description
I	>750	1.0	Solid rock, cemented or very dense granular soil.
II	>400 ≤750	1.3	Very fractured rock, dense granular or hard cohesive soils.
III	>200 ≤400	1.6	Granular soil of average compaction or cohesive soil with a firm to very firm consistency.
IV	≤200	2.0	Granular soil or soft cohesive soil.

To classify the different layers of soil, the velocity of the transverse elastic waves or shear waves is used (v_s). When said velocity cannot be determined, some of the following procedures can be used to determine the thickness of each layer. For granular soils, the static or dynamic penetration tests are used; for cohesive soils, the unconfined compressive strength test is used, and for both, the propagation speed of longitudinal elastic waves measure is used.

The seismic code NCSE02 provides a series of geotechnical characteristic values for each soil type: the propagation speed of the longitudinal elastic waves (v_l); the number of blow counts in the SPT test normalised to 60% of the free-fall energy; point resistance of the static penetrometer (q_c) and unconfined compressive strength (q_u), which are shown in table 3.

Table 3. Soil types. Geotechnical characteristic values.

Soil type		v_l	No. SPT blow counts	q_c	q_u
I		>2000 m/s	>50	>20 MPa	—
II	Granular	>1000 m/s	>40	>15 MPa	—
	Cohesive		—	—	>500 kPa
III	Granular	—	>15	>6 MPa	
	Cohesive	—	—	—	>200 kPa
IV		Soil layers that cannot be classified as I, II or III			

2.3.2.1.b. Probabilistic seismic hazard analysis

In the NCSE02, seismic hazard is calculated in terms of intensity, in accordance with the European Macroseismic Scale (EMS) and using the data from the IGN

SUMARY

seismic catalogue. Horizontal acceleration is determined through correlations. The base ground acceleration values are average values corresponding to a return period (P_R) of 500 years. It is important to highlight that the return period is not a physical recurrence time but corresponds to a probabilistic interpretation. It is associated with a given probability fractile in the probability distribution of maximum potential accelerations (per year). Said value corresponds, in the case of this code, to a probability of exceedance of the potential (yearly) ground acceleration of 2 per thousand ($1/P_R$).

2.3.2.1.c. Construction of the response spectrum

This code establishes a normalised elastic response spectrum at surface level. For the calculation, this spectrum must reach the base ground acceleration and be modified according to the damping (if different from 5%) and the ductile behaviour of the building. The value of the spectral ordinate, $\alpha(T)$, represents the quotient between the peak absolute acceleration of a linear elastic oscillator (S_a) and the peak acceleration applied to its base (a); that is, when the base of the oscillator suffers a peak ground acceleration earthquake a, the response of the oscillator has a peak acceleration $S_a = a \cdot \alpha(T)$, with $\alpha(T)$ being a function of the oscillator's own natural period T. The spectrum is defined through the following values:

$$\begin{aligned} &\text{If } T < T_A && \alpha(T) = 1 + 1.5 \cdot T/T_A \\ &\text{If } T_A \le T \le T_B && \alpha(T) = 2.5 \\ &\text{If } T > T_B && \alpha(T) = K \cdot C/T \end{aligned}$$

Being:

- $\alpha(T)$ *Value of the normalised elastic response spectrum.*
- T *Oscillator's own natural period in seconds.*
- K *Contribution factor. It takes into account the influence of the different types of earthquakes expected for the seismic hazard of each area.*
- C *Ground factor.*
- T_A, T_B *Characteristic parameters of the response spectrum, with the value of:*

$$T_A = K \cdot C/10 \text{ and } T_B = K \cdot C/2.5.$$

SUMARY

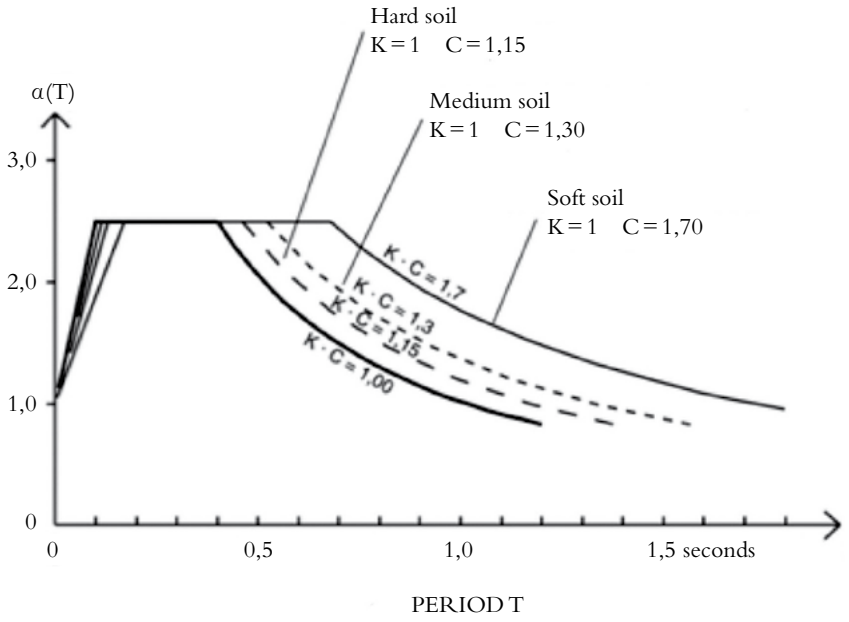

Figure 3. Elastic response spectrum for different values of C and K (NCSE-02).

Fully taking into account all of the factors that influence the shape and the ordinates of the response spectrum is very complex. In this code, a simplified formula, of acceptable accuracy in relation to the available data, has been used. The spectrum is established in accordance with the foundation soil and the differentiating characteristics of the seismicity of the Azores-Gibraltar zone, whose influence is introduced through the factors *C* and *K*, respectively.

Factors *C* and *K* affect the spectral branch in which the velocity is constant (high periods) (figure 3); soft soils and the greater epicentral distance amplify the spectral velocity of this branch and displace the value T_B, where the range starts, to greater periods.

Factor *K* takes into account the different contributions of seismicity of the peninsula and adjacent areas, and of the closest one, corresponding to the Azores-Gibraltar zone, to the seismic hazard in each area of Spanish territory. The *K* values range between 1,0 –at the points where the seismic hazard comes from continental earthquakes or adjacent maritime areas– and 1,5 at the points where the contribution to hazard originates wholly from earthquakes of the aforementioned Azores-Gibraltar region.

In table 4 the base ground acceleration values a_b are included for the municipalities of the province of Huelva established in Annex 1 of the NCSE02. The contribution factor *K* varies between 1,2 and 1,3.

SUMARY

Table 4. Base ground acceleration values (a_b) of the municipalities of the province of Huelva.

Municipality	a_b	Municipality	a_b
Alájar	0,06	Galaroza	0,06
Aljaraque	0,10	Gibraleón	0,10
El Almentro	0,11	La Granada de Río-Tinto	0,06
Almonaster la Real	0,07	El Granado	0,12
Almonte	0,08	Hieguera de la Sierra	0,06
Alosno	0,09	Hinojales	0,06
Aracena	0,06	Hinojos	0,08
Aroche	0,07	Huelva	0,10
Arroyomolinos de León	0,05	Isla Cristina	0,13
Ayamonte	0,14	Jabugo	0,06
Beas	0,09	Lepe	0,12
Berrocal	0,07	Linares de la Sierra	0,06
Bollullos Par del Condado	0,08	Lucena del Puerto	0,09
Bonares	0,09	Manzanilla	0,08
Cabezas Rubias	0,09	Los Marines	0,06
Cala	0,05	Minas de Riotinto	0,07
Calañas	0,08	Moguer	0,10
El Campillo	0,07	La Nava	0,06
Campofrío	0,06	Nerva	0,07
Cañaveral de León	0,05	Niebla	0,09
Cartaya	0,11	La Palma del Condado	0,08
Castaño de Robledo	0,06	Palos de la Frontera	0,10
El Cerro de Andévalo	0,08	Paterna del Campo	0,08
Corteconcepción	0,06	Paymogo	0,11
Cortegana	0,07	Puebla de Guzmán	0,10
Cortelazor	0,06	Puerto Moral	0,06
Cumbres de Enmedio	0,06	Punta Umbría	0,10
Cumbre de San Bartolomé	0,06	Rociana del Condado	0,09
Cumbres Mayores	0,06	Rosal de la Frontera	0,09
Chucena	0,08	San Bartolomé de la Torre	0,10
Encinasola	0,06	San Juan del Puerto	0,09
Escacena del Campo	0,08	Sanlúcar de Guadiana	0,13
Fuenteheridos	0,06	San Silvestre de Guzmán	0,12

SUMARY

Table 4. Base ground acceleration values (a_b) of the municipalities of the province of Huelva *(cont.)*.

Municipio	a_b
Santa Ana la Real	0,06
Santa Bárbara de Casa	0,09
Santa Olalla del Cala	0,05
Trigueros	0,09
Valdelarco	0,06
Valverde del Camino	0,08
Villablanca	0,13

Municipio	a_b
Villalba del Alcor	0,08
Villanueva de las Cruces	0,09
Villanueva de los Castillejos	0,11
Villarrasa	0,08
Zalamea la Real	0,07
Zufre	0,06

2.3.2.1.d. Construction criteria

This Code establishes four types of ductility behaviour: very high, high, low and very low. The type of ductility behaviour depends on the layout, materials and constructive details, and determine a ductility behaviour faactor. The following conditions must be verified in order to adopt a ductility behaviour factor:

- Very high ductility ($\mu = 4$): horizontal seismic action must be resisted by frames with stiff nodes or through stiffening systems especially designed for dissipating energy. In structures with reinforced concrete beams, these must be sharp-edged. Furthermore, they must comply with the requirements related to dimensioning and constructive details.
- High ductility ($\mu = 3$): resistance to horizontal seismic action is achieved through reinforced concrete uncoupled wall panels or tension diagonals. In structures with reinforced concrete beams, these must be sharp-edged. Furthermore, they must comply with the requirements related to dimensioning and constructive details.
- Low ductility ($\mu = 2$): in this group, inverted pendulum structures and structures with flat slabs, waffle slabs or one-way slabs with plane beams are included.
- Very low ductility ($\mu = 1$): in this group, synthetic structures that do not have the capacity to dissipate energy are included, particularly those built with masonry, brick or concrete block walls.

SUMARY

2.3.2.2. Update of the seismic hazard maps

In 2012, an update of the seismic hazard maps drawn up by the IGN was published. The study included the most up-to-date knowledge of the seismicity of the peninsula and advances in techniques for creating new seismic hazard maps, together with the information contributed by recent studies on fault activity. Likewise, the study was adapted to European codes, and a standardisation process was carried out with neighbouring countries.

2.3.2.2.a. Probabilistic seismic hazard analysis

For the proposition of new updated seismic hazard maps, a probabilistic seismic hazard analysis (PSHA) was carried out, using a Poissonian probabilistic model. This model determines the probability of occurrence of an event within a given time frame, using a mean value distribution.

To prepare the database, the seismic catalogue was taken from the IGN, expanding the period considered to 2011 and eliminating earthquakes with a greater depth than 65 km. Given that the information available on many past earthquakes is not expressed in the parameters that are currently used to measure the severity of an earthquake, a standardisation of the catalogue was carried out according to the moment magnitude scale (M_w), using intensity correlations. Moreover, attenuation laws that have been tested and proved valid were used, and a new establishment of seismic zones was undertaken. In total, the catalogue accounted for 6 999 seismic events.

2.3.2.2.b. Results obtained and relation to the NCSE02 code

The results obtained from the updated seismic maps of 2012 are not directly comparable to those used in the NCSE02. In this code, the seismic hazard map defines the seismic hazard of the territory, for a return period of 500 years, using the base ground acceleration value, a_b, and the contribution factor, K. This base ground acceleration was defined for a type II soil and, based on this, the design ground acceleration is calculated a_c, by multiplying a_b by the importance factor, ρ, and the soil factor, S.

The new seismic hazard map is, in reality, a collection of maps with different parameters, peak ground accelerations (PGA) and spectral accelerations calculated for various probabilities of exceedance or return periods. The results obtained in PGA for a return period of 475 years cannot be compared with the a_b obtained in 2002. Furthermore, the map obtained in PGA for a return period of 475 years has been determined for a type I soil in order to adapt it to European codes.

SUMARY

Therefore, to use the elastic response spectrum of the NCSE02, the a_b has to be replaced with this new PGA and the soil factor S must be modified. The adjustments would consist of the following:

For $\rho \cdot a_r \leq 0.1$ g $\quad S = C$

For 0.7 g $< \rho \cdot a_r < 0.4$ $\quad S = 1 + 3.33 \cdot (1 - C) \cdot (\rho \cdot \frac{a_r}{g} - 0.4)$

For 0.4 g $\leq \rho \cdot a_r$ $\quad S = 1.0$

Being:

C *the soil factor, dependent on the geotechnical characteristics of the foundation soil (NCSE-02 art. 2.4).*

a_r *the new PGA acceleration reference ($T_R = 475$).*

Table 5. PGA Values ($T_R = 475$) of the municipalities of the province of Huelva.

Municipality	PGA	Municipality	PGA
Alájar	0,06	Huelva	0,12
Aljaraque	0,12	Isla Cristina	0,13
El Almentro	0,09	Jabugo	0,06
Almonaster la Real	0,07	Lepe	0,12
Almonte	0,10	Linares de la Sierra	0,06
Alosno	0,08	Lucena del Puerto	0,10
Aracena	0,06	Manzanilla	0,09
Aroche	0,07	Los Marines	0,06
Arroyomolinos de León	0,06	Minas de Riotinto	0,07
Ayamonte	0,12	Moguer	0,11
Beas	0,09	La Nava	0,06
Berrocal	0,07	Nerva	0,07
Bollullos Par del Condado	0,10	Niebla	0,10
Bonares	0,10	La Palma del Condado	0,09
Cabezas Rubias	0,07	Palos de la Frontera	0,12
Cala	0,06	Paterna del Campo	0,09
Calañas	0,07	Paymogo	0,08
El Campillo	0,07	Puebla de Guzmán	0,08
Campofrío	0,07	Puerto Moral	0,06

SUMARY

Table 5. PGA Values ($T_R = 475$) of the municipalities of the province of Huelva *(cont.)*.

Municipality	PGA
Cañaveral de León	0,06
Cartaya	0,12
Castaño de Robledo	0,06
El Cerro de Andévalo	0,07
Corteconcepción	0,06
Cortegana	0,07
Cortelazor	0,06
Cumbres de Enmedio	0,06
Cumbre de San Bartolomé	0,06
Cumbres Mayores	0,06
Chucena	0,09
Encinasola	0,06
Escacena del Campo	0,09
Fuenteheridos	0,06
Galaroza	0,06
Gibraleón	0,10
La Granada de Río-Tinto	0,07
El Granado	0,09
Hieguera de la Sierra	0,06
Hinojales	0,06
Hinojos	0,10

Municipality	PGA
Punta Umbría	0,13
Rociana del Condado	0,10
Rosal de la Frontera	0,07
San Bartolomé de la Torre	0,09
San Juan del Puerto	0,10
Sanlúcar de Guadiana	0,09
San Silvestre de Guzmán	0,10
Santa Ana la Real	0,07
Santa Bárbara de Casa	0,08
Santa Olalla del Cala	0,06
Trigueros	0,10
Valdelarco	0,06
Valverde del Camino	0,08
Villablanca	0,11
Villalba del Alcor	0,09
Villanueva de las Cruces	0,08
Villanueva de los Castillejos	0,09
Villarrasa	0,09
Zalamea la Real	0,07
Zufre	0,06

2.3.3. Recommended code: Eurocode 8

Eurocode 8 (1998) arose as a way of standardise criteria relating to the seismic design of structures throughout Europe. However, each country draws up their own National Annex, in which the criteria established in the EC8 are completed or adapted. It is divided into 6 parts, being part 1 (EC8-1) (AENOR, 2018a) and part 3 (EC8-3) (AENOR, 2018b) the most important ones for this project. In part 1, the general rules, seismic actions and construction rules are presented. Part 3 includes the seismic evaluation and adaptation procedure for existing buildings.

SUMARY

2.3.3.1. Determining the response spectrum

In part 1, the process of determining the elastic response spectrum is set out. Seismic hazard is expressed through the reference peak ground acceleration (a_{gR}) for soil type A and determined according to the National Annex. This is the result of multiplying the design ground acceleration (a_g) by the importance factor (γ_I) according to equation (2). In this part 1, a different importance factor is determined according to the construction type, with a value of 0.8 for structures of moderate importance; 1.0 for structures of normal importance; 1.2 for structures of great importance; and 1.4 for structures of special importance. However, this requirement must be compared with what is set out in the National Annex of each country.

$$a_{gR} = a_g \cdot \gamma_I \qquad \text{Eq. (2)}$$

The horizontal elastic response spectrum [$S_e(T)$] is defined in accordance with the following expressions:

$0 \le T \le T_B \qquad S_e(T) = a_g \cdot S \cdot \left[1 + \frac{T}{T_B} \cdot (\eta \cdot 2.5 - 1)\right]$

$T_B \le T \le T_C \qquad S_e(T) = a_g \cdot S \cdot \eta \cdot 2.5$

$T_C \le T \le T_D \qquad S_e(T) = a_g \cdot S \cdot \eta \cdot 2.5 \left[\frac{T_C}{T}\right]$

$T_D \le T \le 4s \qquad S_e(T) = a_g \cdot S \cdot \eta \cdot 2.5 \left[\frac{T_C T_D}{T^2}\right]$

Where:

$S_e(T)$ *is the elastic response spectrum.*
T *is the vibration period of a linear single-degree-of-freedom system.*
a_g *is the value of the design ground acceleration on type A soil.*
T_B *is the lower limit of the period of the constant spectral acceleration branch.*
T_C *is the upper limit of the period of the constant spectral acceleration branch.*
T_D *is the value defining the beginning of the constant displacement response range of the spectrum.*
S *is the soil factor.*
η *is the damping correction factor with reference value $\eta = 1$, for 5% viscous damping.*

SUMARY

The values of parameters T_B, T_C and T_D and the soil factor S depend on the soil type. In Table 6, the criteria for determining the soil type are outlined. In this case, the EC8-1 establishes 5 soil type compared to the 4 determined by the NCSE02 standard.

Table 6. Classification of soil types.

Soil type	Description
A	Rock or another rock-like geological formation, including at most 5 m of weaker material at the surface
B	Deposits of very dense sand, gravel or very stiff clay, at least a few tens of metres in thickness, characterised by a gradual increase of mechanical properties with depth
C	Deep deposits of dense or medium-dense sand, gravel or stiff clay with thickness from several tens to many hundreds of metres
D	Deposits of loose-to-medium cohesionless soil (with or without some soft cohesive layers), or of predominantly soft-to-firm cohesive soil
E	A soil profile consisting of a surface alluvium layer with values of vs (shear wave velocity) of type C or D and a thickness varying between 5 m and 20 m, underlain by stiffer material with vs > 800 m/s
S_1	Deposits consisting of, or containing a layer at least 10 m thick, of soft clays/silts with a high plasticity index (IP > 40) and a high water content
S_2	Deposits of liquefiable soils, of sensitive clays or any other soil profile not included in types A – E or S_1

Furthermore, the EC8-1 differs from the NCSE02 by proposing 2 types of elastic response spectra: 1 and 2 (figure 4). According to the EC8, the type 1 response spectrum is used when the earthquakes that contribute the most to the seismic hazard are far away and of a moderate to high magnitude ($M_w < 5{,}5$). The type 2 spectrum is used for nearby earthquakes with a surface-wave magnitude not greater than $M_w < 5{,}5$. The parameters and the soil factor vary depending on the type of spectrum according to table 7.

SUMARY

Table 7. Values of parameters T_B, T_C and T_D and soil factor S according to the type of spectrum.

Soil type	Seismic Action Type 1				Seismic Action Type 2			
	S_{max}	T_B (s)	T_C (s)	T_D (s)	S_{max}	T_B (s)	T_C (s)	T_D (s)
A	1.00	0.15	0.40	2.00	1.00	0.05	0.25	1.20
B	1.20	0.15	0.50	2.00	1.35	0.05	0.25	1.20
C	1.15	0.20	0.60	2.00	1.50	0.10	0.25	1.20
D	1.35	0.20	0.80	2.00	1.80	0.10	0.30	1.20
E	1.40	0.20	0.50	2.00	1.60	0.05	0.25	1.20

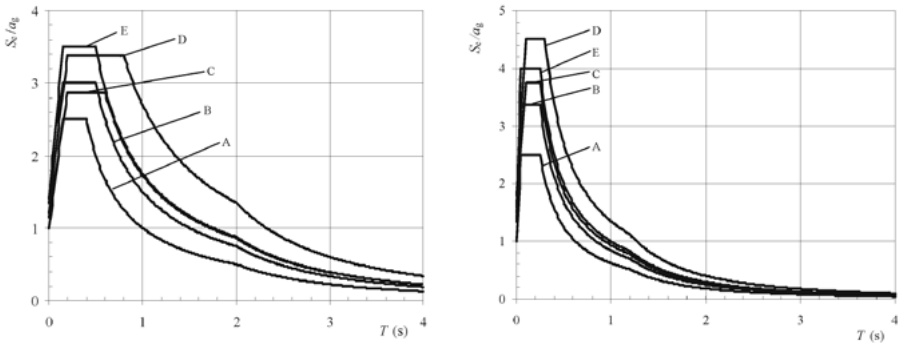

(a) (b)

Figure 4. Elastic response spectrum of type 1 (a) and 2 (b) for each type of soil.

The EC8-1 also proposes the design of an elastic response spectrum to account for the effects of the vertical forces caused by seismic action.

In the linear analyses, the elastic response spectrum is reduced by a factor called the behaviour factor (q) which considers the type of structural system and its ductility. The determination of this factor is specified in the EC8-1 only for the design of new buildings. However, this process cannot be applied to existing buildings, which is why other codes are used such as the American one.

2.3.3.2. Spanish National Annex

For the use of the response spectrum in EC8-1, the National Annex establishes a series of criteria related to the ground acceleration value and the importance factor.

SUMARY

The a_{gR} of the EC8 is established for a type A soil and a T_r of 475 years. however, the base ground acceleration values of the NCSE02 are established for a type II soil and a T_r of 500 years. Thus, in order to use them, the a_b values must be multiplied by a reduction factor of 0.8, according to the equation (3). When using the updated seismic hazard values of 2012, there is no need to make any changes to the PGA, given that it is already expressed for a type I ground and a return period of 475 years.

$$a_{gR} = 0.8 \cdot a_b \qquad \text{Eq. (3)}$$

The Spanish Annex proposes a modification of the importance factor established in the EC8-1: the highest importance factor is increased from 1.2 to 1.3. This change affects this project, as schools are included in this importance class.

2.4. SEISMIC HAZARD IN PORTUGAL

In this section, the chronological evolution of seismic codes in Portugal and the requirements of the currently applied seismic codes are analysed.

2.4.1. Historical seismic codes: Decree law no. 235/83

The first seismic building code in Portugal was the *Decree no. 41 658* (RSCCS, 1958) (Nacional, 1958). The second seismic code was the Decree 44 041 (RSEP, 1961) (Nacional, 1961), which changed the seismic action due to the earthquake that occurred in Agadir in 1960. The *Decree Law 235/83, Reglamento de Segurança e Acçoes para Estructuras de Edificios e Pontes (Safety regulation and actions for buildings structures and bridges)* (RSAEEP) passed in 1983 (Imprensa Nacional-Casa da Moeda, 1983), was the first seismic code to include modern dynamic analysis principles in the design of structures.

2.4.1.1. Probabilistic seismic hazard analysis

The map of the six seismic zones considered in the RSAEEP (figure 5) was influenced by a study on seismic hazard, which resorted to a Poisson model and a type-III extreme value distribution, for a return period of 1 000 years (Oliveira, 1977). In this study, three sources of information were used: 1) a historical catalogue from the 10th century; 2) the Portuguese instrumental catalogue from 1902 (the earthquakes in the Spanish catalogue were also used for border zones); and 3) the maximum intensities observed after the earthquakes of 1902 (Oliveira, 1977).

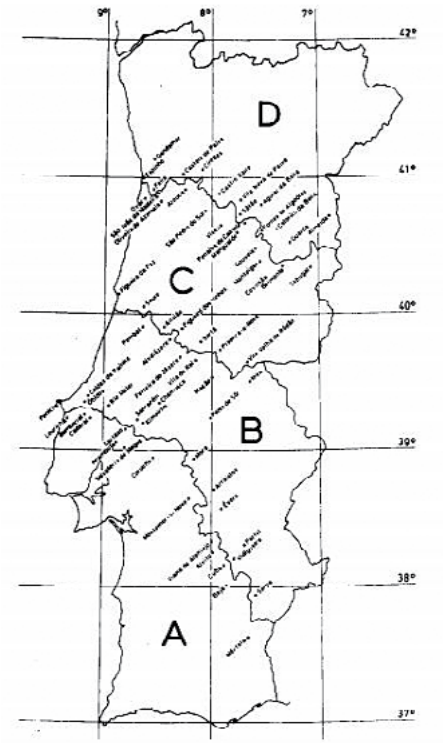

Figure 5. Seismic zonation of Portugal (Decree law no. 235/83).

In terms of the ground type, 3 types were established: type I, rocks; type II, hard soils of a medium consistency; and type III, soft soils.

2.4.1.2. Determination of seismic action

Seismic action was defined through the power spectral densities of acceleration, for two types of earthquakes: 1) a moderate-magnitude earthquake not far from the focus, and 2) an earthquake of a high magnitude at a greater distance from the focus. The response spectra were determined using power spectra, though this was a difficult process. The influence of seismicity is taken into account through factor α for each seismic action.

2.4.2. Mandatory code: Eurocode 8

Since December 2019, Eurocode 8 has been the seismic code in force in Portugal.

SUMARY

2.4.2.1. Construction of the response spectrum

Establishing the response spectrum is carried out in a similar way to that specified in the EC8-1. However, the National Annex specifies the values of parameters T_B, T_C and T_D, of the soil factor S and the importance factor.

2.4.2.2. Portuguese National Annex

The Portuguese National Annex specifies the requirements set out in the EC8-1 for earthquakes of two kinds, as is the RSAEEP, but in this case type 1 is the distant earthquake and type 2 is the nearby earthquake. It proposes new importance factor values according to the importance class and for each type of seismic action (table 8). In the case of schools, the importance class is III, therefore, in the context of a type I response spectrum, it corresponds to an importance factor of 1.45, a higher value than that established by the Spanish National Annex.

Table 8. Importance factors (γ_I).

Importance class	Seismic Action Type 1	Seismic Action Type 2	
		Continent	Azores
I	0.65	0.75	0.85
II	1.00	1.00	1.00
III	1.45	1.25	1.15
IV	1.95	1.50	1.35

It also proposes an update of the values of parameters T_B, T_C and T_D and of the soil factor S for each type of seismic action (table 9).

For $a_g \leq 1$ m/s^2 $\quad S = S_{max}$

For $1 < a_g < 4$ m/s^2 $\quad S = S_{max} - \frac{S_{max} - 1}{3} \cdot (a_g - 1)$

For 4 m/s$^2 \leq a_g$ $\quad S = 1.0$

SUMARY

Table 9. Values of T_B, T_C and T_D and S for each type of response spectrum.

Soil type	Seismic Action Type 1				Seismic Action Type 2			
	S_{max}	T_B(s)	T_C(s)	T_D(s)	S_{max}	T_B(s)	T_C(s)	T_D(s)
A	1.00	0.10	0.60	2.00	1.00	0.10	0.25	2.00
B	1.35	0.10	0.60	2.00	1.35	0.10	0.25	2.00
C	1.60	0.10	0.60	2.00	1.60	0.10	0.25	2.00
D	2.00	0.10	0.60	2.00	2.00	0.10	0.30	2.00
E	1.80	0.10	0.60	2.00	1.80	0.10	0.25	2.00

In (Campos Costa *et al.*, 2008) a proposal to update the National Annex was made in 2008. In this study, new seismic zones were proposed (figure 6) and a new probabilistic seismic hazard analysis was carried out using a Cornells method.

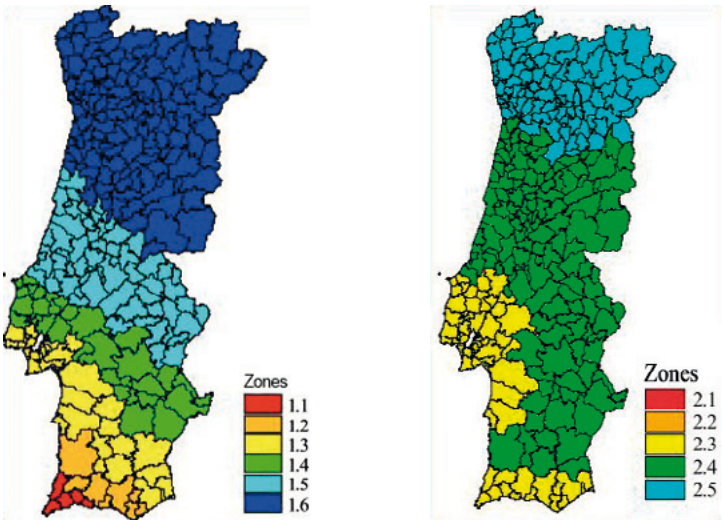

(a) (b)

Figure 6. Seismic zonation annex type 1 (a) and type 2 (b).

SUMARY

Table 10. Reference peak ground acceleration a_{gR} (m/s^2) in various seismic zones.

Ground acceleration Type 1		Ground acceleration Type 2	
Seismic zone	a_{gR} (m/s^2)	Seismic zone	a_{gR} (m/s^2)
1.1	2.5	2.1	2.5
1.2	2.0	2.2	2.0
1.3	1.5	2.3	1.7
1.4	1.0	2.4	1.1
1.5	0.6	2.5	0.8
1.6	0.35	—	—

In this study, new values of a_{gR} were proposed for each seismic zone and for each type of response spectrum according to table 10. These values do not have to be modified by factors, as they are determined for soil type I or A, for a return period of 475 years.

2.5. COMPARISON OF SEISMIC HAZARD IN THE ALGARVE-HUELVA REGION

Despite the fact that, in the case of an earthquake, the border areas of the Algarve and Huelva would be equally affected, the seismic codes of each country differ considerably (Estêvão *et al.*, 2019). The main difference is the value of seismic action due to the different approaches used in the probabilistic seismic hazard analyses. In terms of other requirements, such as ductility or constructive criteria, they are very similar.

It is important to note that, despite the fact that EC8 arose as a standardisation tool for seismic design at the European level, the National Annexes serve to help each country specifying their own parameters. As in (García-Mayordomo *et al.*, 2004), the main differences in the seismic parameters and their values are outlined in table 11.

In the Spanish NCSE02 and in the values update in 2012, a seismic hazard analysis was used based on a Poissonian distribution, hence using mean values. However, for the Portuguese code and the National Annex to the EC values update in 2008, a Poisson and Gumbel I distribution was used, resulting in a distribution of maximum values. Due to this and other factors that influence the results (Estêvão and Oliveira, 2001), the acceleration values obtained for Portugal and Spain differ in some locations.

SUMARY

Table 11. List of basic parameters for determining the ground acceleration according to each code.

Parameter	Decree Law RSAEEP	EC8	NCSE02	Spanish maps update	Spanish Annex to EC8	Portuguese Annex to EC8
Date	1983	1998	2002	2012	2010	2010
Seismic scale	Magnitude	—	Intensity	Magnitude	—	—
Seismic estimation	Historical Parameters Attenuation laws Gumbel III	—	Historical Parameters	Historical Parameters Attenuation laws	—	—
Attenuation functions	Acceleration	—	Macroseismic	Acceleration	—	—
Hazard analysis	Gumbel I	—	Poisson	Poisson	—	—
Hazard descriptor	PGA	$a_g = a_{gR} \cdot \gamma_I$	$a_c = S \cdot \rho \cdot a_b$	PGA	$a_{gR} = 0.8 \cdot a_b$	a_{gR}
Importance factor	—	$\gamma_I = 1$	$\rho = 1$	$\rho = 1$	$\gamma_I = 1{,}3$	γ_I-$T_1 = 1{,}45$ γ_I-$T_2 = 1{,}25$
Type of spectrum	Type 1 and 2	Type 1 and 2	Type 1	Type 1	Type 1 and 2	Type 1 and 2
No-collapse limitation values	$T_{NCR} = 1000$ years	$T_{NCR} = 475$ years $P_{NCR} = 10\%$	$T_{NCR} = 500$ years $P_{NCR} = 2$ ‰	$T_{NCR} = 475$ years $P_{NCR} = 10\%$	$T_{NCR} = 475$ years $P_{NCR} = 10\%$	$T_{NCR} = 475$ years $P_{NCR} = 10\%$
Severe damage limitation values	—	$T_{DLR} = 95$ years $P_{DLR} = 10\%$	$T_{DLR} = 95$ years $P_{DLR} = 10\%$	$T_{DLR} = 95$ years $P_{DLR} = 10\%$	$T_{DLR} = 95$ years $P_{DLR} = 10\%$	$T_{DLR} = 95$ years $P_{DLR} = 10\%$
Ground acceleration value (m/s^2)	—	—	Ayamonte $a_c = 1.597$ $a_g = 1.428$	Ayamonte $a_c = 1.763$ $a_g = 1.5$	—	Vila Real $a_{g-T1} = 2.2$ $a_{g-T2} = 2.1$

Regarding the return period, significant differences are also found. The NCSE02 used a value of 500 years whilst for the EC8 and the Spanish and Portuguese update, this value was 475 years. This difference is important in the case of the Portuguese code, as in the seismic hazard analysis a return period of 1 000 years was considered. Therefore, the seismic action is considerably greater than that established in the NCSE02 or in the Spanish values update.

SUMARY

Another important issue is that the seismic accelerations are expressed for different types of soil. The NCSE02 determines the acceleration for a type II ground, whilst the rest consider a type I. Therefore, when using the EC8 response spectrum, the acceleration of the NCSE02 must be modified by a reduction factor specified in the Spanish National Annex. Furthermore, the NCSE02 considers one single response spectrum. However, the EC8 and the Portuguese code establish two types of seismic action.

In terms of the importance factor, the Spanish code determines a factor of 1,0 for schools. However, this value differs considerably when using the EC8 response spectrum, being 1,3 and 1,45, according to the Spanish and Portuguese National Annexes, respectively. This increase results in considerably higher values of a_g for the case of Portugal.

In the framework of the PERSISTAH project, a comparison has been carried out of the seismic action for two municipalities located on the Spanish-Portuguese border, according to each seismic code. The municipalities selected for the analysis were Vila Real de Santo Antonio and Ayamonte (figure 7). Both are separated only by the Guadiana river and are characterised by the presence of soft soils with similar properties.

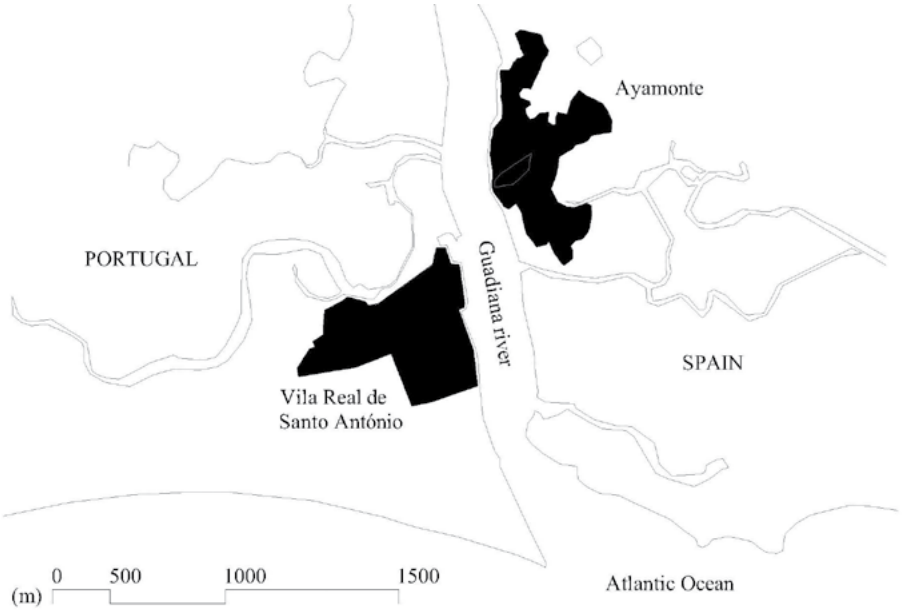

Figure 7. Municipalities considered in the study.

SUMARY

The response spectra were determined based on figure 8: acceleration and frequency tables of the Portuguese code RSAEEP for the corresponding seismic zone; the response spectrum of the NCSE02 considering the base ground acceleration from Annex 1 for Ayamonte and the PGA established in the seismic hazard values update of 2012 for Ayamonte; the EC8 response spectrum considering the two previous accelerations, and that established in (Campos Costa *et al.*, 2008) for the corresponding seismic zone and taking into account the requirements established in each National Annex. The soil type selected has been type III in the case of the national code and C in the European codes, respectively.

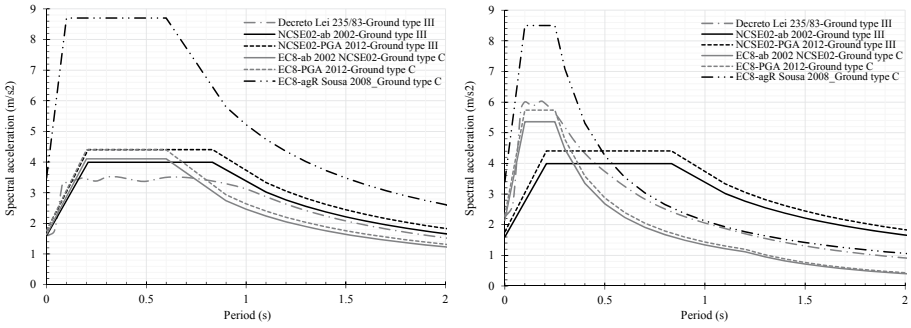

Figure 8. Comparison of the response spectra for each seismic code for a distant earthquake scenario (type 1) (a) and a nearby earthquake scenario (type 2) (b).

From this comparison, it can be stated that there are considerable differences in terms of the value of seismic action, differing by up to 60%. In any case, according to (Oliveira *et al.*, 2000), the seismic hazard analyses considered in the codes are not up to date. In addition, the study should underscore the definition of the ground accelerations by using current and valid attenuation laws, as well as considering different seismic risk scenarios.

SUMARY

SUMARY

Chapter 3. Characterisation of schools

3.1. SOURCES OF INFORMATION

A total of 138 primary schools have been identified in Huelva, each of them consisting of one to six different buildings. A total of 269 buildings have been identified. Figure 9 shows the number of schools according to the number of buildings into which they are divided. Most of them (52%) present only one building, while 26% are composed of two and 13% of three. The remaining 9% presents four or more buildings.

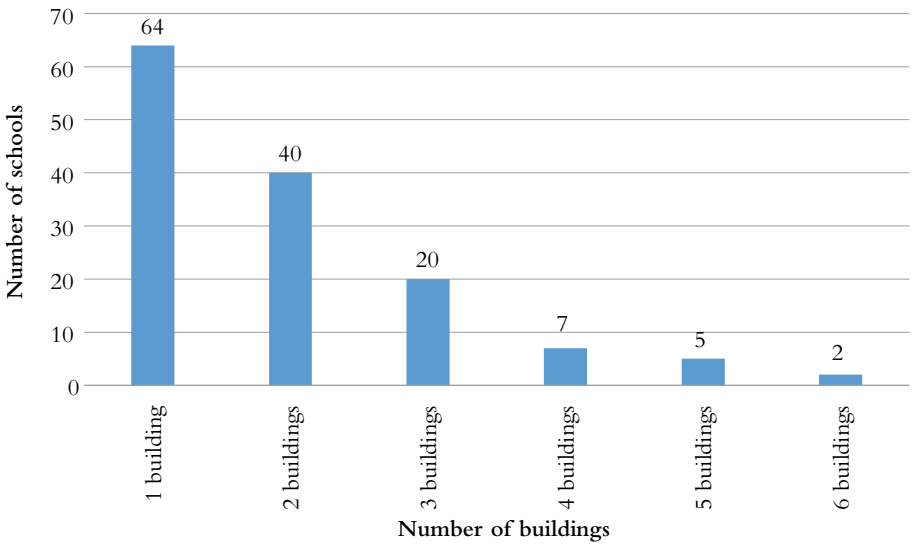

Figure 9. Schools according to the number of buildings into which they are divided.

SUMARY

The characterisation of school buildings is carried out using the information available from each school: aerial images, on-site visits, surveys and original and refurbishment projects (both including descriptive and graphic reports) obtained from different municipal archives of Huelva, the College of Architects of Huelva and the Ministry of Education of the Andalusian Government.

The process followed for the analysis and processing of the information obtained from each source is described below.

3.1.1. Creation of the database

Based on the information obtained, a database has been created and implemented in the software developed within the framework of the research project. This database is divided into the following sections:

- School identification.
- General characterisation of the school campus.
- General characterisation.
- Type of construction.
- Elements for seismic evaluation.
- Existence of damage and level of maintenance of the building.
- Risks and internal characteristics.
- Envelope and exterior risks of the building.

The fields included in each section are expecified in table 12.

3.1.2. Creation of building specification sheets

When detailed enough information of a building was available, a specification sheet was drafted. These sheets collect specific information on the structural and constructive characteristics needed for the calculation of the seismic behaviour of the buildings. Table 13 shows the sections included in a sample building sheet. In total, 36 building specification sheets have been completed.

SUMARY

Table 12. Sections included in the database.

School identification	Characterisation of the school campus
Building number	Total area of the school
Building reference	Number of buildings
Land registry reference	Land area
Type of school	Percentage of free land
Name of the school	Morphology of the school grounds
Country	Is there any possible landslide hazard?
Province	Is it near a cliff?
Municipality	Distance from the coastline
Address	Firefighter capacity
UTM coordinates	Distance from nearby fire station
Contact: phone number and email	
Designation of school year level	
Services	
Institutional nature	
Number of students	
Aerial image of the school	
Image of the school's façade	
General characterisation	Type of construction
Distance from the nearest hospital	Main structural system
Conditions of evacuation and access and conditions of evacuation for emergency services	Average distance between vertical structural elements
Designation	Average dimension of the columns section
Main use	Average dimension of the shear wall section
Total area	Average dimension of the beam section
Maximum building height	Average thickness of the load-bearing wall
Number of floors	Horizontal structural system
Maximum building length	Stiffness of the horizontal structural system
Maximum building width	Middle edge of the slab
Average distance between floors	Structural type of roof
Date of construction	Level of deterioration
Has the school been restructured?	Type of plane irregularity

SUMARY

Table 12. Sections included in the database *(cont.)*.

General characterisation	Type of construction
Date of last retrofit	Is there any chance of different buildings colliding?
Main type	Stiffness of the floor system
Subtype	
Elements for seismic evaluation	Existence of damage and maintenance of the building
Is the distance between floors uniform?	Is there a maintenance plan?
Is there a problem in the building?	Time between maintenance works
Is there an atrium (areas without walls inside the building)?	Who is in charge of the maintenance work?
Are there any stairs or lifts with shear walls?	Is there a foundation problem?
Is there mass eccentricity?	Is there a problem of beam deformation?
Is there a soft floor?	Is there a problem of floor deformation?
Are there short columns?	Are there cracks in the walls?
Average percentage of short columns	Are there problems with window deformation?
Stratigraphic soil profile	Are there problems with door deformation?
Classification of the foundation	Is there a water infiltration problem?
Risks and internal characteristics	Envelope and exterior risks
Main type of non-structural wall	Façade gap ratio
Wall gap ratio	Characteristics of the roof layout
Non-structural suspended ceiling	Percentage of gaps in the roof
Characteristics of the lighting system	Non-structural materials roof surface
Type of furniture	Is there any ornamental element?
Type of piping	Are there any parapets?
Is there an air conditioner in the suspended ceiling?	Is there a chimney?
Façade wall type	Is there any danger of collision with a tall adjacent building?

SUMARY

Table 13. Building specification sheet for the calculation of the structural model.

SCHOOL	reference	S050				name	XXX														
	address	xxx																			
	date	1988															number of buildings	1			
CHARACTERISTICS	building ref.	S050_1				date	1988			refurbished	SI						area	1432			
	heights	sanit.	0,75			GF	3			1F	3			2F			total	6,75			
	URM					RC frame	X			Steel frame				Waffle slab				Slab			
	beams	RC	X			Steel								Wood							
	materials			RC	HA-175		Steel	AEH-400		Wood							Safety	NORMAL			
STRUCTURAL SYSTEM	VERTICAL	columns		separation		min	2,75						rebar		sanit.	4ϕ12					
						av									GF	4ϕ12					
						max	7,85								1F	4ϕ12					
															2F						
				section	sanit.		30x30						stirrups		sanit.	ϕ6 to 15cm					
					GF		30x30								GF	ϕ6 to 15cm					
					1F		30x30								1F	ϕ6 to 15cm					
					2F										2F						
		load bearing wall											bracing		NO						
		panels				dimension							rebar								
	HORIZ.: SANIT.	floor thickness	22+3			peso				luz											
		load bearing beams	type C1			span							section		40x50						
						rebar															
					sup		6ϕ20		inf		6ϕ20		stirrups		ϕ8 to 15cm						
		tie beams	type A1			span							section		30x40						
						rebar															
					sup		2ϕ14		inf		2ϕ14		stirrups		ϕ6 to 20cm						
	HORIZ.GF AND F	floor thickness	26+4			weight				span											
		load bearing beams	type C1			span							section		60x30						
						rebar															
					sup		3ϕ12		inf		4ϕ20+2ϕ16		stirrups		ϕ8 to 10cm						
		tie beams	type A1			span							section		30x30						
						rebar															
					sup		2ϕ10		inf		2ϕ12		stirrup		ϕ8 to 10cm						
FOUNDATION	footing		dim.			thickness			depth				rebar								
	slab		thickness																		
	pile		type	yes		nº/pile caps	2				diameter	ϕ40			depth	-					
			pile cap	13x70x60							stirrups	sup.4ϕ12/inf.4ϕ20										
	st rut		dimension							rebar					stirrups						
	safe load					ballast coeff.							geotechnical e		no						
	concrete type					steel type															
CONSTRUCTIVE SYSTEM	roof		type	gable					thickness	20-30 cm			weight	-							
	external walls		type	E+L+AT+HS+E					thickness	25-26cm			weight	-							
	parapet		type	NO					thickness				weight								
	partition		type	E+HS+E					thickness				weight								
	susp. ceiling		type	NO					thickness				weight								

3.1.3. Questionnaires sent to schools

In order to complete and verify the gathered data, an online questionnaire was sent to each of the schools, requesting information on the current state of the buildings. The information from the surveys makes it possible to include data on maintenance, possible damage to the building, possible reforms and

SUMARY

extensions, as well as to corroborate existing technical data. The content of the questionnaire is available in table 14. Information has been obtained from 47 schools, 33% of the total number.

Table 14. Questionnaire sent to school management.

School's identification data	
Name of the school	Extra services
Population	Number of students
Educational levels	
School's general information	
Slope of the land	Distance from the nearest hospital
Is it near a cliff or ravine?	Evacuation conditions
Distance from the coastline	Does the building have regular maintenance?
Distance from the nearest fire station	How often is maintenance performed?
Manoeuvrability of the fire brigade	Who is in charge of maintenance?
Building 1: technical details	
Main use of the building	Are there deformations in windows?
Number of floors	Are there deformations in doors?
Date of construction of the building	Are there any damp patches?
Has the building had any structural alterations or extensions?	Is there a suspended ceiling?
Type of structure	Type of light fixtures in classrooms
Level of deterioration of the building	Type of furniture in classrooms
Are there structural joints?	In what condition are the pipes in the facilities?
Is there a covered patio?	Is there an air conditioning installation on the ceiling?
Are there shear walls in the staircase or lift?	Type of roof
Are there heavy elements on the roof?	Are there any ornamental elements (such as cornices or shields) that can come loose easily?
Are there open areas on the ground floor (without infills) and built on the first floor?	Are there chimneys?
Are there foundation problems?	Are there any tall buildings adjacent to the building?
Are there cracks and crevices?	Is there a kitchen?

SUMARY

3.2. SCHOOL BUILDINGS CHARACTERISATION PROCESS

The process of characterising school buildings was carried out based on the information obtained as explained in the previous sections. In this classification, as mentioned before, a sample of 269 buildings was considered. Firstly, the buildings have been grouped according to their structural system and date of construction. Secondly, a classification has been made according to geometry and volumetry. These two classifications are a first approach to the analysis of the large volume of data available. Results obtained from the first and second classification are shown in the following chapters.

3.2.1. Classification according to structural system and year of construction

The way the analysis of the seismic vulnerability of a building is performed depends highly on its structural system. Moreover, retrofitting techniques and rehabilitation measures are specific to each structural system. This is the reason why a first classification of the buildings was made based on their structural type. Figure 10 shows the groups into which the buildings have been divided according to their structural system. Most of the buildings were built with reinforced concrete (RC) frames (82%), followed by unreinforced masonry (URM) load-bearing walls (13%). Steel buildings account for 4% of the total. It has not been possible to identify the structural system for only 1% of the buildings.

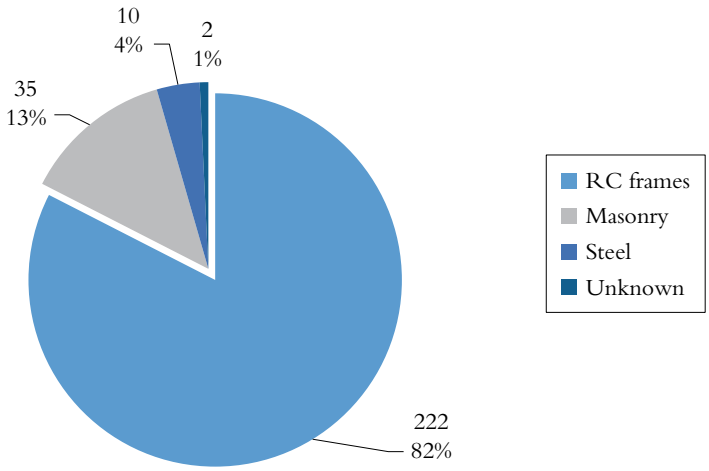

Figure 10. Classification of schools according to their structural system.

SUMARY

The sample was also analysed based on the date of construction of the buildings (figure 11). 31% of the buildings were constructed in the 1980s, 18% during the 1970s and 15% on the 1990s. It is important to highlight the relationship between the date of construction and the structural system. Most of the masonry buildings were constructed before 1970, while most of the buildings that were built during the '70s and '80s are reinforced concrete frame buildings.

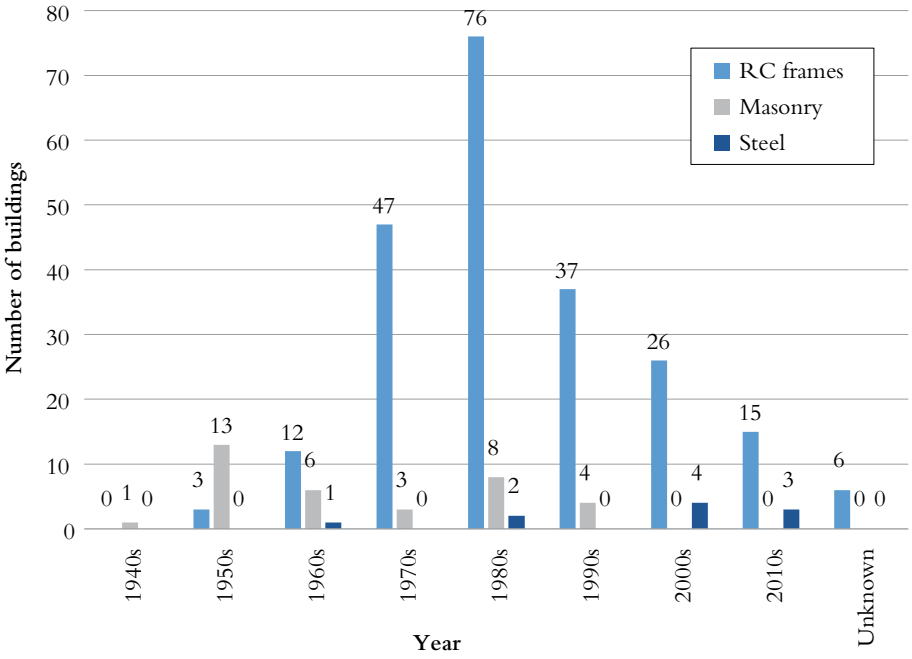

Figure 11. Classification of buildings according to date of construction and structural system (not considering buildings for which the structural system is unknown).

3.2.2. Classification according to geometry and volumetry

The volumetry and footprint of the buildings under study were analysed from available aerial and exterior images. Six main geometrical types have been identified and are shown in figure 12: compact, linear, prism, intersection, juxtaposition and sport. These types are, in turn, divided into several subtypes that allow us to define typologies with expected similar seismic behaviour.

SUMARY

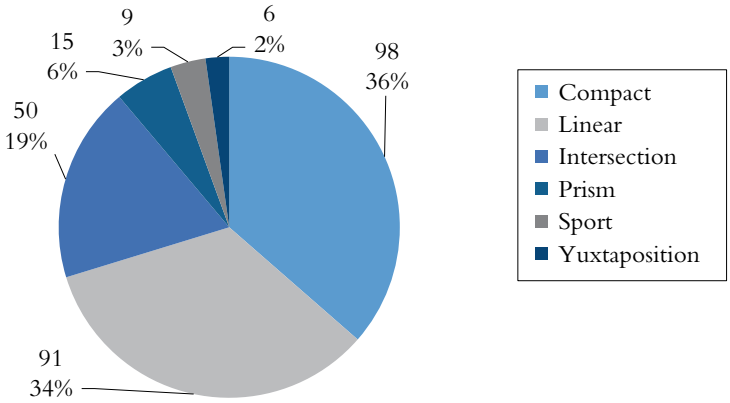

Figure 12. Classification of buildings according to their geometric and volumetric characteristics.

3.2.2.1. Compact type buildings

Compact buildings are characterised by quite square footprints and are very regular in volume. The spans and openings, regardless of the structural type, are small (around 5 m maximum). Therefore, they are mostly buildings without structural joints (67%). Construction dates range from 1955 to 2015. 91% of the buildings consist of RC frames and the remaining 9% of URM walls. In addition, this type is subdivided into several subtypes, as listed below.

3.2.2.1.a. No courtyards

Number of buildings: 59.
Description: the dimensions and built area of these buildings are not very high. Their main feature is that they do not have any courtyards or gaps in the slabs (except for the stairwells). They are mostly composed of a single floor (72%) and have no structural joints. The largest dimension reaches 35 m, although the average is 23 m. The smaller average dimension is 16 m and the built area is about 517 m^2. In

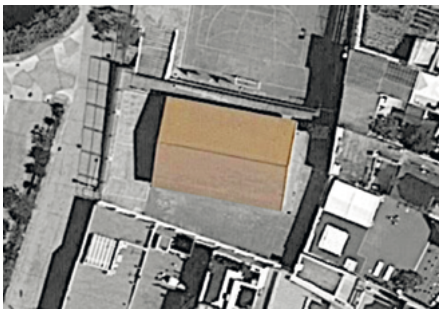

Figure 13. Volumetric classification. School S084. Building: 2. Type: Compact. Sub-type: no courtyards.

SUMARY

addition, they are very regular in floor plan and height, with only 16% of them having atriums or porches for access to the building. 84% have a sloping roof, with ceramic tiles (78%) or metal panels (22%). The rest are characterised by flat roofs with flooring or gravel.

3.2.2.1.b. H-shape

Figure 14. Volumetric classification. School S006. Building: 1. Type: compact. Subtype: H-shape.

Number of buildings: 15.
Description: these are identical buildings, a prototype. The floor plan is rectangular with dimensions of around 48 × 25 m with setbacks of the edge of the slab at the ends. The structural system consists of RC frames with structural joints. They are three stories high and have entrance atriums to the building in the central bays. Construction dates range between 1970 and 1988. The sloping roof is finished with ceramic tiles.

3.2.2.1.c. Compact

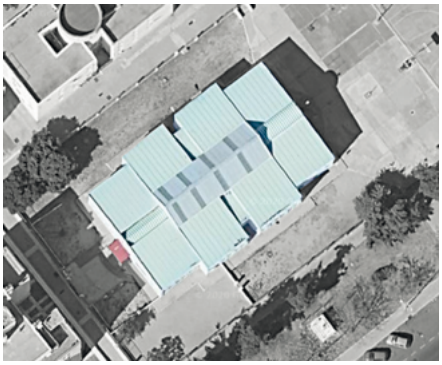

Figure 15. Volumetric classification. School S050. Building: 1. Type: compact. Sub-type: compact.

Number of buildings: 12.
Description: these are buildings of larger dimensions in terms of floor plan and surface area when compared to the subtype "no courtyards". 50% has one floor and the rest, two. Dimensions range from 30-50 m long to 20-30 m wide. Their average built area is 1,352 m^2. 33% have atriums and most of them do not have setbacks in the slab. 60% have flat roofs finished with flooring or gravel, with the rest having a gable roof with ceramic tiles. All have reinforced concrete frames and most (60%) have no structural joints. Construction dates range from 1958 to 2015.

SUMARY

3.2.2.1.d. With courtyards

Number of buildings: 59.
Description: these buildings are the largest, as well as the most irregular and complex. The structural system consists of RC frames, with structural joints in most cases analysed (70%) and two floors (80%). Their length ranges between 25-60 m and the width between 20-30 m. The average value of the built area is 1 642 m^2. 60% has a sloping roof with ceramic tiles and the rest has a flat roof with gravel or flooring. Construction dates range from 1979 to 2010.

Figure 16. Volumetric classification. School S026. Building: 1. Type: compact. Sub-type: with courtyards.

3.2.2.1.e. Symmetrical

Number of buildings: 8.
Description: these are identical buildings that represent a prototype. They are symmetrical in plan and volume, although the perimeter is very irregular with several protrusions and entrances. They have two courtyards in their central part and have atriums along the end bays. They have two floors and their dimensions are 60 × 35 m, with a built area of about 2 100 m^2. The roof is sloped with metal panels. The structure is made of RC frames.

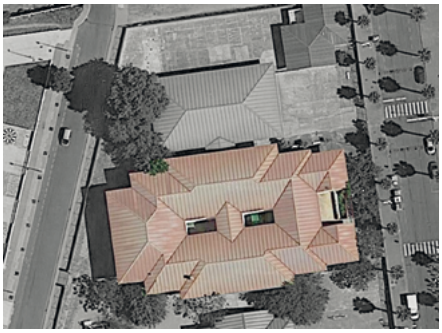

Figure 17. Volumetric classification. School S076. Building: 1. Type: compact. Subtype: symmetrical.

SUMARY

3.2.2.2. Linear type buildings

Linear buildings are characterised by their rectangular plan view with a clearly predominant dimension (minimum ratio 3:1). 24% of the buildings in this group were built with URM walls and 72% with RC frames. Linear buildings are divided into the following subtypes.

3.2.2.2.a. Small

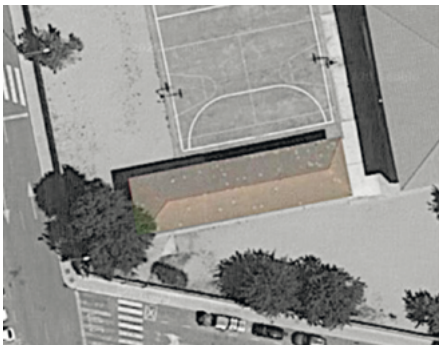

Figure 18. Volumetric classification. School S109. Building: 2. Type: linear. Sub-type: small.

Number of buildings: 25.
Description: these are buildings of average dimensions of 29 m and 10 m in length and width, respectively. 92% are single storey and their built area ranges between 125 and 600 m^2. 84% have sloping roofs with ceramic tiles or metal panels. The rest have flat roofs with a gravel or flooring finish. Construction dates range from 1950 to 2014. 52% have RC frames and 40% are URM buildings. They do not have structural joints.

3.2.2.2.b. Medium

Figure 19. Volumetric classification. School S096. Building: 2. Type: linear. Sub-type: medium.

Number of buildings: 13.
Description: these are larger buildings than the previous ones (up to 85 m long and 30 m wide), with two floors and an average built area of 919 m^2. Most have a sloping roof (76%) with ceramic tiles. Construction dates range from 1955 to 1988. 50% are URM buildings and the rest have RC frames. 70% have no structural joints.

SUMARY

3.2.2.2.c. Large

Number of buildings: 17.
Description: these buildings are the largest (up to 93 m). Their average smallest dimension is 19 m. They are all two storeys high and the average built area is 2 300 m². 47% of the buildings have atriums and setbacks of the slab. They present sloping (70%) and flat roofs (30%). Construction dates range from 1960 to 2010. All the buildings have RC frames and structural joints.

Figure 20. Volumetric classification. School S039. Building: 1. Type: linear. Sub-type: large.

3.2.2.2.d. L-shape

Number of buildings: 18.
Description: they are characterised by an L shaped floor plan. They have two orthogonal arms whose average dimensions are 57 × 25 m. At the intersection of both arms, the vertical communication nuclei are arranged. 66% of the buildings are single-storey, with the rest having two and three floors. They have irregularities such as atriums or recesses of the edges of the slab. They have sloping (50%) and flat roofs (50%). Construction dates range from 1955 to 2005. 77% is made of RC frames with structural joints, the rest are URM buildings.

Figure 21. Volumetric classification. School S057. Building: 1. Type: linear. Subtype: L-shape.

SUMARY

3.2.2.2.e. Various

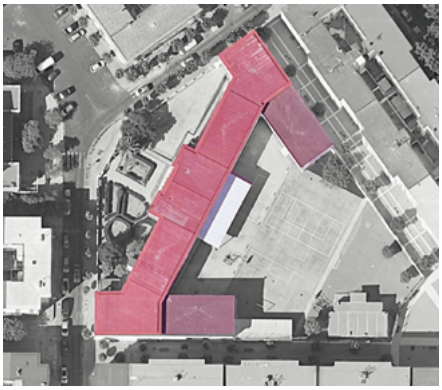

Figure 22. Volumetric classification. School S067. Building: 1. Type: linear. Subtype: various.

Number of buildings: 10.
Description: these buildings have more than two orthogonal arms up to 100 m long and 30 m wide. They have two floors and their built area range between 1 600 and 4 700 m². They have entrance atriums to the building, but they do not have setbacks of the edge of the slab. 60% has a flat roof with flooring and the rest present sloped roofs with ceramic tiles for finishing. Construction dates range from 1954 to 2009. All have RC frames with structural joints.

3.2.2.3. Intersection buildings

Intersection buildings are irregular compared to the other two types mentioned above. 86% of the buildings have RC frames and 11% are URM buildings. They have several volumes that intersect in various ways according to the following subtypes.

3.2.2.3.a. Volumes

Figure 23. Volumetric classification. School S112. Building: 1. Type: intersection. Subtype: volumes.

Number of buildings: 18.
Description: these buildings have several different volumes, but they have normally straight angles, which makes the floor plans regular. These are heterogeneous buildings compared to the two previous groups, which in 40% of cases present irregularities such as porches, atriums or setbacks of the edge of the slab. They have more variable dimensions, ranging from 30-94 m long, 15-58 m wide and 390-3 240 m² of built area. They have up to three floors, but 60% of the buildings have two. They have a

SUMARY

sloping or flat roof at 60 and 40%, respectively. Construction dates range between 1960 and 2012. Most of them present RC frames, with structural joints in 55% of the cases.

3.2.2.3.b. Irregular

Number of buildings: 9.
Description: these are the most irregular buildings in terms of floor plan and elevation. They are composed of several blocks that intersect each other at angles other than 90º. The average built area is between 130 and 3 300 m². 80% are two storeys high. Their length varies between 30-90 m and the width between 17-50 m. They present irregularities and sloping roofs with ceramic tiles or flat roofs with flooring in 50% of the cases. Their structural system is of RC frames with structural joints, and they were built between the years 1974 and 2007.

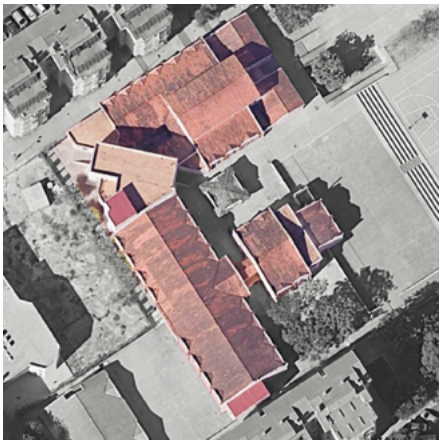

Figure 24. Volumetric classification. School S071. Building: 1. Type: intersection. Subtype: irregular.

3.2.2.3.c. Merged

Number of buildings: 8.
Description: these are buildings formed from the merging of two equal volumes. They are small buildings with an average built area of 714 m² and in 63% of cases, they are two storeys high. 88% of the buildings have reinforced concrete frames and no structural joints. They have irregularities and a gable roof with ceramic tiles.

Figure 25. Volumetric classification. School S109. Building: 1. Type: intersection. Sub-type: merged.

SUMARY

3.2.2.3.d. E-shape

Figure 26. Volumetric classification. School S058. Building: 1. Type: intersection. Subtype: E-shape.

Number of buildings: 6.
Description: this subtype is characterised by an "E"-shaped floor plan. They have a main block to which three other linear blocks are attached. 60% of them are URM structures. The rest have RC frames with structural joints. Their length varies between 30 and 70 m and the width between 20 and 50 m. The number of floors is up to 3 in some buildings with load-bearing walls. The average value of the built area is 1667 m^2. They have irregularities and a sloping roof with ceramic tiles.

3.2.2.3.e. Nexus

Figure 27. Volumetric classification. School S117. Building: 1. Type: intersection. Subtype: nexus.

Number of buildings: 5.
Description: these are buildings made of several equal blocks joined by other smaller volumes. This generates irregularities in the floor plan, with setbacks in the floor slabs. They are large buildings, with an average built area of 620 m^2, two floors, irregularities and a sloping roof with ceramic tiles. Their length varies between 20 and 50 m and the width between 20 and 25 m. They were built between 1970 and 1988 with RC frames (80%) or a steel structure (the rest) and have structural joints.

SUMARY

3.2.2.3.f. Multiple

Number of buildings: 4.
Description: this is the same prototype of a symmetrical building, with a floor plan with several protrusions and entrances, all orthogonal, and with courtyards and irregularities such as atriums and porches for access to the building. All buildings present RC frames systems with structural joints and two floors. The average built area is 3 600 m² distributed over two floors. The largest dimension is 60 m and the smallest is 30 m. They have a sloping roof with ceramic tiles. They were built between 1968 and 1983.

Figure 28. Volumetric classification. School S108. Building: 1. Type: intersection. Subtype: multiple.

3.2.2.3.g. Blade-shape

Number of buildings: 2.
Description: these buildings are identical to each other and have been identified as a prototype. Their main feature is their blade-shaped floor plan. They present RC frames with several structural blocks and two floors. Their built area is 3 000 m² with arms 40 m long and 20 m wide. They have an atrium and a flat roof with a gravel finish. They were built between 1969 and 1977.

Figure 29. Volumetric classification. School S077. Building: 1. Type: intersection. Subtype: blade-shape.

SUMARY

3.2.2.4. Prism buildings

Figure 30. Volumetric classification. School S013. Building: 1. Type: prism.

Number of buildings: 15.
Description: they represent an identical prototype made of a rectangular block which in 46% of the cases has a small annexed building (and which belongs, in most cases, to the compact buildings group). The prototype is built with RC frames and has structural joints. Construction dates range between 1970 and 1989. The average built area is 1 477 m² and their dimensions vary between 25 and 50 m long and 17 and 20 m wide. They are two storeys high and have irregularities such as atriums or setbacks of the slab. They have a sloping roof with ceramic tiles.

3.2.2.5. Juxtaposed buildings

Figure 31. Volumetric classification. School S020. Type: juxtaposed.

Number of buildings: 6.
Description: they serve as a link between buildings belonging to other groups and which have been built recently: from 1990 to 2011. They have flat roofs with gravel or flooring as finishing materials and their dimensions are not very large: 400 m² of average built area, 22 m long and 15 m wide. They have no irregularities and were built with reinforced concrete frames without structural joints.

SUMARY

3.2.3. Sports facilites

Number of buildings: 9.
Description: these are buildings for sports use built mostly (66%) with a steel structure with trusses and finished with metal panels. The dates of construction are recent, from 2004 to 2012. They have one floor and their built area varies from 550 m² to 1 200 m².

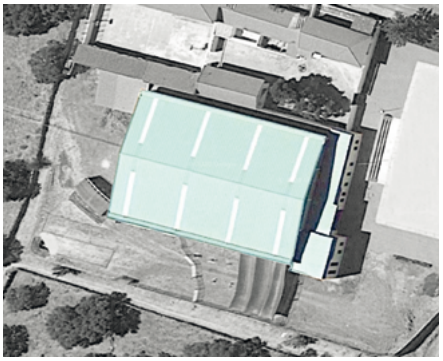

Figure 32. Volumetric classification. School S025. Type: sports facility.

3.3. CHARACTERISATION OF MASONRY BUILDINGS

In total, 35 URM buildings have been identified. These correspond to 13% of the total of those considered in the project. 45% of them are main school buildings (access or main use), while 37% are secondary buildings. 82% of them are classroom buildings, while the use of the remaining percentage could not be identified. From the questionnaires sent to the schools, information could be obtained regarding the level of deterioration of the buildings in 31% of the cases: low (8%), medium (5%) and high (17%). The year of construction of these buildings ranges from the 1940s to the 1990s. However, most of them were built during the 1950s (see figure 11). The technical information contained in the buildings project documentation found is generally very brief. However, it has been possible to identify a number of common building characteristics that have been summarised in table 15.

Eighteen single-storey and sixteen double-storey buildings have been identified. The dimensions of the single-storey buildings range from 15 to 45 m long and 6 to 25 m wide. The construction area varies between 120 and 1 500 m², the average value being 430 m². As for the two-storey buildings, dimensions vary between 22 to 85 m long and 15 to 35 m wide. The construction area of these buildings ranges from 450 to 2 900 m², with an average value of 1 200 m². Single-storey buildings account for 63% of all cases. 74% of the buildings have entrance atriums. This generates an irregularity in floor plan and volume. In the case of the two-storey buildings, no information could be obtained for 37% of them, so no indicative conclusions can be drawn.

SUMARY

Table 15. Common characteristics of URM buildings.

Walls	Type	Unreinforced masonry, heavy-duty brick
	Material	Perforated ceramic brick. 1 cm thick cement mortar bed and head joints
	Thickness	Varies from 25 to 40 cm (figure 33)
	Bonding	The walls are bonded together, so there are no problems in their connections
Slabs	Operation	One-way
	Thickness	Varies from 25 to 30 cm (figure 34)
	Materials	Ceramic vaults and reinforced or prestressed beams with a compression layer
	Type	Sanitary slab on the ground floor: prestressed beams and ceramic vaults. Slab type in the other floors: reinforced beams and ceramic vaults
	Other aspects	Rigid diaphragm behaviour Flat crest beams 20 to 30 cm wide
Roof	Shape	Mainly sloping roof
	Material	Ceramic tile
Geometry	Spans	Between 4 m and 7.2 m
	Number of floors	One to two floors
	Height of the floors	Height of the ground floor: between 0.55 m and 1 m, due to the presence of the sanitary floor slab. Typical floor height: between 3 m and 3.30 m
	Structural joints	No, one single structural block
	Wall openings ratio	Due to their function, they have large openings in their walls

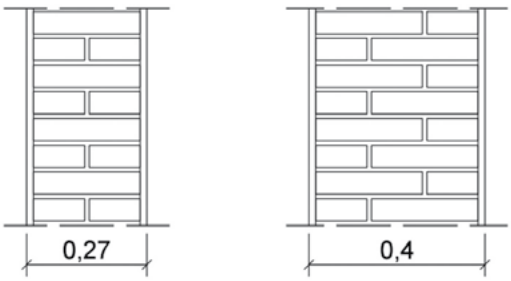

(a) (b)

Figure 33. "Un pie" (a) and "un pie y medio" (b) masonry wall section.

SUMARY

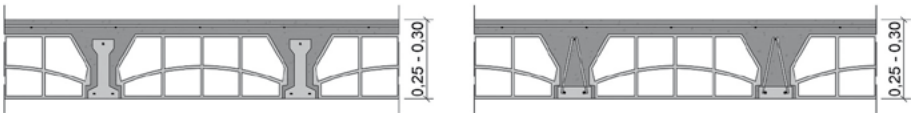

(a) (b)

Figure 34. Sanitary one-way slab (a) and (b) typical section.

As for the type of roof, 32 buildings were built with a sloping roof. 30 buildings are made of ceramic tiles and two are made of metal panels. In addition, three of the buildings were built with a flat roof. The finishing materials are gravel, in two cases, and flooring, in one case.

Due to their teaching function, the classrooms are typically y accessed through a corridor that runs parallel to the main façade of the building. In these cases, it is also common for the wall separating the corridor from the classrooms to be load-bearing. Also, the partitions separating classrooms from each other, usually perpendicular to the longest direction of the building, are usually blind. Furthermore, because of their function, façades tends to have a high percentage of openings in the walls. This significantly affect the seismic response of the structure, causing a concentration of shear stresses and deformations. This effect has been shown to lessen in the presence of load-bearing internal walls. In these cases, the load path will involve these internal load-bearing walls and the role of the façade becomes less relevant. For this reason, it is vital to take these walls into account in seismic assessment, verifying whether they are indeed load-bearing walls or simply interior partitions.

The first regulation concerning the construction of resistant brick masonry walls in Spain was the MV-201 (Ministerio de la Vivienda de España, 1972) published in 1972. These regulations were not very restrictive and, in most cases, were not considered by the designers during the design and construction of the buildings (Andrade, 1993). The minimum strengths established for the construction materials were 100 kg/cm^2 for bricks and 5 kg/cm^2 for mortar, M-5 according to the Spanish designation. A minimum type of cement to be used was also indicated: P-250 (Portland cement with a compressive strength of 250 kp/cm^2). The dimensions of the bricks, as well as the area and position of the gaps, were also limited. In the case of perforated bricks, the dimensions were 24 × 11,5 × 5,3 with a gap area of less than 2,5 cm^2. In addition, a 60 m separation between structural joints was established for oceanic climates. The characteristic factory-produced compressive strength was limited by the strength of the brick, the plasticity of the mortar and the thickness of the joints. For the calculation, a masonry resistance reduction coefficient of 2,5 was indicated.

SUMARY

The next standard was NBE FL-90 (Ministerio de Obras Públicas Trasnportes y Medio Ambiente, 1990) published in 1990. This was more of a revision of the previous regulations, improving the quality control requirements, but it did not introduce new requirements (Andrade, 1993).

In the present book, the mechanical properties of the brick masonry were obtained from the analysis of the applicable regulations, bibliography and available project documentation. The characteristic masonry compressive strength (f_k) has been determined from the ratio set out in Eurocode 6 (EC6) (AENOR, 2013).

$$f_k = K_f \cdot f_b^{\alpha} \cdot f_m^{\beta} \qquad \text{Eq. (4)}$$

The compressive strength of the brick (f_b) has been determined from the regulations applicable in the year of construction. In the project documentation, a brick strength of 15 N/mm² has been identified in all cases. However, the MV-201 standard establishes a minimum value of 10 N/mm², which must be considered in the vulnerability analysis. The mortar strength (f_m) established in the available documentation is 4 N/mm². However, the minimum value is 5 N/mm² according to MV-201. K_f is a constant that depends on the type of brick and mortar determined. In the EC6, values of 0,65 and 0,25 are established for α and β respectively.

The masonry deformation modulus is another parameter involved in the analysis of the seismic behaviour of URM buildings. The ratio of the EC6 is used for recent buildings. However, the deformation modules obtained from this ratio are excessive for older buildings built during the 1970s and 1980s (Martínez *et al.*, 2001). Therefore, the relationship recommended in the French UIC Code 778-3 has been used (Martín-Caro Álamo, 2001). This method is more conservative and realistic, and depends on the elastic modulus of the brick (E_b).

$$E = 0.35 \cdot E_b \cdot f_m^{\beta} \qquad \text{Eq. (5)}$$

In the French code, the E_b determined for a medium-hard brick is 10 000 MPa. Furthermore, this value is similar to the values set in the Italian reference code NTC 2008 (NTC 2008. Decreto Ministeriale 14/1/2008. Norme tecniche per le costruzioni. Ministry of Infrastructures and Transportations. G.U. S.O. n.30 on 4/2/2008; 2008 [in Italian]., n.d.). Therefore, the values determined in the masonry resistance calculation are those set out in table 16.

SUMARY

Table 16. Mechanical parameters of the brick masonry.

Structural parameter	Minimum value	Maximum value	Most likely value
Brick compressive strength (f_b)	10	30	15
Mortar compressive strength (f_m)	5	16	4
Constant K	0,40	0,55	0,45
Masonry compressive strength (f_k)	2,52	7,71	5 MPa
Shear strength (t_0)	—	—	0,24 MPa
Deformation modulus (E)	2800	3500	3500 MPa
Shear modulus (G)	—	—	875 MPa
Density (W)	—	—	18 kN/m^3

In table 17, buildings have been classified according to their characteristics. Parameters such as number of floors, dimensions, built area or presence of irregularities have been taken into account.

Buildings in the same group or subtype present similar seismic behaviour, sharing the main deficiencies, so analogous interventiones may be carried out. The characteristics of each subtype are the following:

- Small linear: one-storey buildings of rectangular proportions with a built area of less than 600 m^2 and a maximum length of 37 m. They have a sloping roof with ceramic tiles. The vulnerability of these buildings is not expected to be among the highest in the group of URM buildings. The percentage of openings is low-medium in the major direction and very low-low in the minor direction.
- Medium linear: buildings of rectangular proportion, but of greater dimensions, up to 85 m long, two storeys high and a maximum built area of 1570 m^2. The type of roofing is still mostly sloping with ceramic tiles. Generally, these buildings are more vulnerable than the previous group. The percentage of openings is medium-high and very low in the major and minor directions, respectively.
- L-shaped linear: the irregularity in the plan of this type of building makes it more vulnerable to earthquakes due to torsional effects. Buildings are comparable to two medium or small linear buildings combined. However, since they do not have structural joints, they work together. The percentage of openings is very high and medium-high in the major and minor directions, respectively.

SUMARY

Table 17. Classification of the types of vulnerability for buildings with load-bearing walls.

Type		Linear			Compact	Intersection
Subtype		Small	Medium	L-shape	No courtyards	E-shape
No. of floors	1 floor (1F)	9	1	1	5	2
	2 floor (2F)	1	6	2	4	4
Dimensions	Length (m)	20-37	25-85	44-76	16-26 (1F) 22-36 (2F)	34-43 (1F) 33-47 (2F)
	Width (m)	6-25	15-35	17-56	7-24 (1F) 13-26 (2F)	20-30 (1F) 21-27 (2F)
Built area (m^2)		125-610	500-1 570	795 (1F) 2 900 (2F)	120-624 (1F) 450-1 200 (2F)	400-900 (1F) 1 260-1 400 (2F)
Date of construction		1950-1994	1955-1970	1955-1969	1955-1986	1955-1980
Atrium	Yes, in the middle	3	1	1	1	2
	No	1	2	1	4	1
	No data	6	4	1	4	3
Type of roof	Inclined	10	5	2	9	6
	Flat	—	2	1	—	—
Roof finish	Ceramic tile	10	5	2	7	6
	Metal panels	—	1	—	2	—
	Gravel	—	—	1	—	—
	Flooring	—	1	—	—	—
% openings (n° of buildings)	In X	Medium (4) Low (3)	High (3) Medium (2) Low (1)	Very high (3)	High (2) Medium (1) Low (1) Very low (2)	Medium (1) Low (2)
	In Y	Medium (1) Low (2) Very low (5)	Low (1) Very low (4)	High (1) Medium (1) Low (1)	Low (2) Very low (5)	Medium (1) Low (3)

SUMARY

— Compact without courtyards: one floor buildings in this category can be compared with small linear ones, and those with two floors with medium linear buildings. However, their higher regularity and square shape makes them less vulnerable. Single-storey buildings have less than 625 m^2 of floor space and are 26 m long. The two-storey buildings are up to 1 200 m^2 in area and 36 m long. All have a sloping roof with ceramic tiles. The percentage of openings is low - very low in the minor direction, and variable in the major.

— E-shaped intersection: these buildings have a comb-shaped floor plan with similar dimensions, both in length (up to 47 m) and width (up to 30 m), regardless of the number of floors. They all have a sloping roof with ceramic tiles. Their shape accentuates their vulnerability. The opening ratio is low-medium in both directions.

3.4. CHARACTERISATION OF REINFORCED CONCRETE FRAME BUILDINGS

In total, 222 RC frame school buildings have been identified. The analysis of the configuration of the buildings leads to the following conclusions.

3.4.1. Date of construction and regulations

The date of construction of these buildings varies between the 1950s and the present day, with the vast majority being built during the 70s and 80s. The structural and construction requirements of reinforced concrete buildings in Spain have evolved considerably over time. These changes have been reflected in table 18.

Table 19 collects the values obtained from the mechanical properties of the RC identified in the documentation. It is important to note that no design information is available for several buildings in this group. Therefore, in the evaluation of its seismic response and vulnerability, the values necessary for the calculation established in the regulations have been considered according to its date of construction.

SUMARY

Table 18. Evolution of mechanical properties and construction criteria for reinforced concrete buildings according to regulations.

	Regulations	EH-68	EH-73	EH-80	EH-88	EH-91	EH-98	EHE-08
	Date	1968	1973	1980	1988	1991	1998	2008
Concrete	f_{ckmin} (N/mm^2)	12	12,5	15	15	15	20	25
Concrete	E (N/mm^2)	No	No	$\sqrt{1900 f_{ck}}$	$\sqrt{1900 f_{ck}}$	$\sqrt{1900 f_{ck}}$	$\sqrt[3]{1000 f_{cm}}$	$\sqrt[3]{8500 f_{cm}}$
Steel	f_y (N/mm^2)	230	220	410 (CS-400)	410 (CS-400)	410 (CS-400)	400 (B400S)	400 (B400S)
Steel	Diameter (Φ_{min}) (mm)	5	6	4	No	4	6	6
Steel	Types bars	Smooth	Smooth and corrugated	Smooth and corrugated	Smooth and corrugated	Smooth and corrugated	Corrugated	Corrugated
Steel	Provision	No	No	On hanger	On hanger	On hanger	On hanger	On hanger
Others	Actions	No	No	Yes	Yes	Yes	Yes	Yes
Others	Coat.	No	No	No	Yes	Yes	Yes	Yes
Others	Coefficient security S: steel C: concrete	No	No	S: 1,15 C: 1,5	S: 1,15 C: 1,5	S: 1,15 C: 1,5	S: 1,15 C: 1,5	S: 1,15 C: 1,5

Table 19. Mechanical properties of reinforced concrete buildings according to available design documentation.

Parameter	Units	Concrete (RC-175)	Steel (CS-400)
Weight by volume (W/V)	kN/m^3	24,51	76,47
Strain modulus (E_c)	kN/m^2	According to regulation	210
Poisson's ratio (U)		0,2	0,3
Coef. Thermal expansion (A)	1/C	10E-05	1,2E-05
Concrete strength (f'_c)	MPa	17,5	
Elastic limit (F_y)	kN/m^2		420
Minimum tensile strength (F_u)	kN/m^2		Fy · 1,10

SUMARY

3.4.2. Area and height

The floor area of these buildings varies between 125 m² and 4700 m². 56% (125) have two floors, and the rest (80) have only one. The latter are the buildings with the smallest built area. Only 20 buildings are three storeys high, with an area between 2000 and 3000 m². Of these, 13 are H shaped and share common characteristics.

A large number of the buildings have a sanitary slab. This rises above the ground, from 0,35 m to 0,8 m, resulting in short columns. This is one of the typical seismic vulnerabilities in RC frame buildings. The shear forces concentrate on these short columns, worsening the seismic behaviour of the building. The height of a standard storey ranges from 3 m to 3,45 m.

3.4.3. Slabs

The slab of virtually all the buildings observed is one-way, with some (few) cases with a two-way or reticular slab. These are used to support higher spans. In both cases, and given the construction techniques used, these slabs can be considered as a rigid diaphragm for calculation purposes. The thickness of both types ranges from 0,25 to 0,3 m. The characteristics of the slabs are as follows (figure 35):

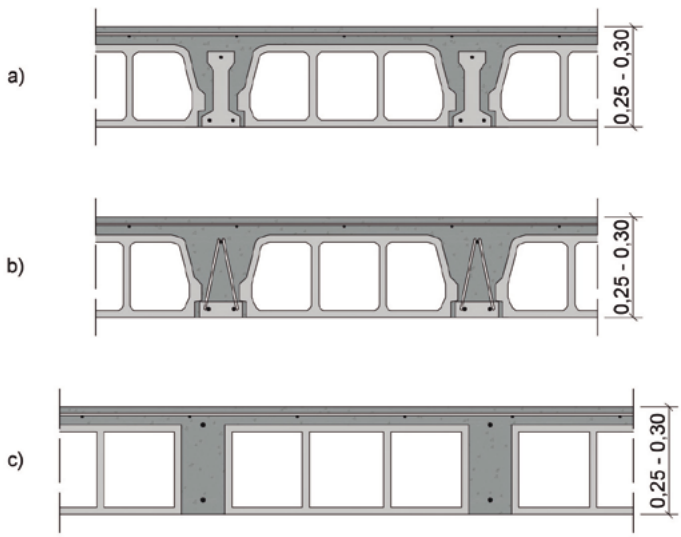

Figure 35. Sanitary (a), one-way (b) and two-way (c) slab typical section.

SUMARY

— Slabs in standard floors: one-way concrete slab with reinforced beams, ceramic or lightweight concrete vaults and compression layer in standard floors; or two-way with lost panels of lightweight or ceramic concrete.
— Sanitary slab on the ground floor: one-way concrete slab with prestressed beams, ceramic or lightweight concrete vaults and compression layer on the ground floor.

3.4.4. Colums and beams

In all cases, the structures lack bracing systems or diaphragm walls, so the horizontal load path relies on the capacity of the nodes between beams and columns to transmit the shear forces and moments.

Buildings with one-way slabs were constructed either with flat or edge beams. It has been found that the dimensions of these beams vary considerably, even when being of the same type. In the case of tying frames, the beams are normally flat and equal in width to the column. In the case of the columns, the dimensions are practically identical in all the buildings analysed. They only vary in size and become rectangular when the spans between columns are greater than 7 m or when the buildings are more than two storeys high. Table 20 shows the main characteristics of columns and beams.

Table 20. Characteristics of the columns and beams of RC buildings.

		Columns	Flat beams	Edge beams	Tie beams	Bar position
Dimensions	Min Max	25×25 cm 30×45 cm	25×25 cm 80×30 cm	25×40 cm 30×60 cm	25×25 cm 30×30 cm	
Longitudinal reinforcement	Min Max	4Ø12 mm 8Ø16 mm	2Ø12 mm 5Ø16 mm	2Ø12 mm 4Ø16 mm	2Ø12 mm 2Ø16 mm	Higher
	Min Max		4Ø12 mm 5Ø20 mm	2Ø12 mm 5Ø20 mm	2Ø12 mm 3Ø16 mm	Lower
Transverse reinforcement	Min Max	Ø6 mm/30 cm Ø8 mm/15 cm	Ø6 mm/30 cm Ø8 mm/15 cm	Ø6 mm/30 cm Ø6 mm/15 cm	Ø6 mm/30 cm Ø6 mm/15 cm	

In addition, it is important to note that many of these buildings were built before the seismic regulations came into force. This means that the details of the beam-column connections may not be enough to consider the frames as rigid, leaving the building without enough resistance to lateral loads.

SUMARY

3.4.5. Infill walls

The infill walls of these buildings are generally composed of a perforated ceramic half-brick wall (11,5 cm), an air chamber (4-5 cm), a simple hollow ceramic brick partition (5 cm) and their respective interior and exterior finishes (figure 36). The total thickness is about 24,5 cm. However, it should be noted that different configurations have been detected. The outer leaf can also be made of ½ foot of solid or perforated ceramic brick or double hollow ceramic brick with water-repellent cement mortar rendering on both sides. The cavity generally has 4-5 cm thick fibreglass thermal insulation. The inner leaf can also be made of a double hollow ceramic brick or glass-type partition.

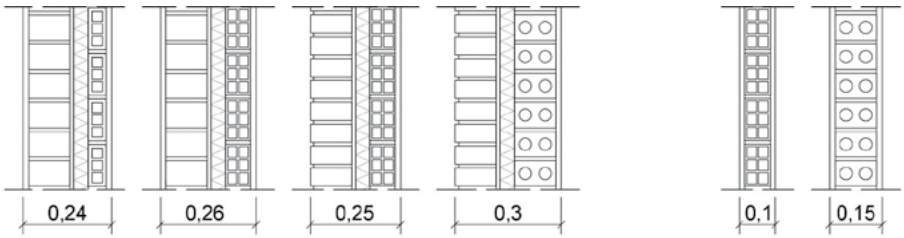

Figure 36. External (a) and internal (b) infill wall typical sections.

Infill walls are not load-bearing and are not connected to the reinforced concrete structure, they just rest on it. In some cases, the half-brick wall can be face-on, but this does not affect the calculation of the seismic behaviour.

Infill walls have not been considered in the calculations. However, some specific situations may count as added vulnerabilities. In particular, when the enclosure does not reach the ceiling and gives rise to short columns, on the one hand; and the absence of external and/or partition infill walls on one of the floors, normally the ground floor, on the other. This second point can be considered as an irregularity in the height of the building. No further irregularities of this type have been observed, as all parts of these buildings are the same height (with the exception of a few isolated staircases).

SUMARY

3.4.6. Irregularities

The main shortcomings of these buildings are due to irregularities in floors and height. The presence of atriums on the ground floor, with no infill walls, gives rise to a sudden change in stiffness, with these infill walls existing on the upper floors. This atrium is not necessarily located along the entire length of the façade, nor in the centre of it, which gives rise to undesirable torsion in the building's seismic response. In addition, when a recessing of the enclosure is made on the ground floor, it generates isolated façade columns, sometimes higher than the other floors, which reinforces this change in stiffness, creating a soft floor.

3.4.7. Subtypes

In the group of RC buildings, several sub-groups can be found. Unlike buildings with load-bearing walls, these are characterised by the presence of expansion joints that cause them to be divided into different structural blocks. Each structural block will behave independently in the face of a seismic event, so the subsequent classification is of the structural blocks and not of the buildings. In some cases, the building consists of a single structural block (shown as adjacency I in the tables). In other cases, the analysed block corresponds to a part of a larger building (in the tables it is reflected as adjacency II).

Four main types are proposed, in which the blocks are grouped based on their expected seismic behaviour. These in turn are divided into several subtypes.

3.4.7.1. Square footprint

These buildings are characterised by their square floor plan and are divided into three subtypes according to their dimensions and number of floors. Table 21 shows the properties of the buildings in this group.

These buildings are mostly built from the 70s onwards. The number of floors ranges from 1 to 3 in equal percentage. It is important to note that the length to width ratio does not exceed 1,5. Finally, there is no correlation between the type of building and the roof.

SUMARY

Table 21. Properties of square floor plan RC buildings.

Type		Small simple		Small compound		Large (compound + courtyard)		
No. of floors		1	2	1	2	1	2	3
No. of buildings		23	30	12	33	11	30	26
Length (m)	Min	11,5	16	11	9	23	19,5	23,5
	Max	31	35	28	68	38	40	25,5
	Mean	19	35	21	24	32,5	28	24
Width (m)	Min	11	8,5	9	9	19	13,5	23,5
	Max	25	28	24	40	24	38	24
	Mean	14	20	18	16	21,5	24	24
Proportion		1,4	1,4	1,2	1,5	1,5	1,2	1,0
Date	By decade	>60	60 70 80	>60	>70	>70	>70	>70
Atrium	Yes	4	14	—	20	1	21	20
	No	7	7	3	7	3	2	4
	Unknown	12	9	9	6	7	7	2
Setback of the slab	Yes	1	3	—	7	1	2	2
	No	22	27	12	26	10	28	24
	Unknown	—	—	—	—	—	—	—
Type of roof	Sloped	11	21	8	27	7	20	26
	Flat	12	9	4	6	4	10	—
Roof finish	Ceramic tile	12	14	5	26	5	19	26
	Metal panels	1	8	3	1	2	1	—
	Gravel	5	6	2	2	—	3	—
	Flooring	7	2	2	4	4	7	—

3.4.7.2. Rectangular footprint

These buildings are characterised by their rectangular floor plan and are divided into four subtypes according to their dimensions, number of floors and adjacency. Table 22 shows the properties of the buildings in this group.

SUMARY

Table 22. Properties of the rectangular floor plan RC buildings.

Type		Small		Medium		Length	In L
Subtype	No. of floors	1	2	1	2	2	2
	Adjacency	I	II	I and II	I and II	I and II	I
No. of buildings		31	26	7	48	14	11
Length (m)	Min.	17	18	25	15	35	13,5
	Max.	50	42	42,3	72	92	93
	Mean	29	29	39	36	60	42
Width (m)	Min.	7	6	11	9	8,5	10
	Max.	26	29,5	16	40	18	30
	Mean	13	12	13,5	15	10	15,5
Proportion		2,2	2,4	2,9	2,4	6,2	—
Date	By decade	>70	60-90	>80	All	All	All
Atrium	Yes	4	17	3	20	4	5
	No	11	6	—	15	4	2
	Unknown	16	3	4	13	6	4
Setback of the slab	Yes	1	4	1	11	—	2
	No	30	22	6	37	14	9
	Unknown	—	—	—	—	—	—
Type of roof	Sloped	25	22	2	36	6	9
	Flat	6	4	5	12	8	2
Roof finish	Ceramic tile	17	22	2	36	6	9
	Metal panels	8	—	—	—	—	—
	Gravel	5	2	3	9	2	1
	Flooring	1	2	2	3	6	1

There is no correlation for some of the parameters researched, such as the date of construction or the existence of atriums. In the case of the proportion, however, it can be seen that proportion increases as the size of the block increases, becoming more elongated. *A priori*, this can be seen as an increase in vulnerability due to greater torsional effects. Furthermore, as the size of the block increases, the probability of having two storeys also increases, which is a further disadvantage in the face of seismic action. Most of these blocks have a sloping roof with ceramic tiles. This involves a large mass located at a high point in the building.

SUMARY

3.4.7.3. Intersection

In this group, buildings are made of various aggregate volumes, giving rise to a floor plan that reflects a certain regularity. The buildings are grouped according to the type of adjacency and the number of floors. Table 23 shows the main characteristics of these buildings.

Table 23. Properties of intersection RC buildings.

Type	Adjacency	I	I	II
No. of floors		2	1	2
No. of buildings		6	2	12
Length (m)	Min.	76	20	35
	Max.	20	30	35
	Mean	35	25	35
Width (m)	Min.	40	18	14
	Max.	20	20	28
	Mean	28	19	21
Proportion		1,3	1,3	1,7
Date	By decade	60 70 80 90 00		50 a 90
Atrium	Yes	5	—	2
	No	1	2	5
	Unknown	—	—	5
Setback of the slab	Yes	—	—	—
	No	6	2	12
	Unknown	—	—	—
Type of roof	Inclined	6	2	12
	Flat	—	—	—
Roof finish	Ceramic tile	6	2	12
	Metal panels	—	—	—
	Gravel	—	—	—
	Flooring	—	—	—

According to the data obtained, it can be concluded that there is a relationship between the number of floors and the size of the building: the more floors, the larger the building. In terms of the adjacency, type II buildings have a more rectangular proportion than type I buildings. Finally, these buildings have a flat roof with a ceramic tile finish.

SUMARY

3.4.7.4. Irregular

The last of the groups identified are the irregular buildings, formed from the aggregation of various volumes of different sizes. This makes the estimation of their seismic behaviour at a typology level more complex. Only 5 structural blocks have been included in this group. In table 24 their main characteristics are listed.

Table 24. Properties of irregular RC buildings.

Type	Adjacency	I	I
No. of floors		1	1
No. of buildings		2	3
Length (m)	Min.	32	50
	Max.	57	65
	Mean	45	57
Width (m)	Min.	24	51
	Max.	29	60
	Mean	27	45
Proportion		1,7	1,3
Date	By decade	90	80 00
Atrium	Yes	1	2
	No	1	1
	Unknown	—	—
Setback of the slab	Yes	—	—
	No	2	3
	Unknown	—	—
Type of roof	Sloped	1	1
	Flat	1	2
Roof finish	Ceramic tile	1	1
	Metal panels	—	—
	Gravel	—	1
	Flooring	1	1

Based on the data obtained, it can be concluded that the fundamental differences between these blocks are their dimensions and proportions. Other characteristics, such as date of construction, type of roof, irregularities and setbacks, are practically identical.

SUMARY

Chapter 4. Structural safety analysis

This section shows the structural safety analysis process, which will be applied in the software developed (Estêvão, 2019).

4.1. METHOD

For the analysis of the seismic vulnerability of the primary education schools, the seismic behaviour of the different types of schools has been analysed through the capacity - demand spectrum method (Freeman, 2004) (performance-based method). Due to the scale of the school buildings, this analysis is the most appropriate for this study.

The evaluation of the seismic safety of school buildings includes:

1. Obtaining and analysing the constructive and structural characteristics of the different school buildings. In addition, information is obtained on the various aspects that influence the building's seismic vulnerability (distance from the nearest fire station, accessibility for emergency teams, evacuation, etc.).
2. Non-linear static calculation to obtain the capacity curves in both directions of the buildings.
3. Determining the elastic response spectrum according to seismic regulations or attenuation laws.
4. Obtaining the performance point of each building, in the two orthogonal directions.
5. Evaluating seismic safety according to different damage limit states.

SUMARY

4.2. CAPACITY ANALYSIS

The vulnerability assessment is based on the capacity curves (figure 37), which graphically represent the non-linear relationship between the base shear and the displacement of the control node, which is generally located at the centre of masses of the top level. It is obtained through a non-linear static or push-over analysis in both directions of the building (X and Y). It consists on the application of an incremental horizontal load until the collapse of the structure is reached, which allows to determine the capacity of the building to resist the seismic action, considering the non-linear behaviour of the structure. The analysis can be carried out with different commercial software depending on the structural system and applying different load patterns. These load patterns are obtained by two methods according to EC8: a uniform pattern providing the mass of each degree of freedom (mass of each floor of the building); and a modal type pattern, which is proportional to the displacement produced by the vibration mode with the highest mass participation.

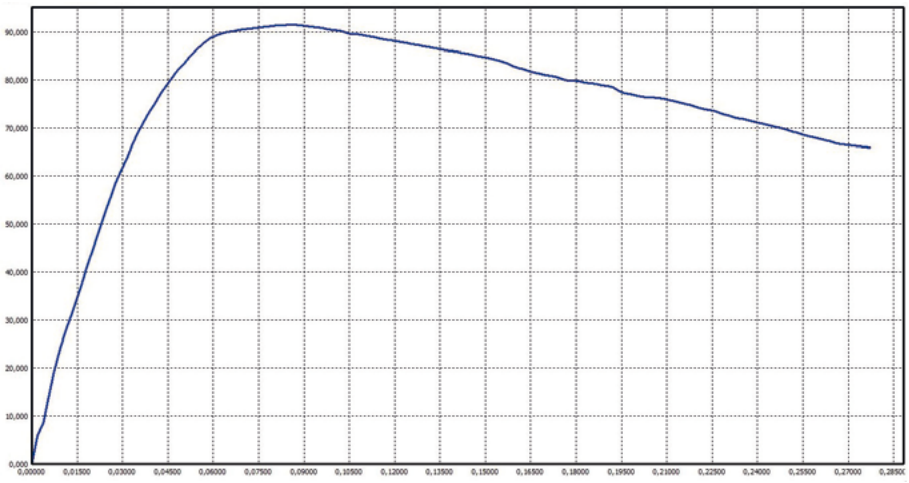

Figure 37. Capacity curve of a system equivalent to a system with multiple degrees of freedom. PERSISTAH Software.

According to the EC8, in order to obtain the capacity curves, the two lateral load patterns must be applied in both X and Y directions, as well as in the positive and negative directions. Accidental eccentricity of the centre of mass (three centres of mass in each direction) should also be considered. Applying all these rules, it is necessary to consider at least 24 capacity curves ($2 \times 2 \times 2 \times 3 = 24$).

SUMARY

The first thing to do in any non-linear static analysis method is to idealise a single degree of freedom (SDOF) system with a K* stiffness and a mass m* which is equivalent to the initial multi-degree of freedom (MDOF) system.

The transformation of the initial system (MDOF) is done through the equivalent mass (m^*) for SDOF and the transformation factor (Γ), according to Annex B of EC8 part 1.

$$m^* = \sum_{i=1}^{N} m_i \phi_i \qquad \text{Eq. (6)}$$

$$\Gamma = \frac{m^*}{\sum_{i=1}^{N} m_i \phi_i^2} \qquad \text{Eq. (7)}$$

Where ϕ_i and m_i are the displacement (configuration of the deformation adopted in the transformation process) and the standardised mass of each floor of the building, respectively (normally $\phi_i = 1$ on the control node).

The capacity curves of the MDOF system can be calculated through the use of any structural analysis software. This is done by applying a set of forces (Fi) Eq. (8) to the structure at each node of freedom (N). It is advisable that the sum of these forces be equal to the unit $\sum_{i=1}^{N} Fi = 1$.

$$Fi = \frac{m_i \phi_i}{m^*} \qquad \text{Eq. (8)}$$

The base shear V is given by the load parameter λ that is normally calculated by the computer program where the non-linear static analysis is executed.

$$V = \lambda \cdot \sum_{i=1}^{N} Fi = \lambda \qquad \text{Eq. (9)}$$

Once the capacity curves for the MDOF structural system are obtained, it is possible to compute them for an SDOF system. Displacement d^* and the equivalent force F^* in the equivalent SDOF system is given by the following functions, through the transformation factor (Γ) and where V is the base shear and d the displacement in the equivalent MDOF system.

$$d^* = \frac{d}{\Gamma} \qquad \text{Eq. (10)}$$

$$F^* = \frac{V}{\Gamma} \qquad \text{Eq. (11)}$$

SUMARY

4.3. PERFORMANCE POINT

The performance point (displacement vs. base shear), which represents the maximum response of the building, is obtained by the intersection of the capacity curve and the linear response spectrum, both in spectral coordinates.

The structural behaviour of each school has been analysed according to the N2 Method (Peter Fajfar, 2000), according to the iterative process proposed by Annex B of EC8 part 1 (AENOR, 2018a). The capacity-demand spectrum method of the ATC-40 standard (Applied Technology Council [ATC], 1996) was also used when considering an actual earthquake scenario (Estêvão, 2019). These routines have been successfully applied previously to evaluate the structural behaviour of buildings in the Algarve (Estêvão, 2016) and in the Azores (Estêvão and Carvalho, 2015), which are two Portuguese earthquake-prone regions.

4.3.1. N2 Method

The N2 method is presented in Annex B of EC8-1 with two possible approaches: an iterative and a non-iterative approach. Both approaches have been used in the analysis method implemented in the software developed for the seismic evaluation of school buildings. The iterative approach of the N2 method has been implemented in the software through the algorithm developed in (Estêvão, 2019; Estêvão, 2020).

To apply this method, the first thing to do is to obtain an elastic-perfectly plastic relationship between the forces (F^*) and the displacements (d^*) in the SDOF (figure 38) system. This ensures that the deformation energy of the equivalent system is the same as in the initial system.

The force corresponding to the elastic limit (F_y^*), which represents the ultimate strength of the equivalent SDOF system, is equal to the base shear in the formation of the plastic mechanism. Where the initial stiffness of the SDOF system has been determined by matching areas, so that the area covered by the MDOF and the bilinear (SDOF) capacity curve are equal. The other necessary parameter is the displacement corresponding to the elastic limit of the SDOF system, d_y^*, defined by the following function Eq. (12), where E_m^* is the deformation energy for the formation of the plastic mechanism (see Eq. [13]). This corresponds to the area under the capacity curve.

$$d_y^* = 2\left(d_m^* - \frac{E_m^*}{F_y^*}\right) \qquad \text{Eq. (12)}$$

SUMARY

$$E_m^* = \int_0^{d_{m^*}} F^* \cdot d(d^*) \qquad \text{Eq. (13)}$$

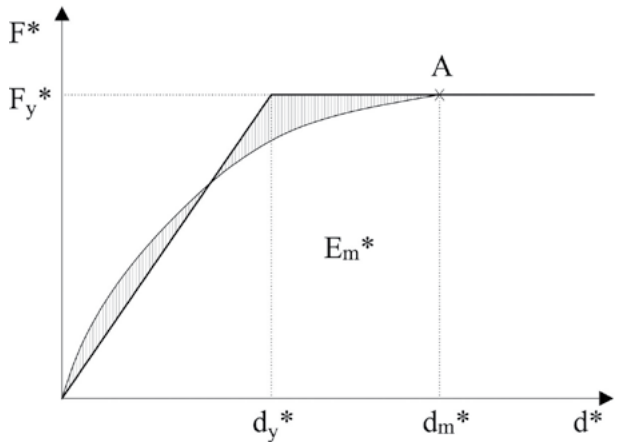

Figure 38. Bilinear capacity curve. SDOF equivalent system. Annex B: EC8, part 1.

The period of the structure for the SDOF system (T^*) has been calculated according to Annex B of EC8 part 1, using the following function:

$$T^* = 2\pi\sqrt{\frac{m^* d_y^*}{F_y^*}} \qquad \text{Eq. (14)}$$

4.3.1.1. Implementation in the PERSISTAH software

In the PERSISTAH software, the user can choose between the iterative and non-iterative approach. The iterative one (figure 39), is the most precise and, therefore, is the default method implemented in the software through the algorithm (figure 39) developed in (Estêvão, 2019; Estêvão, 2020). The different factors that define the bilinear curve, stiffness (k_m*), force (F_y*) and displacement (d_y*), are determined through the following algorithm:

SUMARY

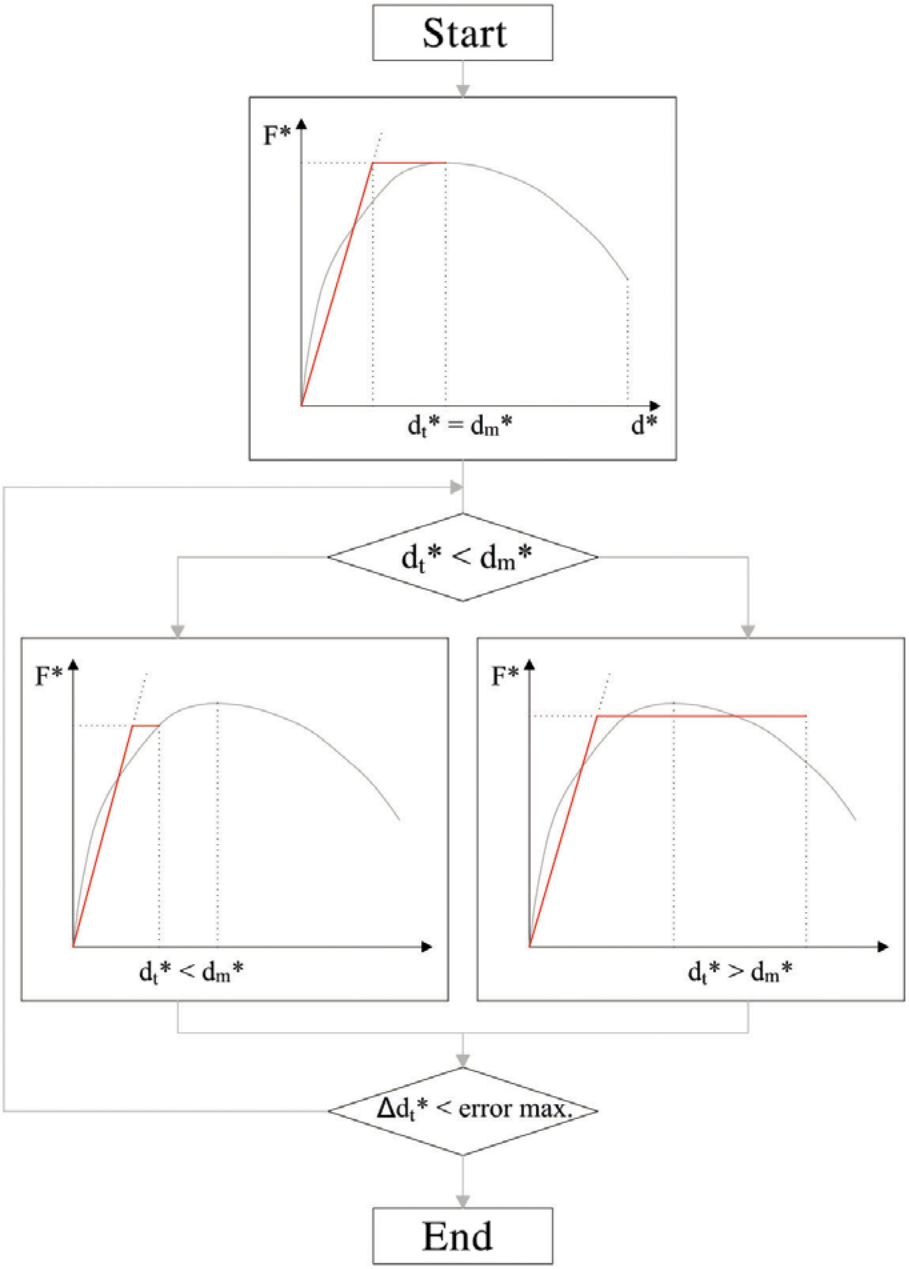

Figure 39. Diagram of the algorithm developed for the N2 iterative method (Estêvão, 2019).

Step 1: Determination of the area under the capacity curve E_m^* delimited by the limit point (d_m^*, F_m^*), which in this case coincides with the maximum

SUMARY

force of the capacity curve, and the stiffness (k_m*) of the elastic-perfectly plastic structural system, in this case the force F_y* is equal to F_m*, and d_t* = d_m* (figure 40):

$$k_m^* = \frac{F_m^*}{2 \cdot \left(d_m^* - \frac{E_m^*}{F_m^*} \right)} \qquad \text{Eq. (15)}$$

$$d_y^* = \frac{F_m^*}{k_m^*} \qquad \text{Eq. (16)}$$

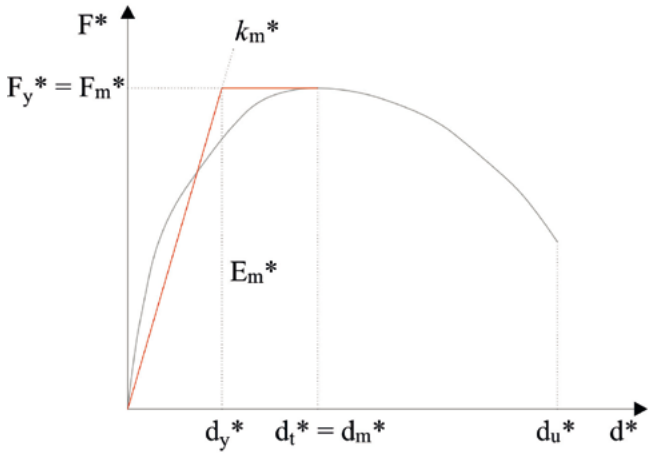

Figure 40. Capacity curve of the elastic-perfectly plastic structural system where dt* = dm*.

Step 2: Determination of the target displacement for the equivalent SDOF system. This displacement is calculated evaluating the elastic response spectrum at T* (period of the equivalent SDOF system).

$$d_{et}^* = S_e(T^*) \left[\frac{T^*}{2\pi} \right]^2 \qquad \text{Eq. (17)}$$

The target inelastic displacement (d_t*) is then determined with different equations for short period range structures ($T^* < T_C$) and for structures where the period range is medium and long ($T^* \geq T_C$).

SUMARY

Table 25. Equations for determining the target displacement. Annex B: EC8, part 1.

Short period range ($T^* < T_C$)		Medium and long period range ($T^* \geq T_C$)
If $\frac{F_y^*}{m^*} \geq S_e(T^*)$ elastic response	$d_t^* = d_{et}^*$	$d_t^* = d_{et}^*$
If $\frac{F_y^*}{m^*} < S_e(T^*)$ non-linear response	$d_t^* = \frac{d_{et}^*}{q_u}\left(1 + (q_u - 1)\frac{T_C}{T^*}\right) \geq d_{et}^*$	

$$q_u = \frac{m^* \cdot S_e(T^*)}{F_y^*} \qquad \text{Eq. (18)}$$

The relationship between the different magnitudes is shown in two spectral acceleration/displacement graphs below (figure 41). The period T^* is represented by the line linking the coordinates origin and the point of the elastic response spectrum with coordinates, d_{et}^* (SDOF elastic displacement) and $S_e(T^*)$.

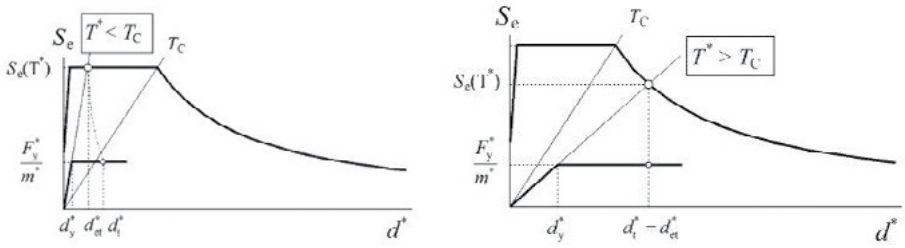

(a) (b)

Figure 41. Determination of the target displacement for an equivalent SDOF system for short periods (a) and long periods (b). Annex B: EC8, part 1.

Step 3: If the difference between the old performance point and the new one is greater than a given maximum error, then the E_t^* area under the capacity curve of the new target displacement d_t^* is calculated.

SUMARY

— If $d_t^* < d_m^*$ (figure 42), then:

$$d_y^* = 2 \cdot \left(d_t^* - \frac{E_t^*}{F_y^*} \right) \quad \text{Eq. (19)}$$

$$k_i^* = \frac{F_y^*}{d_y^*} \quad \text{Eq. (20)}$$

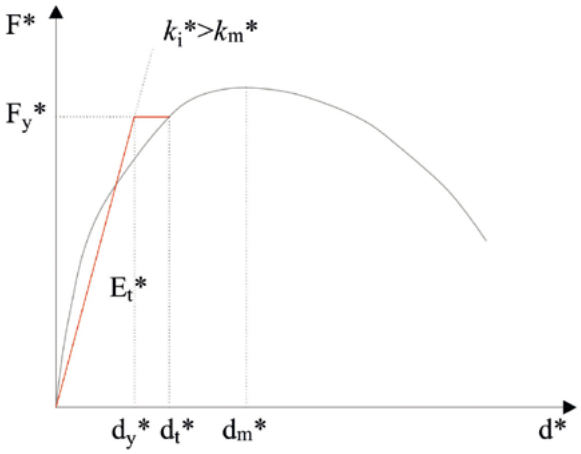

Figure 42. Capacity curve of the elastic-perfectly plastic structural system where $d_{ti}^* < dm$.

— If $d_{ti}^* > d_m^*$ (figure 43), then:

$$F_y^* = k_m^* \cdot \left[d_t^* - \sqrt{\frac{k_m^* \cdot (d_t^*)^2 - 2 \cdot E_t^*}{k_m^*}} \right] \quad \text{Eq. (21)}$$

$$d_y^* = \frac{F_y^*}{k_m^*} \quad \text{Eq. (22)}$$

SUMARY

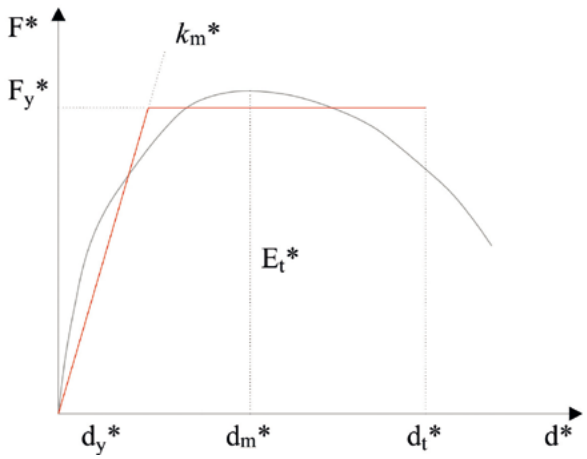

Figure 43. Capacity curve of the elastic-perfectly plastic structural system with $d_{ti}^* > dm$.

The calculation returns to the second step until convergence is reached.

Finally, when the convergence criterion is met, the target displacement (d_t) is determined for an equivalent MDOF system. This displacement corresponds to the control node and is defined by the following equation:

$$d_t = \Gamma d_t^* \qquad \text{Eq. (23)}$$

Where Γ is the transformation factor in Eq. (7).

An example of the output interface of the N2 method in the PERSISTAH software is shown below.

SUMARY

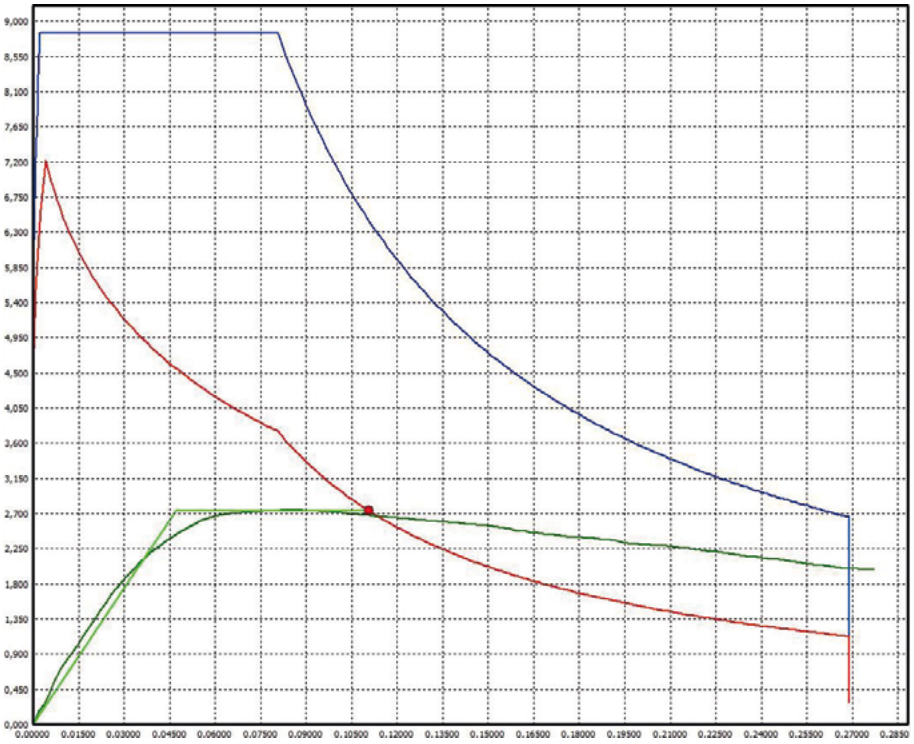

Figure 44. N2 method interface in the PERSISTAH software.

4.3.2. Capacity-demand spectrum method

This method proposed by the ATC-40 standard (Applied Technology Council [ATC], 1996) has also been implemented in the software. The iterative approach of this method is more complicated to apply than the N2 method. However, to implement it, an approach developed in (Estêvão, 2019) and based on the efficiency curve (figure 45) defined in section 4.4 has been used to simplify the process.

$$\%S_e = \frac{F^*_{t,D}}{m^*} \cdot \frac{100}{S_e(T^*_i, \xi_i)} \qquad \text{Eq. (24)}$$

Where $S_e(T^*_i, \xi_i)$ are obtained by the equations presented in section 2.3, and an equivalent damping ξ_i (in percentage) (figure 45). This can be obtained according to the ATC-40 standard (Eq. 25), assuming simplified hysteretic structural behaviour (grey area in figure 45).

SUMARY

$$\xi_i = 5 + k_\xi \frac{200}{\pi} \cdot \frac{F_y^* \cdot d_{t,D}^* - F_{t,D}^* \cdot d_y^*}{F_{t,D}^* \cdot d_{t,D}^*} \qquad \text{Eq. (25)}$$

To take into account the actual hysteresis cycles, the ATC-40 standard uses a modification factor k_ξ, which reduces the area in figure 45, defining the effective damping. This factor depends on the structural behaviour (type of material and structural details) and the duration of the earthquake. The three types of energy dissipation behaviour [A ($k_\xi = 1$), B ($k_\xi = 2/3$) and C ($k_\xi = 1/3$)] presented in the ATC-40 standard have been implemented in the PERSISTAH software.

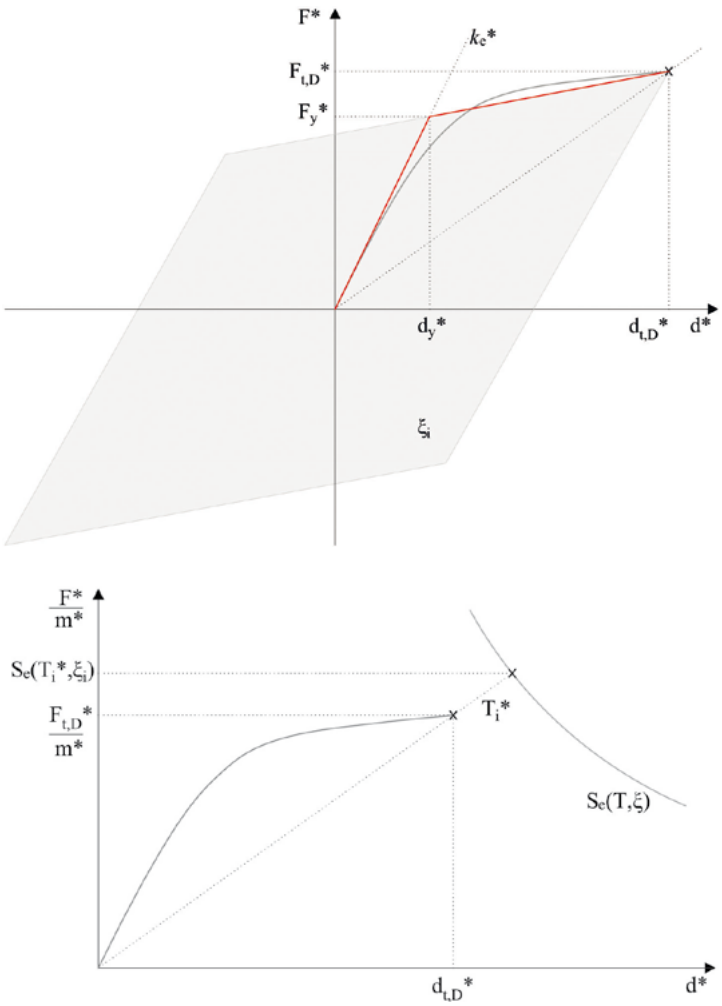

Figure 45. Diagrams of the capacity-demand spectrum method (Estêvão, 2019).

SUMARY

4.3.2.1. Implementation in the PERSISTAH software

For the implementation of the capacity-demand spectrum method in the software, the concept of the efficiency curve (Eq. 24) for the calculation of the c (target displacement) (Estêvão, 2019) has been used.

First, the interval where the performance point d_t^* ($\%S_{e,t} = 100$) is situated must be located. This range is limited by the points d_1^* ($\%S_{e,1} < 100$) and d_2^* ($\%S_{e,2} > 100$). These points are calculated by scanning the points on the efficiency curve (figure 46).

An iterative process is then applied until convergence is achieved with the desired error accuracy:

$$d_t^* = \frac{d_1^* + d_2^*}{2} \qquad \text{Eq. (26)}$$

If $\%S_{e,t} < 100$ then $d_1^* = d_t^*$; if $\%S_{e,t} > 100$ then $d_2^* = d_t^*$.

This iterative process is repeated until $d_2^* - d_1^*$ is less than the maximum error and $\%S_{e,t}$ is very close to 100%.

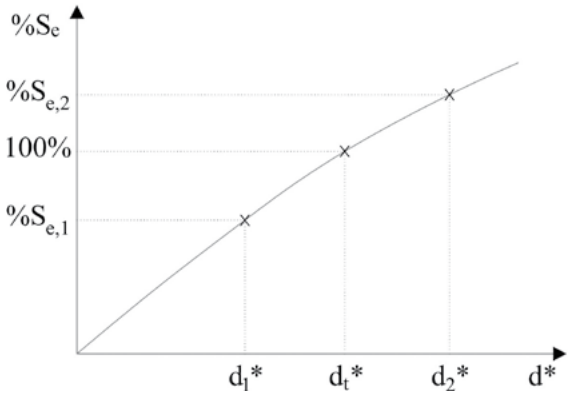

Figure 46. Iterative process of the capacity-demand spectrum (Estêvão, 2019).

4.4. STRUCTURAL DAMAGE ANALYSIS

The seismic safety assessment has been carried out according to the different damage limit states defined in Eurocode 8 part 3 (AENOR, 2018b). This code defines three damage states: near collapse (NC), significant damage (SD), and damage limitation (DL). In addition to this, in the present work, a limit state associated with operation (OP) has been added, as this damage limit will be considered in future European regulations. Seismic safety has been evaluated with

SUMARY

the damage limit SD (Sd3), which is defined below. In such a state of damage, repairing the structure is not cost-effective. EC3 part 3 presents the following definition of each of these damage limit states.

Near collapse (NC) state:

> The structure is seriously damaged, with low residual stiffness and lateral resistance, but the vertical elements are still capable of withstanding vertical loads. Most of the non-structural elements have collapsed. There are significant permanent relative displacements. The structure is near collapse and would probably not withstand another earthquake, even one of moderate intensity.

Significant damage (SD) state:

> The structure is significantly damaged, with some residual stiffness and lateral resistance, and the vertical elements are capable of withstanding vertical loads. The non-structural elements are damaged, although the partitions and fillings have not failed outside their mid-plane. There are moderate permanent relative displacements. The structure can withstand replicas of moderate intensity. Repairing the structure may not be cost-effective.

Damage limitation (DL) state:

> The structure is only slightly damaged, with structural elements that have not undergone significant plastification and maintain their strength and stiffness properties. Non-structural elements, such as partitions and fillings, may have widespread cracking, but their repair is economically viable. Permanent relative displacement is negligible. The structure does not need any repair measures.

The different damage limit states, represented as points in the bilinear capacity curve of each school building, have been obtained according to the displacement corresponding to the elastic limit (d_y) and the ultimate displacement (d_u), as proposed by the EC8-3. As an alternative, the damage limit states OP, DL, SD and NC, can be equal to S_{d1}, S_{d2}, S_{d3} and S_{d4}, respectively (Barbat *et al.*, 2008).

$$S_{d1} = 0.7 d_y \qquad \text{Eq. (27)}$$

$$S_{d2} = d_y \qquad \text{Eq. (28)}$$

$$S_{d3} = d_y + 0.25(d_y + d_u) \qquad \text{Eq. (29)}$$

$$S_{d4} = d_u \qquad \text{Eq. (30)}$$

SUMARY

In the PERSISTAH software, these damage limits are obtained from the bi-linear curve obtained for a single degree of freedom equivalent (SDOF) system, or they can be entered manually.

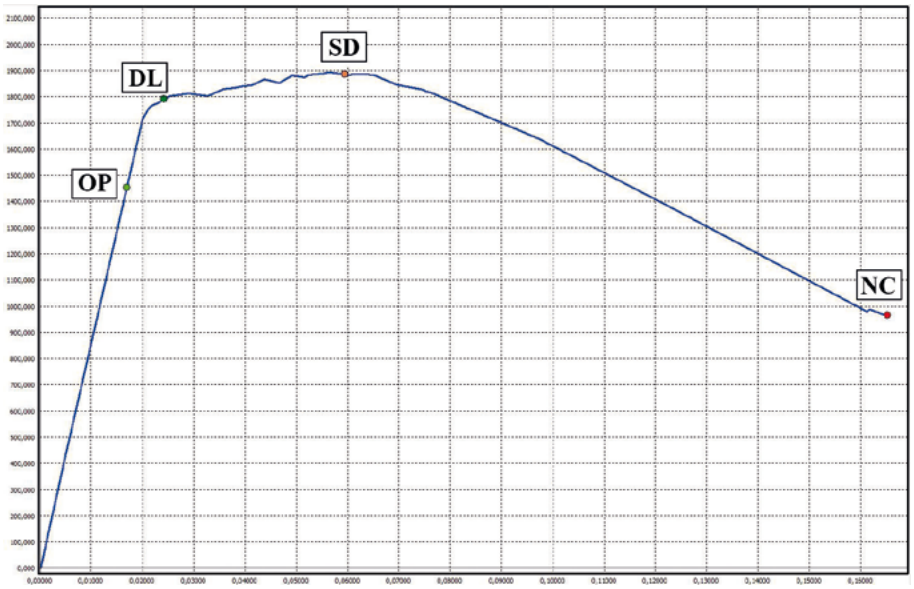

Figure 47. Capacity curve and damage limit states. PERSISTAH software.

Considering the limit states defined above, the school building damage assessment is made on the basis of the performance point (target displacement EC8-3). However, there is great difficulty in determining the damage levels presented in EC8-3, since each capacity curve presents different limit state values. For example, a capacity curve that presents high resistance can present a high level of damage or even collapse, if it has less ductility. In order to implement this method as easily as possible, a new concept, the performance curve, has been applied (Estêvão, 2019).

The efficiency curve represents the relationship between the displacement at the control node and the percentage given by the response spectrum with which the target displacement (performance point) is obtained. In short, this represents the performance points obtained by considering various percentages of the response spectrum. With this approach, the methods are reversed, i.e. the percentage of the spectral acceleration associated with a predefined displacement (damage limit state) is calculated.

SUMARY

The different percentages of spectral acceleration (%S_e) (response spectrum of EC8), corresponding to the displacements $d^*_{t,D}$ associated to a given damage limit state, are obtained from the following equations.

$$\%S_e = \frac{S_a^*}{S_e(T^*)} \cdot 100 \qquad \text{Eq. (31)}$$

— If $T^* \geq T_C$ (medium and long period range):

$$S_a^* = S_{ea}^* = d_{t,D}^* \cdot \left(\frac{2\pi}{T^*}\right)^2 \qquad \text{Eq. (32)}$$

— If $T^* < T_C$ (short period range):

$$S_a^* = \frac{1}{T_C}\left[\frac{4\pi^2 \cdot d_{t,D}^*}{T^*} + \frac{F_y^*(T_C - T^*)}{m^*}\right] \qquad \text{Eq. (33)}$$

If $F_y^*/m^* > S_a^*$, then $S_a^* = S_{ea}^*$.

With this, the efficiency curve is obtained (figure 48), which serves to obtain the most unfavourable capacity curve for a given damage limit state.

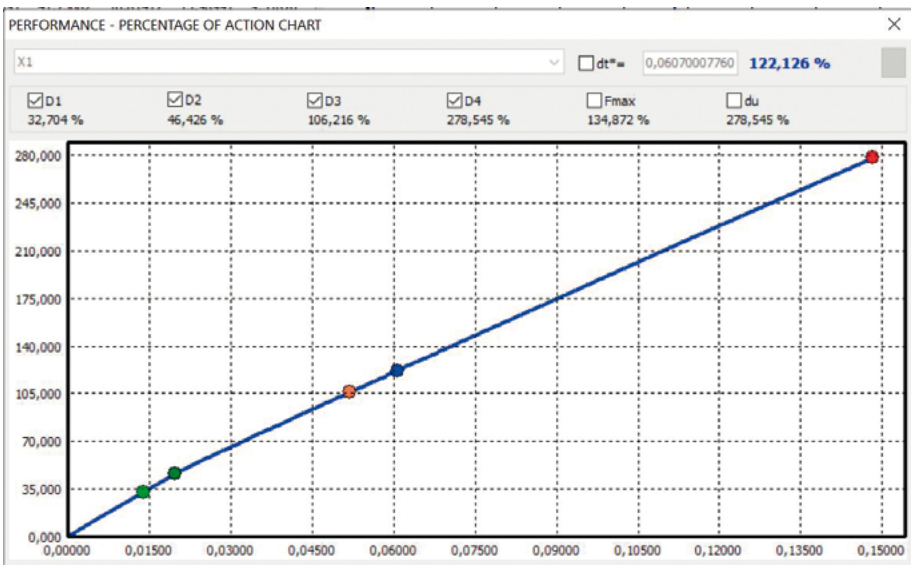

Figure 48. Efficiency curve. PERSISTAH software.

SUMARY

Once the different damage limit states have been defined, the software develops the fragility curves (figure 49). These curves define the probability that the expected overall damage of a structure will reach or exceed a certain specific damage limit state (Barbat *et al.*, 2008). These curves have been determined according to the lognormal RISK-EU probability distribution. Fragility curves can be calculated for each performance point (target displacement d_t) (Eq. 34). A curve is defined for each damage state, which is defined by plotting $P[D_i \mid d_t]$ (Estêvão, 2019).

$$P[D_i \mid d_t] = \Phi\left[\frac{1}{\beta_{Di}} ln\left(\frac{d_t}{d_{Di}}\right)\right] \qquad \text{Eq. (34)}$$

where **Φ** is the cumulative distribution function for the normal distribution, d_{Di} the mean displacement for a given damage state and β_{Di} the corresponding standard deviation of the logarithm of the displacement d_{Di}. This value β_{Di} can be defined by the user in the PERSISTAH software.

The probability of obtaining a given damage limit state (D_i), considering the different damage states defined above as OP = D1, DL = D2, SD = D3, NC = D4 and D5 = collapse is given by the following equations:

$$\rho_{D5} = P[D4 \mid d_t] \qquad \text{Eq. (35)}$$

$$\rho_{D4} = P[D3 \mid d_t] - P[D4 \mid d_t] \qquad \text{Eq. (36)}$$

$$\rho_{D3} = P[D2 \mid d_t] - P[D3 \mid d_t] \qquad \text{Eq. (37)}$$

$$\rho_{D2} = P[D1 \mid d_t] - P[D2 \mid d_t] \qquad \text{Eq. (38)}$$

$$\rho_{D1} = 1 - P[D1 \mid d_t] \qquad \text{Eq. (39)}$$

Fragility curves are defined by the relationship between a displacement and the probability of reaching a given limit state ρ_{Di}.

SUMARY

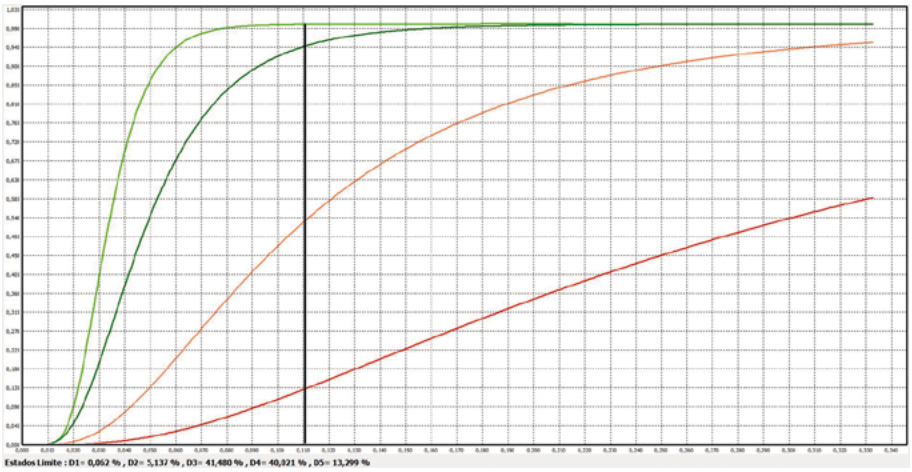

Figure 49. Fragility curves. PERSISTAH software.

Once the seismic evaluation of each school building has been carried out by applying the method developed (by obtaining of the performance point and with the evaluation of the damage limit states), the School-score is according to Eq. (40). This value will make it possible to classify school buildings according to their seismic risk (Estêvão, 2019).

$$School\text{ - }core = \frac{100}{\%S_e} \qquad \text{Eq. (40)}$$

SUMARY

Chapter 5. PERSISTAH Software

The PERSISTAH software (Estêvão, 2019; Estêvão, 2020) follows the Eurocode 08 part 1 and 3, considering the national annexes of Spain and Portugal (NP EN 1998-1: 2010 and NP EN 1998-3: 2017). First, using any structural analysis software and according to EC3-3, a set of capacity curves is obtained for each building. Then, the curves are fed into the PERSISTAH software, where the seismic analysis methods described in the previous section are applied to obtain the seismic safety of each building (performance point, fragility curves, damage analysis and school-score) school building (Estêvão, 2019).

This software can be used by the relevant authorities and civil protection bodies both in Spain and Portugal. It will be available on the research project website (<https://datalab.upo.es/persistah>) for public use and information. The software is easy and intuitive to use, and is available in three languages: Portuguese, Spanish and English. The collaboration between the various institutions, the University of the Algarve and the University of Seville, is essential for this software to be used in both countries.

The software has been developed for the management of seismic safety in schools. It is divided into three main modules: the first one, aimed at generating a geo-referenced database of the schools; the second one, for the selection of the seismic action to be considered for the evaluation of each school; and the third one, to determine the degree of damage and the School-score of each school building.

The IT strategy developed and applied in the program is relatively complex (Estêvão, 2020; Estêvão, 2019) and has been outlined in figure 50. It represents the diagram of the software operation, which consists of three different modules each with different routines.

SUMARY

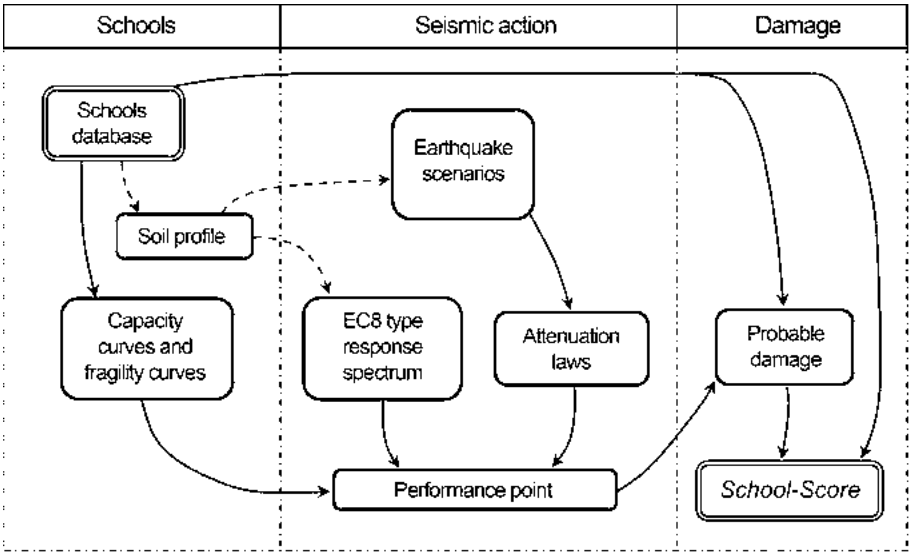

Figure 50. Diagram of the operation of the PERSISTAH software. Obtaining the School-Score.

5.1. SCHOOLS MODULE

Schools, as described in Chapter 3, have been grouped into several types and subtypes. This module presents a school management menu, where it is possible to define the general characteristics of the school (figure 51), and to include its aerial image and georeference.

5.1.1. Menu: School

Within the schools module, a school database is to be found, featuring fields as: schools, buildings and photos.

In this section, it is possible to define the general characteristics of the schools (figure 51), such as: reference code, name, address, telephone, e-mail, level of education, ownership, no. of students, built area, no. of buildings, plot area, % of surface area, morphology of the land, distance from the coast, operational capacity of the fire brigade, distance from a fire station, distance from the nearest hospital and conditions of access and evacuation. As described in section 3.1.1, this information was collected for each of the schools in the Algarve and Huelva provinces, and was fed into the PERSISTAH software.

SUMARY

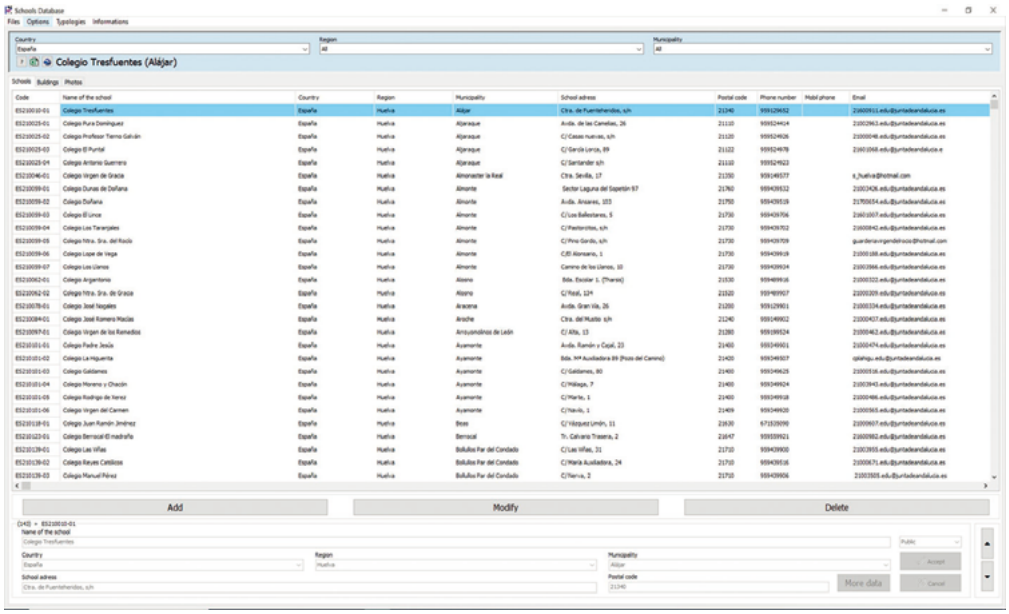

Figure 51. Schools tab. PERSISTAH software.

Figure 52. Menu for georeferencing schools. Aerial image.

For each school, the data concerning the general characterisation (figure 53) and the photographs (figure 52) can be modified or filled in. In fact, during the development of the PERSISTAH project, the database was completed or modified based on new data coming from the school inspections or the answers to the surveys.

SUMARY

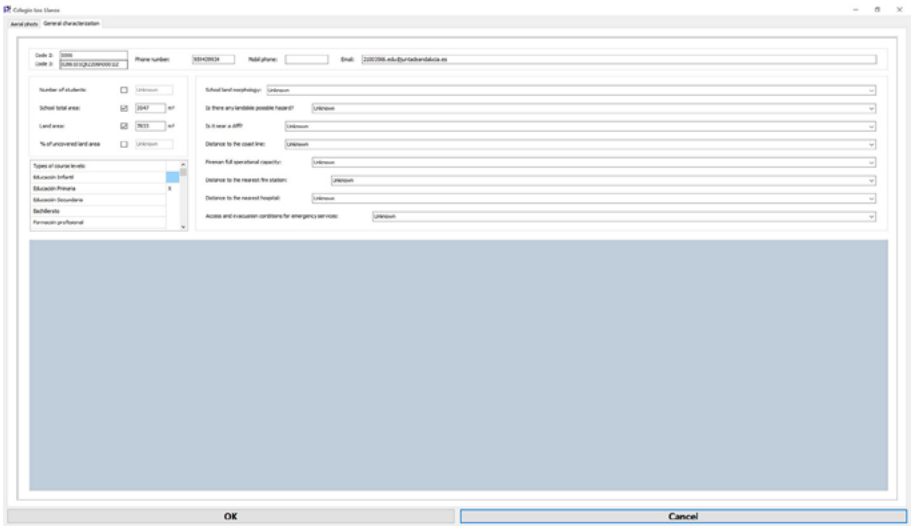

Figure 53. General characterisation of the school.

It is possible to filter the database by country, region and municipality, and to export the filtered results to Google Earth (figure 54) or to Excel. With this, detailed information from any school or group of schools can be easily obtained and effectively presented.

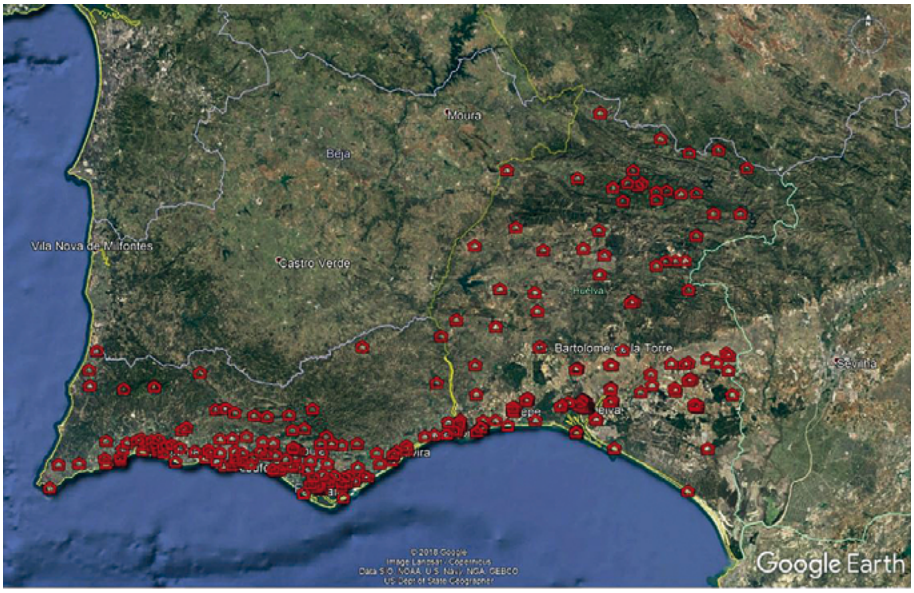

Figure 54. Exporting the location of schools in Google Earth. PERSISTAH software.

SUMARY

5.1.2. Menu: School buildings

In the Buildings menu, information for each building or module that is structurally independent (between joints) is gathered. It is divided into different sections (structural data, irregularities and foundations, non-structural elements, building maintenance and location and photos) (figure 55).

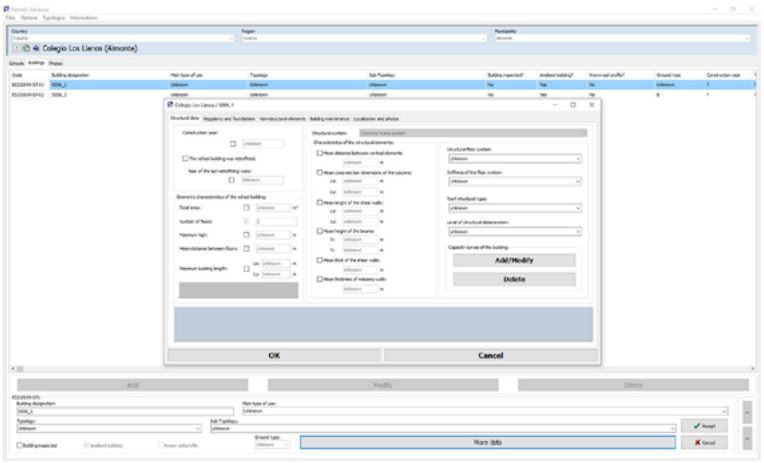

Figure 55. Buildings tab. PERSISTAH software.

The structural characteristics (capacity curve [figure 56]) and photographs of each building (elevations, interiors, aerial, etc.) can be entered independently. The photo section is very intuitive and it is possible to visualise the images of the building in a simple way (figure 57).

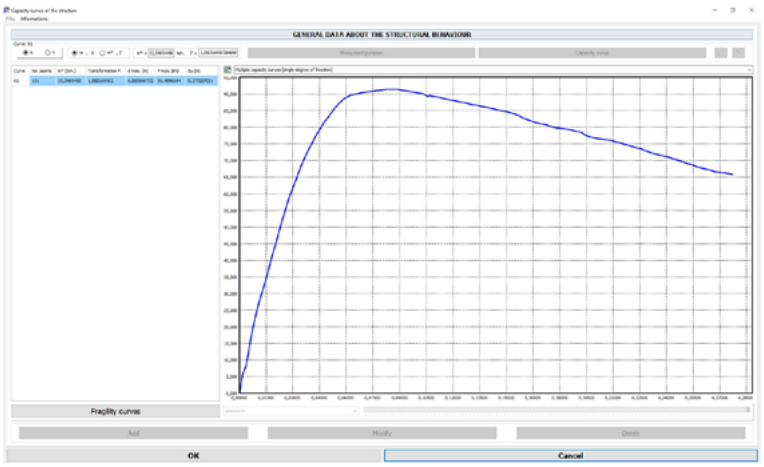

Figure 56. Capacity curve input module.

SUMARY

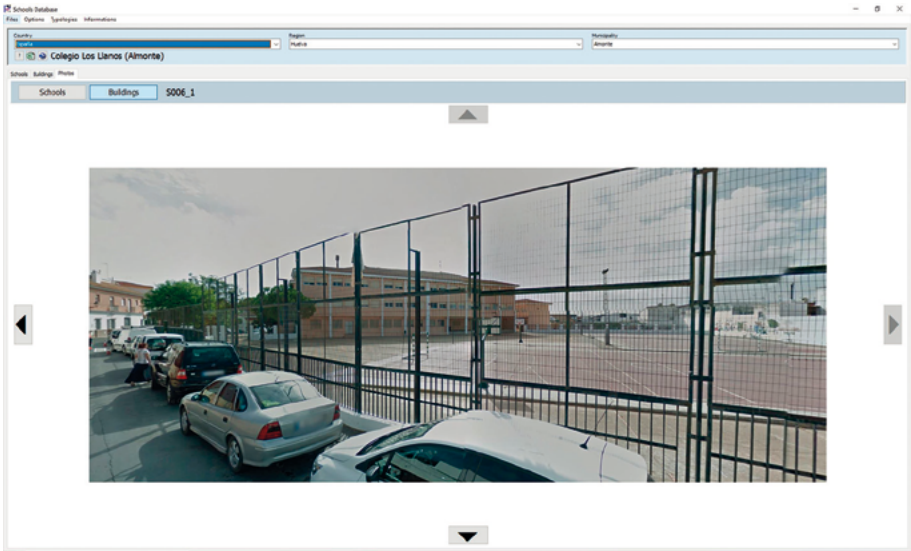

Figure 57. Photos tab. PERSISTAH software.

5.1.3. Importing capacity curves

The PERSISTAH software is able to import capacity curves in text format (.txt) were shear (kN) and displacement (m) values are displayed in columns. In addition, the equivalent mass values (m*) for SDOF and the transformation factor (Γ) must be calculated externally, calculated according to Annex B of EC8, part 1, and fed to the software. Once this data is entered, the program draws the capacity curve (figure 56).

Several capacity curves can be incorporated in each direction, making it possible to compare different capacity curves for the same building. For example, this can be used to compare the capacity curves of the original building with the capacity curves of various retrofitting models.

5.2. SEISMIC ACTION MODULE

In this module, the user can define the seismic action by means of two different methods. The first is based in the hazard stipulated by the codes (essentially for the verification of retrofitting needs). The second defines the seismic action through a seismic scenario (which is particularly important for civil protection).

SUMARY

In the code based definition (figure 58), the seismic actions of several seismic codes have been implemented: the Eurocode-08, the Spanish seismic standard NCSE-02, and the Portuguese NP EN 1998-1:2010.

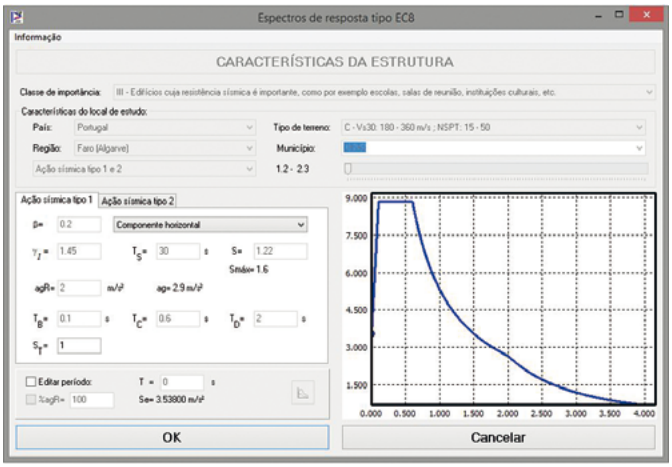

Figure 58. Seismic action module. Response spectrum.

When the seismic action is defined through a seismic scenario with a certain magnitude and epicentre (figure 59). The response spectrum is obtained by applying attenuation laws.

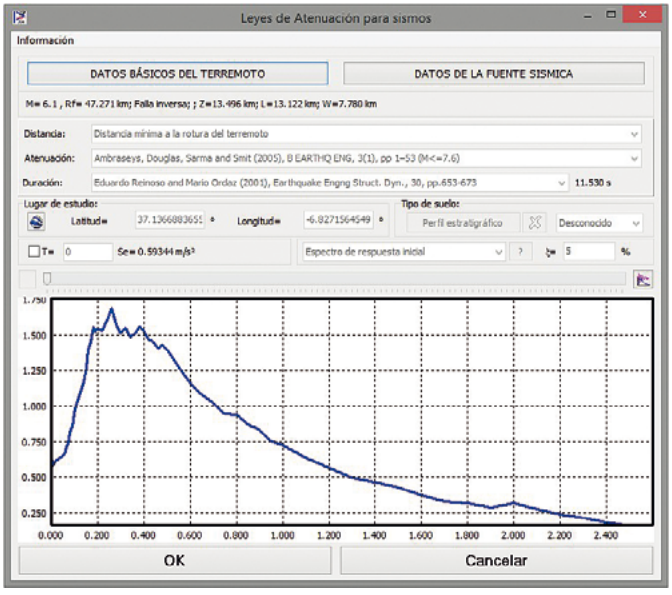

Figure 59. Seismic action corresponding to a seismic scenario.

SUMARY

5.3. DAMAGE MODULE

In this module, the calculation of the School-score is made according to the data entered in the previous module and the capacity curves of each school building. Below, the operation of this module and the obtaining of the School-score is presented.

5.3.1. Operation

In the "Damage" section, the list of schools is arranged according to their seismic vulnerability. This classification is made according to the School-score, in which the higher the value, the more vulnerable the school building is (figure 60).

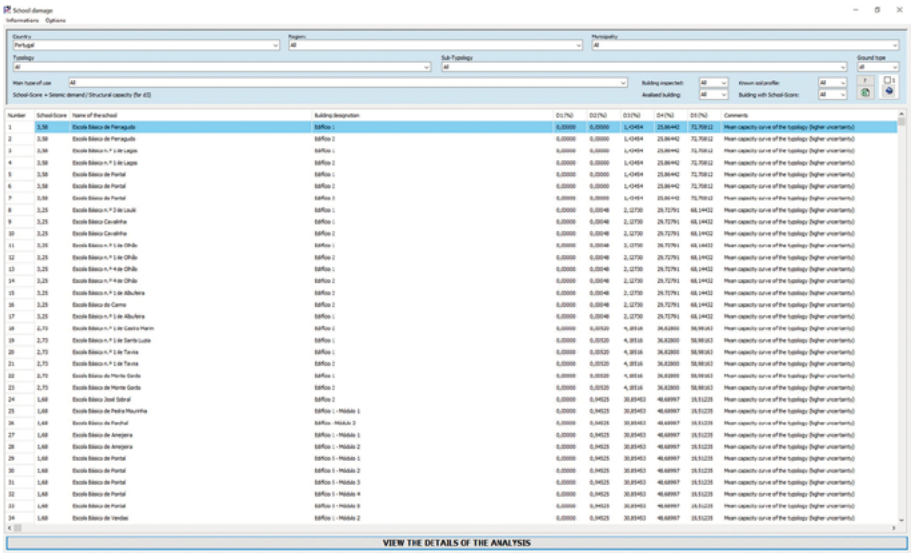

Figure 60. Classification of schools according to School-Score. PERSISTAH Software.

An analytical method for damage assessment in schools has been implemented, based on the non-linear static analysis method included in the Portuguese standard NP EN 1998-3:2017. The performance point of the structure can be determined through the N2 method, as explained above. It is obtained through the intersection of the response spectrum with the bilinear capacity curve, both in spectral coordinates (figure 61).

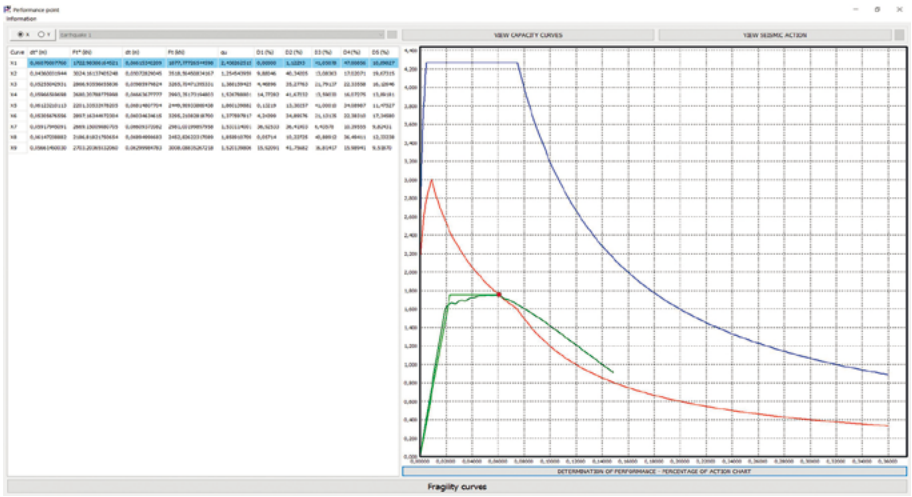

Figure 61. Performance point. N2 Method.

There are two hypotheses of seismic analysis of schools: the first hypothesis consist on a non-linear static analysis of each building, to obtain its capacity curve. This task is complicated due to the large number of schools and the information available. In the second hypothesis, average capacity curves are defined for each typology.

Based on the capacity curves and the performance point, the software obtains the fragility curves of each building. With these curves, the probabilities of exceeding the different damage limit states are determined, as well as the action level associated with each limit state (figure 62).

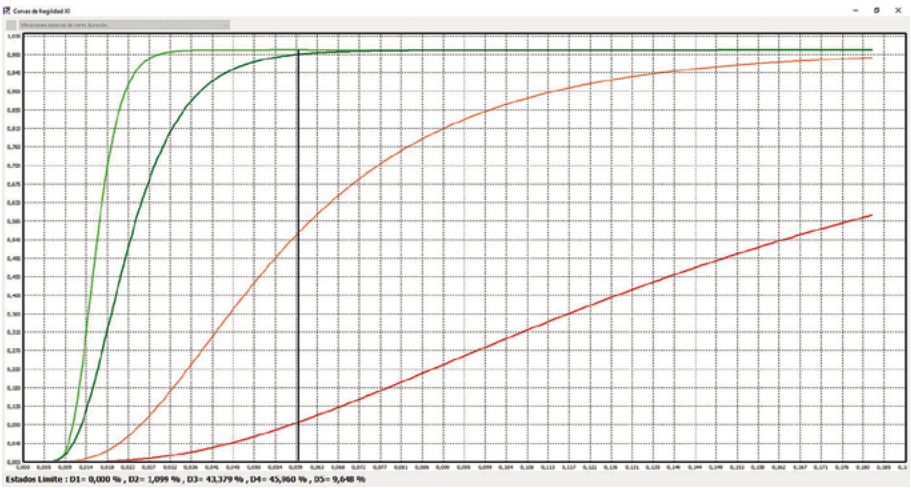

Figure 62. Fragility curves.

SUMARY

Finally, the School-score is determined through various available options.

5.3.2. Obtaining the School-score

Finally, the School-score of each building is obtained. The School-score depends on the level of structural damage. Therefore, a higher value of the school score indicates that the school is less resilient in the event of an earthquake. A classification of the different school buildings in each country has been made according to this factor, in order to establish a hierarchy for future seismic retrofitting interventions. This classification will help the different regions to study the need for seismic retrofitting of their school buildings.

The values of the School-score can be automatically exported and presented in Google Earth (figure 63).

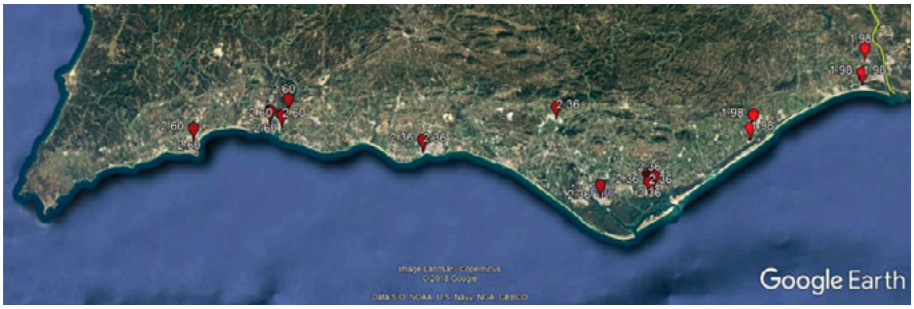

Figure 63. Example of export of filtered results to Google Earth.

SUMARY

Chapter 6. Sismic retrofitting strategies

Most of the school buildings studied were built before the current seismic regulations, therefore, without taking into account the seismic action, considering only the gravitational loads. For this reason, many of them present a high seismic vulnerability, which must be reduced to guarantee the safety of these buildings in case of an earthquake. To reduce this vulnerability, the technician must evaluate different strategies (or a combination of strategies) for rehabilitation: increase in stiffness, reduction in seismic demand or increase in the building's deformation capacity, depending on the deficiencies observed in the evaluation of the building and considering the design restrictions it may present. In this case, seismic demand reduction techniques have been ruled out, due to the configuration of the buildings, as will be seen in the following sections.

Once the strategy or strategies have been chosen, a selection of the most appropriate retrofitting method is made and a preliminary design is developed. In the present work, an exhaustive bibliographic review of these techniques has been carried out, including an analysis of the different strategies and methods of intervention proposed by different seismic regulations (ATC-40, FEMA 356 and Eurocode 08), which are presented in the following sections. The analysis has been completed with a series of images and constructive details to illustrate the main methods studied.

The different seismic retrofitting techniques have been examined in terms of their feasibility for the retrofitting of the school buildings studied, but also taking into account other factors, such as architectural integration (both aesthetic and functional), ease of construction and minimization of the interference of the implementation of the measures with teaching activity.

Of each of the viable retrofitting techniques, the effectiveness has been analysed, in terms of increasing the resistant capacity of the structure and reducing the damage caused to the building, in the event of an earthquake. The evaluation was carried out by applying the methodology outlined in the previous sections, and then comparing the performance and level of seismic damage in the retrofitted and unretrofitted building. Finally, a classification has been made

SUMARY

of the retrofitting methods and configurations analysed in order to choose the most efficient one for the building under study.

This methodology points to the possibility that the results obtained on the seismic retrofitting systems analysed in various typologies of schools could be extrapolated to other buildings with a similar typology (typology and structural system). This means that the most efficient retrofitting configurations can be easily and quickly applied to other buildings with a similar typology and configuration.

Two primary education buildings, one in the Algarve and another one in Huelva, have been selected as pilot rehabilitation projects, in which the most relevant techniques have been implemented in each case. These buildings have one of the most unfavourable School-score coefficients, that is, they are among the most seismically vulnerable and need more urgent intervention. In addition, they are buildings that adapt to the scale of intervention of the research project, due to their characteristics, dimensions and proximity.

This chapter presents a set of seismic retrofitting measures that can be adapted to the characteristics of schools in Huelva and their seismic hazard.

6.1. INTERNATIONAL CONTEXT

In this section, the different retrofitting techniques proposed by the American seismic standards (ATC-40 and FEMA 356) and the European Eurocode 08 regulations will be addressed. The different seismic retrofitting techniques will be presented in a schematic way in order to offer an overall view of the different strategies and specific retrofitting solutions proposed by these standards, based on the different deficiencies that the buildings studied may have.

6.1.1. ATC-40

The American standard ATC-40 (Applied Technology Council (ATC), 1996), in its chapter 6, "Retrofitting strategies" proposes four general strategies for rehabilitation: improvement of the overall performance, increase of the stiffness, increase of the deformation capacity and reduction of the seismic demand (see table 26).

SUMARY

Table 26. Seismic adaptation strategies of the ATC-40 standard.

Improving overall performance	Diaphragm stiffening (slabs)		
	Slab – vertical elements connectivity		
	Anchoring and bracing of non-structural components		
Stiffening and reinforcement	Shear walls	Steel	
		Concrete	
	Triangulated (braced) frames	Shape: diagonal, X, V, K	
		Including dampers	
	Buttresses		
	Moment-resisting frames		
	Diaphragm stiffening (slabs)		
Increase in deformation capacity	Addition of infill	Concrete or steel jacket	
	Reinforcement of columns	Different types of FRP	
	Reduction of local stiffness		
	Supports/Supplementary supports		
Reduction of seismic demand	Base isolation		
	Energy dissipation elements (dampers)	Fluid-Viscous	
		Friction	
		Metals	Steel sheet or plate
			Steel rods
			Honeycomb
			Cracks, joints
	Reduction of mass		

In the table, the retrofitting methods considered in the studies carried out have been highlighted in grey. In order to select them, the type of building studied, the seismic action existing in the area and the economic means available to the administration for this type of intervention have been considered, and these strategies are the best-suited and most used ones. However, the engineer is the one who has the final choice when it comes to applying any retrofitting system, once the first evaluation of the building has been carried out and as long as the different factors involved come into play. One of the most widely used techniques is the strategy of stiffening and reinforcing by means of diaphragm walls or triangular frames (bracing) (figure 66 and figure 78) with different configurations. Also, in school buildings, the structures are usually simple and two

SUMARY

or three storeys high, so seismic demand reduction systems —which are expensive and recommended for complex or higher buildings— are not applied. The buildings under study behave well on a global level, i.e. the floors have a satisfactory stiffness and the structural elements are correctly joined together, so the first group of strategies is excluded. For illustrative purposes, techniques relating to diaphragm stiffening are presented in figure 64.

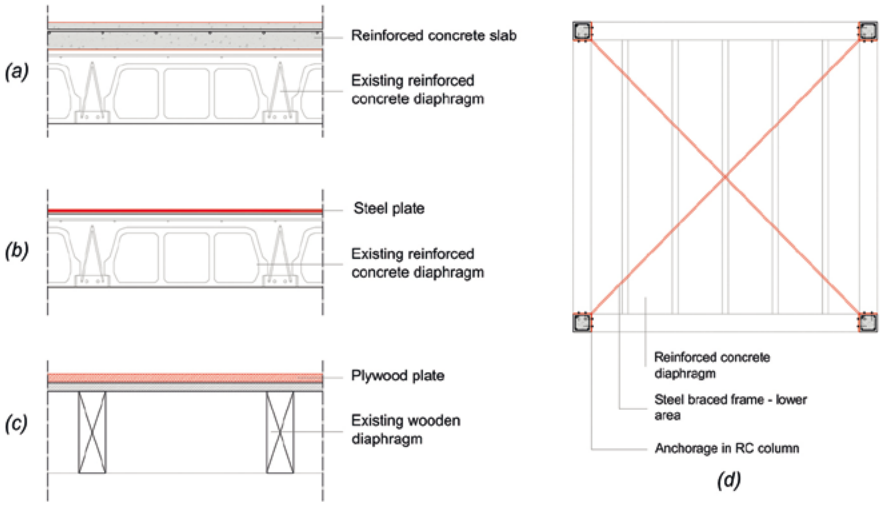

Figure 64. Horizontal diaphragm stiffening systems: a) Reinforced concrete slab on existing slab; b) Steel plate on existing slab; c) Thickness increase by means of plywood layer (Wooden slab); d) Bracing under existing slab.

Furthermore, the retrofitting scheme selected must be in line with the building's configuration, allowing the normal development of teaching activities, minimising inconveniences during its execution and reducing the architectural impact. This excludes a number of alternatives such as the use of moment resisting frames or buttresses. The latter are illustrated by way of example in figure 65.

SUMARY

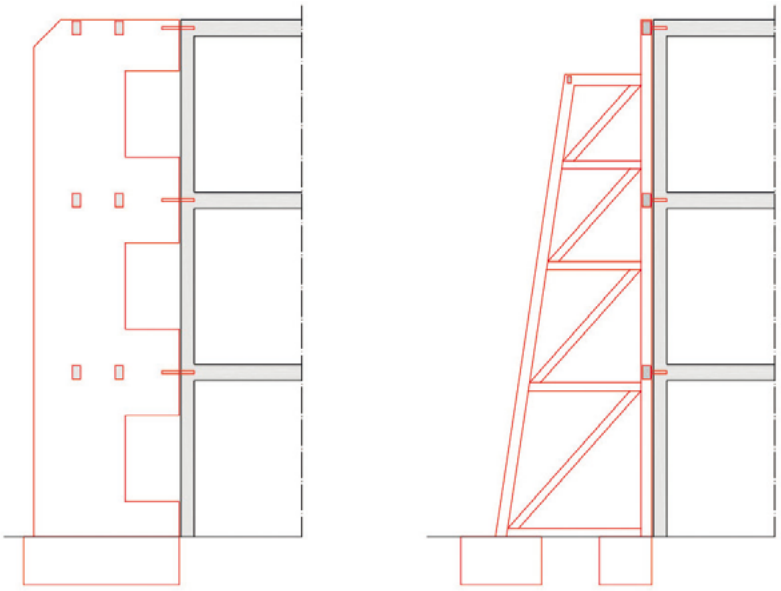

(a) (b)

Figure 65. Stiffening systems using buttresses: a) Reinforced concrete; b) Steel profiles.

6.1.2. FEMA 356

The American standard FEMA 356 (American Society of Civil Engineers [ASCE], 2000) proposes different intervention strategies depending on the deficiency to be corrected: local modification of components, elimination or reduction of irregularities, increase of global stiffness, global retrofit of the structure, reduction of mass, seismic isolation, and supplemental energy dissipation. These strategies are presented in table 27, together with the corresponding methods of intervention. In the table, the methods considered in this guide have been highlighted in grey according to various criteria (see 6.1.1). According to this standard, each retrofitting measure must be evaluated in conjunction with other measures on the existing structure, and with the structure itself, verifying its effects on the structure's stiffness, strength and deformability. It is also necessary to check the compatibility of new and existing elements.

SUMARY

Table 27. Retrofitting Strategies in FEMA 356.

Strategy	Deficiencies	System/Method
Local modification of components	– Resistance – Deformation capacity – Stiffness	Steel cladding on beams and columns
		Addition of plywood in wooden slab
		Jacketing of RC columns
		Reduction of the cross section
Elimination or reduction of irregularities	– High demand for inelastic deformation – Irregular displacement	Triangulated (braced) frames
		Shear walls
		Bending-resistant frames
		Partial demolition (> building impact)
		Removal of parts from the structure (towers or side flanges)
		Creation of structural joints (irregular building – various regular structures)
Overall structure stiffness	– Excessive lateral deformations – Structural elements without adequate ductility to resist deformation	Triangulated (braced) frames
		Shear walls
Global retrofit of the structure	– Inelastic behaviour low levels of ground movement – Inadequate overall resistance	Triangulated (braced) frames
		Shear walls
		Bending-resistant frames
Mass reduction	– Excessive mass in building – Global structure flexibility – Global structural weakness	Demolition of upper floors
		Replacement of heavy cladding and interior partitions
		Removal of large storage and equipment loads
Seismic isolation	– Excessive seismic forces – Demand and excessive deformation – Protection of important building elements – Protection of non-structural elements	Bearings between the structure and the foundation
		Energy-dissipating bearings (dampers)
Supplemental energy dissipation	– Excessive deformation due to the overall flexibility of the structure	Viscous fluid dampers (hydraulic cylinders)
		Deformation expiration plates
		Friction pads

SUMARY

In school buildings, structures are usually simple and have two or three floors, so the base isolation and supplemental energy dissipation systems, which are expensive and recommended for buildings of greater complexity or height, are not applied. Mass reduction strategies with high architectural impact are not applied either, as these buildings have a low storage load, lightweight cladding, and low height. Even so, the engineer criterion prevails, so an individual study must be carried out when selecting a strategy.

Figure 66 shows two of the most commonly used seismic retrofitting systems: triangular or braced frames and shear walls.

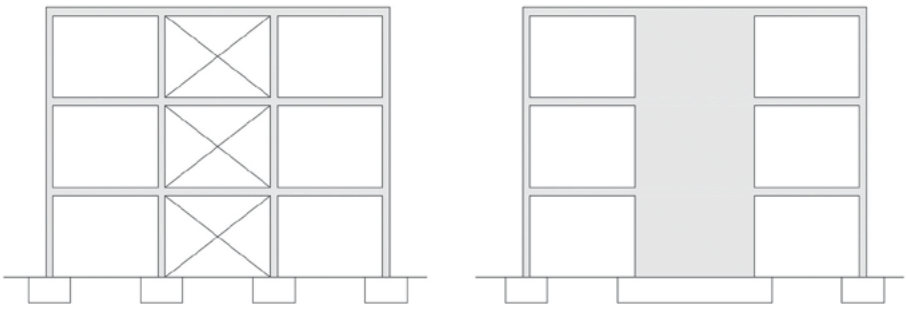

Figure 66. Stiffening systems: (a) Bracing systems; (b) Shear walls.

6.1.3. EC8

European regulation EC8, part 3, presents a series of general criteria for intervention in the structure and general information on the types of intervention possible. According to this standard, seismic enhancement strategies should increase the capacity of systems resistant to lateral forces and horizontal diaphragms, and/or reduce the demand imposed by seismic actions. The general classification of the different types of intervention (table 28), is very similar to those proposed by the American standard FEMA 356: stiffness and reinforcement of the structure and its foundation, improvement of ductility, reduction of mass, base isolation and additional damping. As in previous sections, the techniques considered in this study have been highlighted in grey in this table.

SUMARY

Table 28. Types of intervention. Eurocode 08 part 3.

Local or global modification of the damaged or undamaged elements, considering the stiffness, resistance and/or ductility of these elements	Repair
	Reinforcement
	Complete replacement
Addition of new structural elements	Bracing systems
	Shear walls
	RC, wood or steel straps (load-bearing walls)
Modification of the structural system	Elimination of some structural joints
	Widening of joints
	Elimination of vulnerable elements
	Modification to obtain more regular and/or more ductile arrangements
Addition of a new structural system to resist all or part of the seismic action	Transformation of existing non-structural elements into structural elements
Introduction of passive protection devices	Dissipative bracings
	Base isolation
Restricting or changing the use of the building	
Partial demolition	

Unlike the American standards (ATC-40 and FEMA 356), where a series of specific interventions are presented within each general strategy, the European regulations present a series of strategies in a general way, as well as a series of criteria to be taken into account when intervening in a structure.

In each annex according to the different structural systems (masonry buildings, RC structures and steel and mixed structures), a series of strategies and methods of intervention are presented specifically, which are set out, in a schematic way, below.

6.1.3.1. Masonry buildings

The Eurocode 08, part 3, in its Annex C "Masonry buildings" presents different retrofitting strategies within which the different methods of repair and reinforcement of buildings with URM load-bearing walls are classified. These retrofitting techniques are presented schematically in table 29.

SUMARY

Table 29. Retrofitting strategies, Eurocode 08 part 3 Annex C Masonry buildings.

Strategy	Deficiencies	System/Method
Repairing cracks	Small opening (<10 mm); thin wall	Sealing with mortar
	Small opening (<10 mm); thick wall	Injections with cement paste
		Epoxy-based concrete paste injections
	Wide opening (>10 mm)	Mastering with bricks or elongated stones
		Crack connection (dovetail clips, metal plates or polymer grids)
		Sealing with cement mortar
	Vertical cracking (walls with levelled tendons)	Small diameter wire in bed-joints
		Polymeric grid strips in bed-joints
	Large diagonal cracks	Concrete ribs
		Polymeric grids (one or both sides) + mortar and plaster
Repair and reinforcement of wall intersections	Poor connection between concurrent walls	Reinforced concrete strap
		Steel plates or mesh on guide line
		Insertion of inclined steel reinforcements in holes with fluid mortar
		Post-tensioning
Reinforcement and stiffening of horizontal diaphragms	Distortions in the plane	Additional layer – wood panels (perpendicular or oblique)
		RC overlay + welded mesh (shear connections and wall anchorage)
		Mesh in two diagonal directions (anchored to beams and perimeter walls)
	Roof trusses	Bracing and anchoring to support wall
		Horizontal diaphragm (bottom chord level)

SUMARY

Table 29. Retrofitting strategies, Eurocode 08 part 3 Annex C Masonry buildings *(cont.)*.

Strategy	Deficiencies	System/Method
Tie beams	Damaged tie beam	Repair or reconstruction
		If there are none, add
Reinforcement of buildings by means of steel braces	Bad connection and overall behaviour (out-of-plane failure)	Longitudinal or transverse braces to walls, external or in perforations
		Post-tensioning straps (improves tensile strength)
Reinforcement of rubble-filled masonry walls (multi-leaf walls)	Rubble filling	Reinforcement by means of fluid mortar
		Mortar + steel reinforcement anchored to the outer leaves
Reinforcement by means of reinforced concrete jackets or steel profiles	Out-of-plane failure	Shotcrete reinforced with wire mesh or steel bars (one or two sides with cross ties)
		Steel profiles (one or two sides)
Reinforcement by polymer grid jackets	Out-of-plane failure	Polymeric grids (one or both sides) + ductile pastes (lime and cement with fibre-based reinforcement), should be anchored to the perpendicular walls

It can be established that the school buildings under study analysed in the province of Huelva (Spain) generally present the following characteristics:

- They have wall crest beams (tying beams) and a good connection between the competing walls, so there is no need to resort to strategies to reinforce the wall intersections or between walls and slabs.
- They have rigid diaphragms, generally one-way span reinforced concrete slabs, so they do not need to be stiffened.
- They have single-leaf ceramic brick walls of various thicknesses, so the techniques of reinforcing multi-leaf walls with rubble filling are not applied.
- They do not have structural joints. In some cases the largest dimension reaches 70 m in length.

SUMARY

According to the above, and based on its low architectural impact on the building, and its ease and speed of application (only the external part of the wall is involved, without interrupting teaching activities), the most relevant techniques proposed by this standard are: reinforcement by steel straps, reinforcement of walls by means of reinforced concrete jackets or steel profiles, and reinforcement by means of sheet metal jackets or polymer mesh (table 29).

The study of retrofitting techniques for URM school buildings is discussed in more detail in section 6.2 of this guide.

6.1.3.2. Reinforced concrete buildings

The Eurocode 8, part 3, in its Annex A "Reinforced concrete buildings" generally develops a series of techniques for the repair and reinforcement of buildings with a reinforced concrete structure. The three retrofitting techniques proposed in this annex are presented schematically in table 30.

Table 30. Retrofitting strategies, Eurocode-08 part 3 Annex A Reinforced concrete buildings.

System/Method	Improvement/Enhancement
Concrete jacketing	Bearing capacity
	Bending and/or shear resistance
	Deformation capacity
	Poor splice resistance due to overlaps
Steel jacketing	Bearing capacity
	Poor splice resistance due to overlaps
	Ductility by confinement
Plating and wrapping with fibre reinforced polymers (FRP)	Shear strength of columns and walls
	Ductility by confinement at the ends of structural elements
	Prevention of poor overlap failure

As we can see in this standard, three specific retrofitting methods are presented (table 30) unlike the American standards (ATC-40 and FEMA 356), which present a more exhaustive classification of these systems (table 26 and table 27). However, in Annex B "Steel and composite structures" it is specified that the local seismic retrofitting systems proposed for the structural elements and for the connection between elements (table 32), can be applied to any

SUMARY

structural system. Therefore, most of them are compatible and can be applied to reinforced concrete structural elements.

The study of retrofitting techniques for reinforced concrete school buildings is developed in detail in section 6.3 of this guide.

6.1.3.3. Other buildings

The European seismic standard EC8, part 3, in its Annex B "Steel and composite structures" presents a series of seismic rehabilitation strategies for buildings with steel or mixed structures, which are a minority among schools in the province of Huelva.

Unlike the systems proposed for reinforced concrete buildings, for buildings with steel or composite structures this annex presents a more complete classification with a series of strategies at the global (table 31) and local (table 32) level, within which the various specific retrofitting systems are classified. The retrofitting strategies proposed for these buildings are in fact applicable, according to this annex, to any structural system.

The objective of the general seismic retrofitting strategies is to increase the overall capacity of the structure and the horizontal diaphragms to resist lateral forces, and to reduce the seismic demand, very similar to those mentioned in the American standards ATC 40 and FEMA 356 (table 26 and table 27, respectively) for reinforced concrete structures. Comprehensive seismic retrofitting interventions should include one or more strategies, as can be seen in table 31.

Regarding the assessment and local seismic adaptation of structural elements, the standard indicates a number of general requirements that will not be discussed in detail in this document. The different types of local seismic retrofits proposed in this standard for structural elements are shown below schematically (table 32).

SUMARY

Table 31. Global Retrofitting Strategies Eurocode-08, Part 3, Annex B Steel and composite structures.

Strategy	Intervention		
Stiffness and reinforcement of the structure and its foundation system	Bending-resistant frames	Improved mixed action steel beams and RC slab (higher overall stiffness)	Connectors
			Embedding beams and columns in RC
		Semi-rigid and/or partially resistant steel or composite joints	
		Bracings (greater overall stiffness)	
	Triangulated (braced) frames	Off-centre bracing and tapering (brace connection in dissipative zone) better than concentric bracing	
		Improves ductile response and prevents beam-column instability	Steel, RC or composite walls
		Increased overall stiffness	Bracings in moment-resisting frames
Improved ductility of the structure	The systems proposed in Table 21 for structural elements can be applied		
Reduction of mass	Replacement of heavy plating with lighter systems		
	Disposal of unused equipment and stored loads		
	Replacement of masonry partitions with lightweight systems		
	Removal of one or more floors		
Seismic isolation	Base isolation	Structures with fundamental periods >1.0 s	
Additional damping			

SUMARY

Table 32. Local retrofitting strategies, Eurocode 08, part 3, Annex B: Steel and composite structures.

Beams		
Insufficient stability	Beams span-height ratio between 15 and 18 (energy absorption). Incorporation of intermediate supports to shorten the large spans	
	Constraint of lateral movements of the flanges	
Insufficient resistance	Increase in bending capacity	Addition of steel plates in the flanges
		Addition of longitudinal reinforcement
	Ductility class M (Standard EN 1998-1:2004)	
	Increase in shear capacity	Addition of steel plates in web (H section and double T)
		Addition of steel wall plates (Hollow Sections)
Repair of bent or broken flanges	Reinforcement or replacement with new steel plates	
	Addition of full height web stiffeners on both sides (thickness = beam web)	
	Orientation of the plates longitudinally to the rolling direction	
	Steel beam shell in reinforced concrete (RC)	
Weakening of the beams	Improved ductility. Weakening of the wing in desired areas (moving dissipative areas away from connections)	
	Reduced beam sections (RBS). Premature fracture protection in beam-column connection.	
Mixed elements	Shear connection between steel beams and RC slab	
	Do not use or remove – shear connectors in dissipative areas	
	Wing-bolt welded connection (avoid rivets or screws)	
	Maximum tensile deformation does not cause wing tearing	
	Provide stirrups to the RC-wrapped beams	

SUMARY

Table 32. Local retrofitting strategies, Eurocode 08, part 3, Annex B: Steel and composite structures *(cont.)*.

Columns		
Insufficient stability	Reduced width/thickness ratio	Welding of steel plates on web and/or flanges (H profile)
		Welded external steel plates (hollow profile)
	Lateral constraints on both flanges (lateral stiffeners)	
Insufficient resistance	Increase in bending capacity	Welding of steel plates on web and/or flanges (H profile)
		Welded steel plates on walls (hollow profile)
		Structural steel profile wrapping in RC
Repair of bent and broken flanges and broken joints	Bent or broken flanges / Broken joints	Reinforcement or replacement with new plates
	Bent and broken flanges	Replacement by similar plate
		Direct flame stretching
	Broken joints	External plates on flanges (e plate = e wing)
		Alignment with rolling direction
		Small crack edge perforation (prevent spreading)
		Tests for magnetic particles or tinted liquids (to avoid later defects or discontinuities)
Joint requirements	New – middle third of free column height	
Panel area	Column-beam connection – elastic in limit state DL	
	Avoiding premature denting (action of inelastic shear deformation)	
Mixed Elements	RC wrapping (improve stiffness, strength and ductility)	
	Transfer shear stresses (connectors along the column)	

SUMARY

Table 32. Local retrofitting strategies, Eurocode 08, part 3, Annex B: Steel and composite structures *(cont.)*.

Triangulations (bracings)		
Insufficient stability	Reduce width/thickness ratio	Welding of steel plates in web and/or flanges (H-profile)
		Welded external steel plates (hollow profile)
	Envelope - to comply with EN 1998-1:2004	
	Improve lateral stiffness	Increased stiffness of external connections
	Preference for X-bracing versus V-bracing or inverted V. Do not use K-bracing	
	Improve post-bending resistance	Closely spaced reinforcing plates
Insufficient Resistance	Limit state DL. Axial compression $N \leq 80\% N_{pl,Rd}$ (plastic resistance to normal cross-section stress)	
	Frames with concentric bracing. $N > 50\%$ $N_{pl,Rd}$	
Mixed elements	Increased strength, stiffness and ductility	RC wrapping on the steel profile. H-profiles can be partially or totally embedded
	Good connection	Stirrups and stiffeners (total embedded)
		Straight connections (partially embedded)
	Tensile capacity	Only consideration of the structural steel section
Non-adhesive triangulations	Non-adhesive incorporation (non-stick material)	Reinforced concrete walls
		Concrete filled pipes
	Steel fibre reinforced concrete (non-stick material)	

SUMARY

Table 32. Local retrofitting strategies, Eurocode 08, part 3, Annex B: Steel and composite structures *(cont.)*.

Connections between elements (reinforced and existing)		
Column-Beam Connections	Welding replacement	Replacing filler material
		Transverse stiffeners lower and upper part in panel area (e ≥ and beam flanges)
	Weakening	Reduced beam section connections
		Semi-rigid connections
	Reinforcement	Connections with gussets
		Flashing plate connections
Triangulation and seismic coupling connections	Dimensioning according to the effects of the cyclical behaviour after buckling	
	Preference for rigid connections	
	No interruption in the continuity of the beam and columns	
	Beam shaft – triangulation must intersect within seismic coupling	
	Avoid welded connection seismic coupling to weak shaft of a column	

6.2. MASONRY BUILDINGS

Unreinforced masonry (URM) buildings are characterised by a poor performance in earthquakes due to their lack of ductility. The seismic retrofitting for these buildings can be grouped into reinforcement of the joints (wall to wall, wall to slab or wall to roof), stiffening of horizontal diaphragms (relevant for flexible slabs), strapping/tying, and reinforcement of walls.

In the case of the province of Huelva, in most of the buildings with load-bearing walls, the elements are properly connected to each other: the walls are locked, and there is a crest beam that links walls and slabs or roofs. In addition, these buildings have rigid diaphragms, generally RC slabs. In any case, techniques for the retrofitting of connections and diaphragms can be found in the previous section.

SUMARY

On the other hand, these schools have, due to their function, large openings in many of their walls. There are studies (Sanaz and Armen, 2012) that show that the presence of openings in the walls significantly affects the seismic behaviour of the building, causing a concentration of shear forces and deformations. Thus, the presence of high opening ratios considerably increases the seismic vulnerability of the building, making the strategies of wall and openings reinforcement the most relevant in this case. From this point onwards, this document will focus on such strategies.

6.2.1. State of the Art

After the bibliographic review of the different retrofitting techniques (Abeling *et al.*, 2018; Maio *et al.*, 2017; Meireles and Bento, 2012), a summary table (table 33) has been prepared with a series of local and general interventions in load-bearing wall structures. It should be noted that in the case of school buildings, generally, deficiencies have been detected in the general seismic behaviour of the structure, while no local deficiencies have been observed in the structural elements. If a local deficiency is detected, some of the retrofitting techniques presented in table 33 can be applied.

Table 33. Local seismic retrofitting strategies in load-bearing wall buildings.

Local action	Steel	Plates
		Reinforcement (drilling)
		Braces
	Polymeric bands	Reinforced with fibre (FRP) CFRP, GFRP, AFRP
		Reinforced with steel (SRP)

Generally, deficiencies have been detected in the global behaviour of the load-bearing wall structure in schools, so a series of general actions to intervene in these cases are developed below (table 34).

SUMARY

Table 34. Global seismic retrofitting strategies for URM load-bearing wall buildings.

Global Action	Wire mesh	Ferrocement (wire)
		Shotcrete (round)
	Steel bands	Crossbars
		Grid
		3D
	Injections	Cement grout
		Epoxy resin
	Reinforced concrete elements	Rigid core
		Confinement by means of tie beams or columns
	Carbon fibre reinforced polymer (CFRP) bands	One-way bands
		X-bands
		Gridded bands
	Steel rebaring of gaps	Laminated profile (tubular or angular)
		Increase in the amount of reinforcement

A wide variety of materials are used in the seismic reinforcement of URM load-bearing, which can be grouped into five types: steel (in profiles, bands or meshes); carbon or glass fibre reinforced polymers (FRP) used as bands, glass fibre or textile reinforced mortars, cement or epoxy resin grout injections; and, finally, reinforced concrete. The latter is used to create new bracing frames or as a rigid core inside the walls (figure 74) as proposed by (Fulop and Suppola, 2011). Finally, it should be noted that two of these materials are the most implemented. Firstly, steel in meshes or profiles, due to its low cost and easy implementation. Secondly, carbon-fibre reinforced polymers (CFRP), because of their high efficiency and the considerable improvement in the strength and dissipative capacity of the walls that they achieve.

Below are the diagrams of the elevation and construction details (figure 67-figure 74) of the seismic retrofitting techniques for URM buildings shown in the table above (table 33). These are different systems of global intervention in the structure with various materials and techniques. These systems are also well integrated into the building configuration, which minimise their architectural impact on the building.

SUMARY

6.2.1.1. Wire mesh

The global retrofitting techniques by means of meshes (figure 67 and figure 68), are techniques that have a good architectural integration, being inserted inside the wall. Furthermore, they are cheap and easy to apply that are normally used in rehabilitation works. They provide the wall with increased confinement and resistance to tensile forces, preventing the formation of cracks. In addition, they increase both the in-plane and out-of-plane resistance of the wall.

Steel has been widely used to reinforce walls by placing meshes anchored to the masonry and covered with shotcrete or cement mortar. Depending on the type of mesh and the installation technique, various solutions can be found. In the case of ferro-cement (figure 67), the meshes are made of welded wire or other fibres and are covered with concrete micro-mortar (Fulop and Suppola, 2011). It is also possible to implement meshes with intermediate diameters (4-6 mm) applied on one or both sides of the wall with the same construction solution, as in (Diz *et al.*, 2015). Finally, there are retrofitting techniques through the use of shotcrete (figure 68). In this case, a larger diameter mesh (6-14 mm) is used, covered with shotcrete (Shabdin *et al.*, 2018).

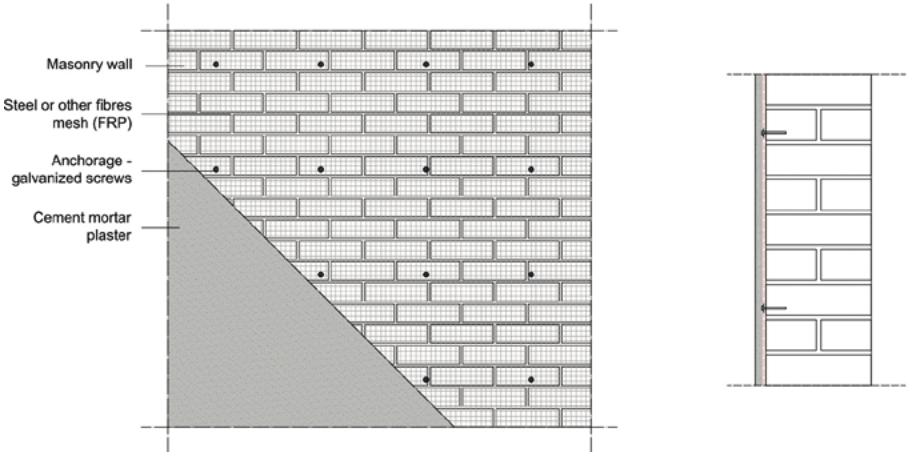

Figure 67. Ferro-cement. Diagram and construction detail.

SUMARY

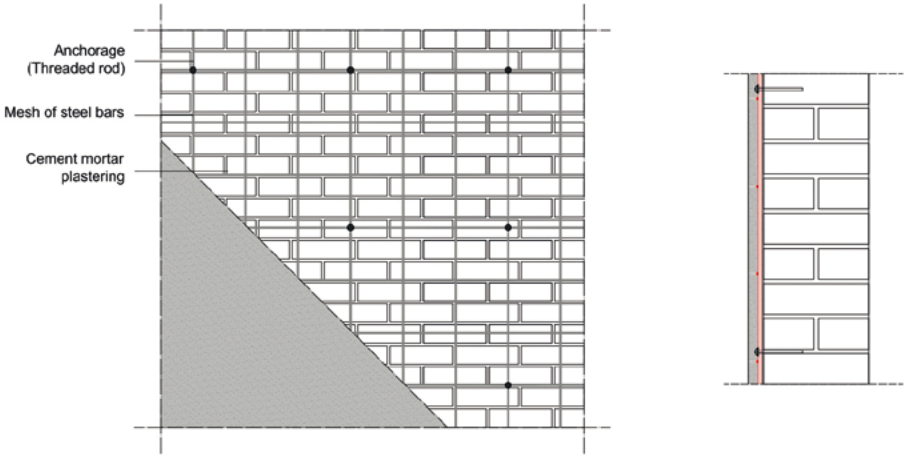

Figure 68. Steel rod mesh covered by shotcrete. Diagram and construction detail.

6.2.1.2. Steel sheet bands

Steel can also be applied to the outside of the wall by means of cross bracing (figure 69) or forming a grid (figure 70) with steel sheet bands. These systems provide an improvement in the tensile behaviour of the wall, out-of-plane resistance and an increase in stiffness. Cross bracing presents a difficulty in achieving the necessary strength at the ends, where the bands are more concentrated. They are usually easy and fast to execute and low cost, both in terms of material and execution. They are usually used only on one side of the wall but can be placed on both sides.

A variant of the techniques mentioned above is the three-dimensional tying system (figure 71). In this case, stainless steel strips (thickness 0,8 mm; width 20 mm) are used instead of bands or meshes. These are placed on both sides of the wall and connected together to form a 3D wall tying system. A pre-stressing is applied to these strips, which gives a slight compression to the wall (Dolce *et al.*, 2009). Studies on this solution have concluded that it is an effective reinforcement (Spinella, 2019), due to the considerable increase in the overall strength and ductility of the structure. It is a more invasive technique than the previous ones, which requires a series of perforations to be made through the wall.

SUMARY

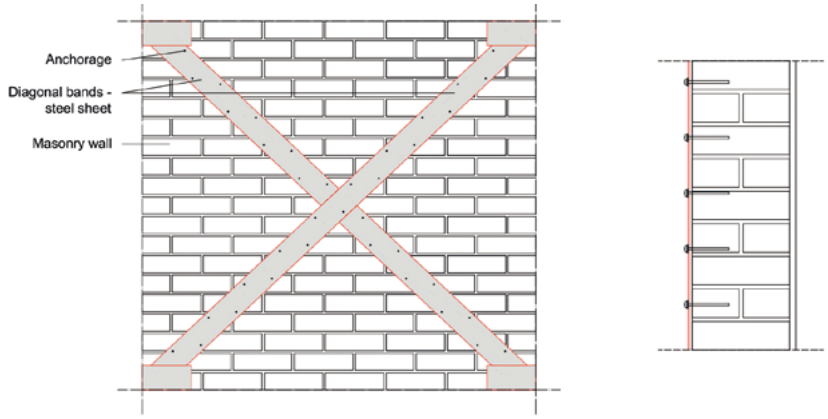

Figure 69. External steel bands.

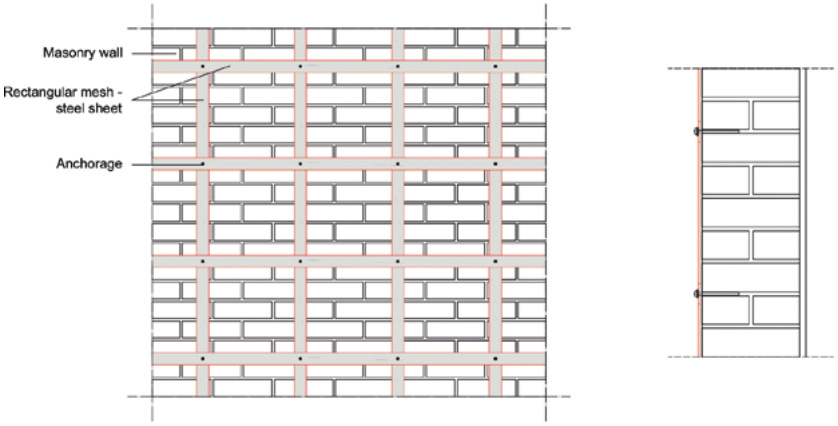

Figure 70. Rectangular steel band mesh.

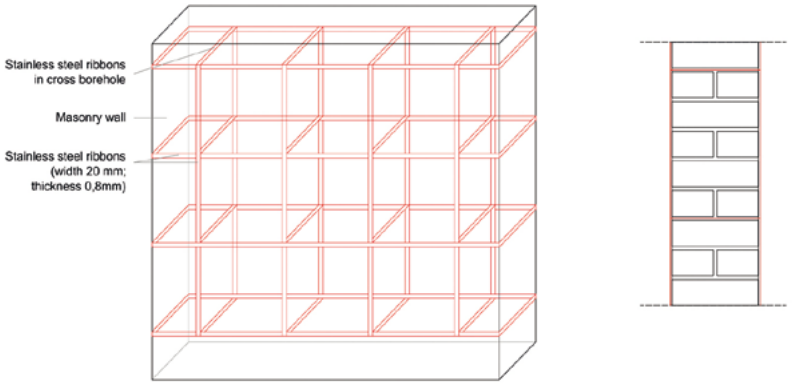

Figure 71. Three-dimensional tying system.

SUMARY

6.2.1.3. Injections

Another type of global intervention are the injections of cement or epoxy resin grout into the wall (figure 72) or into cracks in the wall (figure 73). This type of intervention does not change the appearance of the wall, and also restores the continuity of the wall, covering the possible flaws and cracks. In multi-leaf walls, they seal the potential internal holes of the wall, providing a considerable increase in its stiffness and resistance.

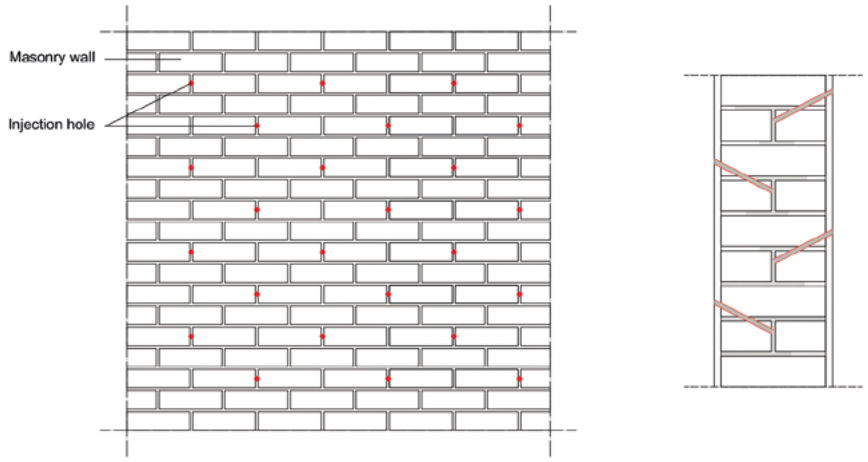

Figure 72. Injection of grout or epoxy resin.

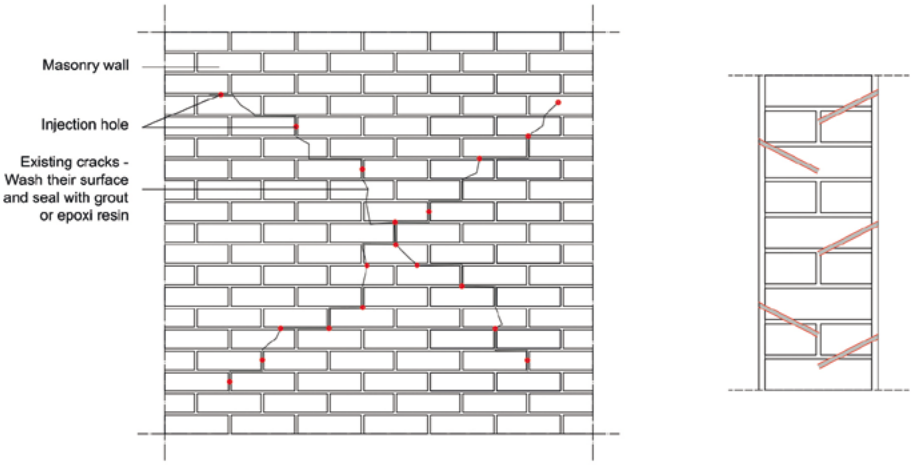

Figure 73. Injection of grout or epoxy resin in cracks.

SUMARY

6.2.1.4. Reinforced concrete elements

As for global actions using reinforced concrete elements, two techniques can be highlighted: rigid core and confinement by means of tie beams or columns (figure 74).

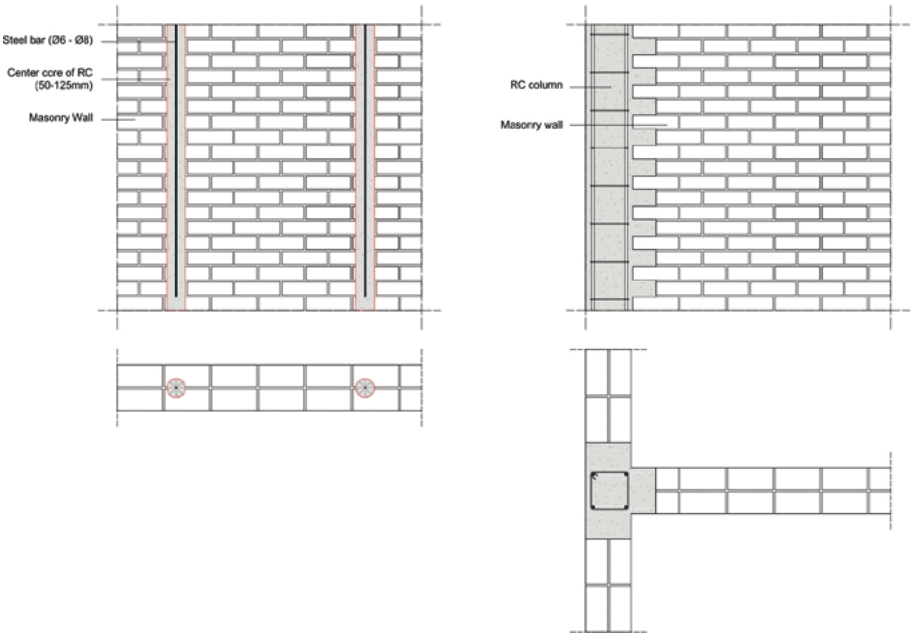

Figure 74. General action with reinforced concrete elements. (a) rigid core and (b) confinement with RC columns and beams.

The rigid core system is executed by drilling holes in the centre of the wall along its entire height up to the foundation. The usual diameter of the hole is 50-125 mm, depending on the thickness of the structural element and the characteristics of the intervention. After placing the reinforcement in the hole, cement grout or polymer/epoxy sand is pumped in, until the hole is filled. This method increases the lateral resistance and the energy dissipation capacity of the wall. Furthermore, it has no architectural impact on the building.

SUMARY

When using a confinement system, reinforced concrete columns are introduced at each corner, at the ends and in the wall gaps. In the case of long walls, the columns are inserted at regular intervals. These columns are connected horizontally by means of tie beams on each floor or, in the case of a great height, at regular intervals. These elements are made of reinforced concrete with variable dimensions according to the characteristics of the reinforcement. This system improves the ductility, the energy dissipation capacity of the wall, and its out-of-plane behaviour.

However, the execution of these two retrofitting techniques is complicated, compared to the ones, in which only the outside of the wall is involved.

6.2.1.5. Carbon fibre reinforced polymers (CFRP)

Carbon fibre reinforced polymers (CFRP) (figure 75) is one of the most widely used materials in the seismic retrofitting of URM buildings. There are various configurations, which can be executed on one or both sides of the wall. However, they are usually placed on the outside of the wall to obtain greater ease and speed of execution. These reinforcements are usually covered with shotcrete or mortar and are completely integrated into the wall. The method considerably improves the strength, displacement capacity and energy dissipation capacity of walls.

It has several advantages: low weight, high mechanical properties, lack of corrosion and high feasibility of installation (Proença *et al.*, 2012). Most CFRP studies focus on the analysis of the strength of compression diagonals through the application of cyclic loads and analyse the behaviour of reinforced walls. In (Martinelli *et al.*, 2016), the authors examined broad bands of fibre vertically, horizontally, and diagonally. In (Turco *et al.*, 2006), the bands used were narrow and the reinforcement was embedded in channels. As concluded in (Papanicolaou *et al.*, 2011; Faella *et al.*, 2010; Capozucca, 2013), this technique has two main weaknesses: the lack of adhesion between the bands and the wall, and its high price. In (Fathalla and Salem, 2018), a four-storey residential building was reinforced with CFRP bands of different thicknesses and configurations. The analysis concluded that CFRP bands have a high capacity to prevent structural collapse with less local damage.

SUMARY

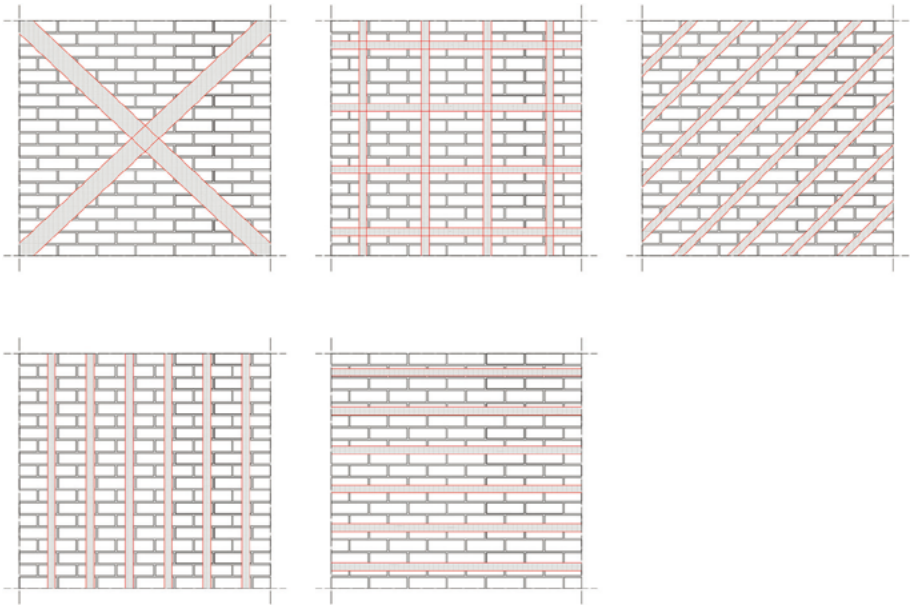

Figure 75. Reinforcement configurations using CFRP bands.

6.2.1.6. Rebaring

An important aspect in this type of building is the presence of openings in the wall, which reduces its seismic capacity. In (Sanaz and Armen, 2012), the authors conclude that the openings significantly affect the seismic behaviour of the wall, causing a concentration of shear forces in some areas of it. Similar conclusions were obtained in the experimental analysis presented by (Reyes *et al.*, 2018), in which the influence of window and door openings in load-bearing walls is analysed. In this study, openings are shown to be a key influencing factor in the shear strength of walls, and damage patterns are generally concentrated in the areas between them. This phenomenon has also been corroborated by inspections of school buildings following major earthquakes (Augenti *et al.*, 2004). In the case of the earthquake in the Italian region of Molise in 2002, masonry walls with a greater number of openings were found to have deeper and more severe cracks. All these studies establish that the presence of a high opening ratio considerably increases the seismic vulnerability of URM buildings.

SUMARY

A recent experimental study analysed a new technique for reinforcing masonry walls (Proença *et al.*, 2019), which consists of installing steel bars in the openings perimeter. A wall sample was tested cyclically until failure, first without reinforcement and then with a steel rebar. The results showed that the rebaring produced a significant increase in resistance and deformation capacity in plane, as well as in the energy dissipation accumulated until collapse. Although it is a very efficient and novel technique, studies and experimental data on it are currently limited.

This system can be executed with a tubular profile embedded in the perimeter of the opening (figure 76) or, externally, by means of another type of steel profile, such as the one in (figure 77). If a surface reinforcement is carried out using steel rod mesh (see section 6.2.1.1 Wire mesh in this chapter), the opening can be reinforced by increasing the amount of reinforcement on the perimeter itself.

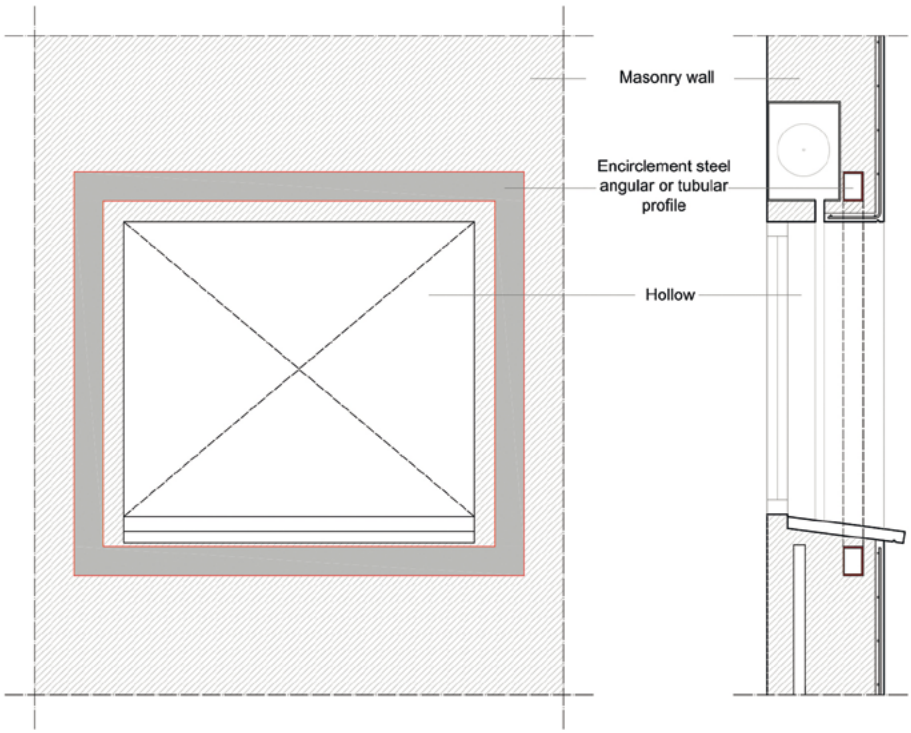

Figure 76. Steel rebar in opening perimeter. Elevation and cross-section.

SUMARY

6.2.2. Retrofitting schemes considered

In accordance with the characteristics of the buildings studied, several of the solutions set out in the previous section have been selected as suitable: wire mesh on the outer surface of the wall, CFRP mesh, and metal rebars for openings (figure 77). These solutions have been studied in depth.

All of them can be implemented working exclusively from the outside of the building, without affecting the rooms. They are cheap and easy to carry out and, furthermore, do not interfere with the configuration and use of the wall on which they are applied. The retrofitting is fully integrated into the building, without causing any visual impact. Furthermore, these solutions are reversible and do not change the configuration of the building.

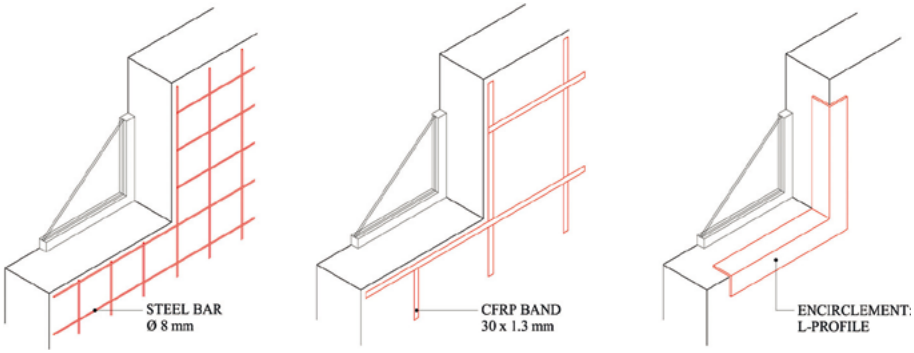

(a) (b) (c)

Figure 77. Retrofitting systems analysed: steel mesh (a), CFRP mesh (b), and steel rebar (c).

The first technique is based on the addition of a steel mesh on the outside of the load-bearing walls, as shown in figure 77 (a). For its execution, it is necessary to remove the existing paint and plaster and to apply a bonding layer of acrylic resin. Then, the meshes are placed by means of mechanical anchors, and finally they are plastered and painted. The technique requires the use of skilled labour. The work is carried out exclusively outside the wall and, therefore, does not involve interrupting the normal development of the teaching activity in the school. Another advantage of this technique is its low cost and easy implementation.

The second technique consists of reinforcing the walls with carbon fibre reinforced polymer mesh (CFRP), figure 77 (b). The execution procedure is similar to that used in the previous technique, but in this case the bands are stuck on with epoxy resin. CFRP is a very efficient material that also allows to

SUMARY

considerably improve the resistance conditions and capacity of the wall; however, it is expensive. As with wire mesh, the execution is carried out from the outside of the building, making it easier to implement, and the solution does not change in any way the aesthetics or functionality of the wall on which it is applied.

With the third technique, metal rebaring (figure 77 [c]), the properties of the wall are improved by intervening in the openings, which are the weak points of this type of structures. To do this, the window sills must be removed and then metal profiles made of rolled steel must be placed in the outer corner of the openings. The profiles, which form a frame, are fixed to the wall by means of mechanical anchors. Finally, the existing sill is replaced. Like the two previous methods, rebaring has good architectural integration in the building, as well as an easy and fast execution that is carried out from the outside of the building. When the behaviour of a wall reinforced with this technique is compared with that of a solid wall (without openings), the results are similar, especially in terms of maximum resistance. In addition to this, this technique presents an outstanding cost-benefit ratio.

In the studies carried out in this project, the relative effectiveness of the selected techniques was studied by carrying out non-linear static numerical analyses of as built and retrofitted models. The results obtained show that all the retrofitting techniques improve the seismic behaviour with respect to that of the original structure, greatly increasing its resistant capacity and notably reducing the target displacement at the performance point.

In the model reinforced with rebaring, a decrease in the openings deformation has been observed, thus causing an increase in the stiffness of the structure. This retrofitting technique is the best in terms of cost-benefit ratio, since the retrofit is carried out locally, and not in the entire surface of the wall and with very cheap materials.

The addition of a steel mesh with ø8 rods spaced 20 cm and L120.12 rebars has caused the greatest reduction in damage levels. Generally, most retrofitting systems have improved the level of damage, except for some configurations.

In terms of cost, CFRP band reinforcement is the most expensive reinforcement technique. However, this solution has not reached maximum efficiency in terms of improving seismic behaviour. In general, the addition of L120.12 bars has been shown to have the best cost-benefit ratio.

The addition of bars has reduced deformation, increasing thee stiffness of the structure. The addition of a steel mesh has caused the greatest increase in maximum strength. However, the addition of bars has led to the greatest reduction in displacement of the performance point.

SUMARY

6.3. REINFORCED CONCRETE BUILDINGS

Most of the school buildings studied have a reinforced concrete structure (see section 3.2), generally RC columns and beams, and one-way spanning RC floors. Most of them have a sanitary slab on the ground floor, typically a one-way reinforced concrete slab. School buildings with two-way reinforced concrete slabs can also be found, but to a lesser extent. There is a multitude of configurations and dimensions (dimensions of columns and beams, spans, no. of load-bearing frames, no. of columns, etc.).

These buildings have, in a significant number of cases, one or more of the following weaknesses:

- Short columns due, generally, to horizontal openings, infills that do not reach the ceiling or sanitary slabs.
- Soft storey in the ground floor due to the presence of a diaphanous ground floor or an exterior covered porch designed for a recreation area.
- Two-way slabs, which have low ductility and inadequate functioning in the face of seismic action.
- Irregularities (atriums / setbacks).
- High mass at high points.

It is important to carry out a first analysis where these weak points are detected, since the directly affect the seismic behaviour of the structure. Furthermore, their detection is relevant to decide what type of retrofitting scheme to use and the possible areas to reinforce.

There are numerous retrofitting techniques for improving the seismic behaviour of reinforced concrete buildings. The most widely used strategies are generally based on systems of reinforcement, stiffening and improvement of the building's deformation capacity, which make it possible to correct the deficiencies observed in the buildings studied (short columns, soft storey, etc.). The reduction of seismic demand has also been widely studied, with the incorporation of base isolation devices. However, these are expensive and sophisticated systems, designed for more complex and higher buildings; therefore, they do not apply in the case of the school buildings studied, since they only have one or two floors.

SUMARY

6.3.1. State of the art

There are numerous studies on the different techniques of seismic retrofitting for reinforced concrete buildings —some carried out on real buildings and most of them on theoretical laboratory models. Reinforcement systems and increased stiffness are the most widely used, and are essentially based on the incorporation of bracing with various configurations (figure 78), energy dissipation systems, jackets (figure 81) and shear walls (figure 79 and figure 80).

6.3.1.1. Bracings

The steel bracing stiffening system is one of the most widely used. It increases the strength and stiffness of the structure, and can be applied in several configurations (figure 78). Special attention should be paid to the anchorage points to the existing structure, where stresses are concentrated.

This method is relatively inexpensive and easy to implement in existing structures, with a short execution time. In addition, it is easily reversible. On the other hand, it can compromise the aesthetics of the building and even, in some cases, interfere with its functional configuration.

The behaviour of structures in which steel braces were incorporated was analysed experimentally in (TahamouliRoudsari *et al.*, 2017; Ozcelik *et al.*, 2012). In (Ozcelik *et al.*, 2012), a comparison was made between the improvement produced by shear walls and steel bracing, respectively. The results show that models with steel bracing have a higher capacity than models with shear walls.

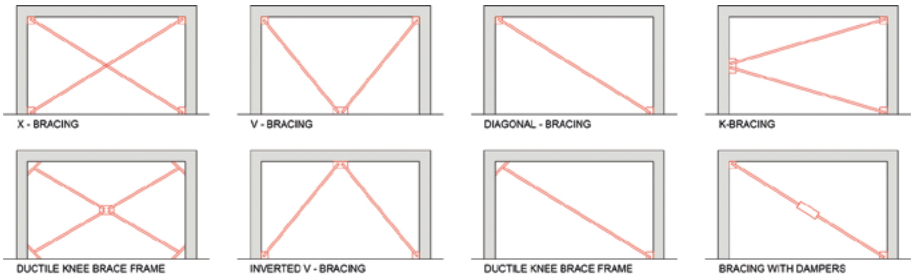

Figure 78. Steel bracing typical configurations.

SUMARY

In other studies, the use of other materials for the execution of the bracing was evaluated, so that the fragile rupture that conventional steel elements can present could be avoided. In (Ju *et al.*, 2014), for example, cross bracing with carbon fibre elements was analysed. This system increases the resistance and does not have fragile rupture, however, it is a relatively expensive and is not necessary for the seismic demand that exists in the area of Algarve and Huelva.

The effects of steel cross bracing on the columns of a building were analysed in (Rahimi and Maheri, 2018). This study concludes that, in the tallest buildings, the elements located on the upper floors have adverse effects on the columns to which they are connected. However, for low-rise buildings, such as school buildings, steel cross bracing has a positive effect on the stiffness and seismic capacity, without adversely affecting the columns to which the bracing is connected.

Other studies, such as (Mazzolani, 2008), analysed different types of stiffening systems in existing structures. These were statically and dynamically tested. The results show the effectiveness of the steel reinforcement systems analysed, improving the stiffness, strength and ductility of the original building.

6.3.1.2. Energy dissipation systems

This type of retrofitting system is tipycally used in areas with very high seismic demand. They are implemented in structures that present a high deformation due to the global flexibility of the structure. There are several types of dissipative elements that can be used: fluid-viscous (hydraulic), metallic or friction elements. Either of them can be implemented in the structure itself or integrated in the bracing systems.

The energy dissipation systems (dampers) included in the steel bracing systems or in the structural elements themselves have been analysed in numerous studies, as well as the effects of the different types of dissipate devises: fluid viscous dampers (Ozcelik *et al.*, 2012), steel plates (TahamouliRoudsari *et al.*, 2018), steel rods (Ozcelik *et al.*, 2011), honeycomb (Lee *et al.*, 2017), or joints (Oh *et al.*, 2009). The results of these analyses show that these systems could considerably improve the seismic behaviour of buildings.

6.3.1.3. Shear walls

Shear walls are one of the most commonly used systems within the stiffening strategies, both in new construction and in the rehabilitation of existing structures. In rehabilitation, it is applied when the structure does not have enough

SUMARY

resistance to lateral loads. The method increases the strength and stiffness of the existing structure. The walls can be built using reinforced concrete (figure 79) or steel elements (steel laminated sheets) (figure 80), in one or more heights, and must be rigidly anchored on their perimeter to the frame they are reinforcing.

Figure 79. Reinforced concrete shear wall.

The added walls must, of course, be blind, so they could potentially interfere with the functionality of the building.

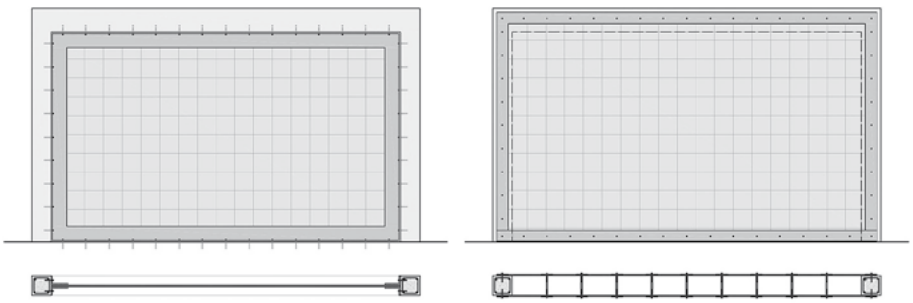

Figure 80. Steel shear wall.

SUMARY

6.3.1.4. Confinement jackets

To use the confinement method via jackets, one or more columns are wrapped with steel plates, reinforced concrete or carbon fibre (FRP) (figure 81). This method increases the strength of the vertical structural element, increasing its ability to resist lateral forces induced by seismic action. In addition, it provides confinement to the column, improving its deformation capacity or ductility. It should be noted that this type of system improves the seismic behaviour of short columns too, which are one of the most common weak points in the type of structures under study.

The jackets are fully integrated in the structure, not interfering with the functionality and aesthetics of the building. On the other hand, the elements that are reinforced can be interior, the implementation in this case having a greater impact on the normal development of the activities in the building. In addition, the intervention could involve the temporary removal, full or partial, of some partitions attached to the reinforced columns.

Many approaches have been proposed to improve the deformation capacity of buildings. The effects of incorporating reinforced concrete and reinforced polymer fibre (FRP) (figure 81) jackets into columns were evaluated in (Oh *et al.*, 2009). In these studies, non-linear analyses and physical tests were performed. The effects of these systems were compared with those resulting from the addition of steel bracing and reinforced concrete shear walls. Results showed that non-linear static analyses could be considered an important tool for evaluating aggregate reinforcement interventions in existing reinforced concrete buildings. The effects of the addition of reinforced concrete jackets in columns were experimentally compared with those by adding carbon fibre reinforced polymer (CFRP) in (Oh *et al.*, 2009; Raychowdhury and Hutchinson, 2009; Colomb *et al.*, 2008). Furthermore, it was noted that the position of the reinforcements is important to avoid unfavourable torsional effects.

In (Valente and Milani, 2018), the effectiveness of the following three reinforcement solutions was evaluated: reinforced concrete jacket (figure 81), steel bracing (figure 78) and RC shear (figure 79). It was concluded that steel bracing reduces the demand of displacement and increases the deformation and dissipation capacities of the structure. However, this type of reinforcement increases the stresses in the connection between the reinforcing element and the structure.

Finally, (Seo *et al.*, 2018) presented a new algorithm to obtain the required amount and optimal position of FRP reinforcements.

SUMARY

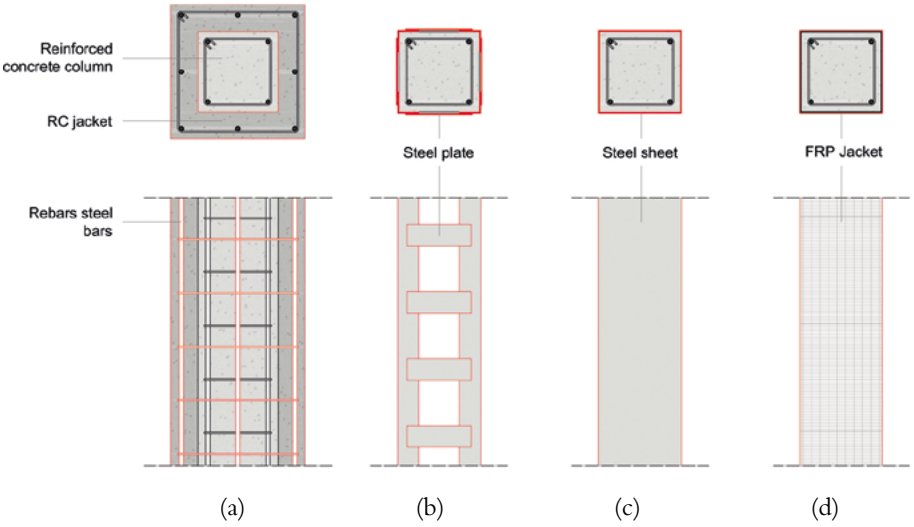

Figure 81. Systems for improving the deformation capacity by additional confinement: a) Reinforced concrete jacket; b) Steel jacket; c) Continuous steel jacket; d) FRP jacket.

6.3.2. Retrofitting schemes considered

In the studies conducted in this project, a series of retrofitting schemes were chosen, as they are the most suitable ones when considering the characteristics of the main types of buildings studied (linear and compact, see chapter 3.2).

The main shortcomings of these buildings are due to irregularities in floors and height. The presence of atriums on the ground floor, with no infills, gives rise to a sudden change in stiffness, with these infills present on the upper floors. This atrium is not necessarily located along the entire length of the façade, nor in the centre of it, which gives rise to undesirable twists in the building's response. In addition, as the infills are set back on the ground floor, there are isolated façade columns, sometimes higher than the other floors, which reinforce this change in stiffness, creating a soft floor. To improve these aspects, the following solutions are selected (figure 78):

— steel bracings in "X" configuration,
— steel bracings in "V" configuration,
— steel bracings in "K" configuration.

SUMARY

On the other hand, on the upper floors, infills with horizontal openings can lead to the formation of short columns. These can be corrected by (figure 81):

— reinforced concrete jackets,

— steel jackets.

Additionally, many of these buildings were built before seismic regulations came into force, which means that the details of the beam-column connections may not be enough to consider the frames as rigid, leaving the building with insufficient resistance to lateral loads. This situation can be improved by:

— individual steel braces at column-beam joints,

— reinforced concrete shear walls (figure 79).

The effectiveness of each proposed solution has been studied exhaustively based on its cost-effectiveness, efficiency and architectural integration. To speed up the process, a reinforcement index where all these factors are applied has been developed. It can be seen in the following section (6.4 Seismic Reinforcement Index).

Non-linear static analysis reveals that introducing elements in the most vulnerable direction of the building can lead to higher efficiency values than incorporating few elements in both directions. In this sense, shear walls lead to improvements in both directions. For this reason, it is very important to conduct a first analysis to detect the weak points and the seismic behaviour of the building, to identify which is the most vulnerable direction and the most effective zones to introduce the seismic reinforcement in.

The steel bracing is the solution that produces the greatest improvement in the overall seismic behaviour of the building. This system increases resistance and stiffness, considerably improving the soft floor effect. However, the most effective areas should be carefully studied, as these solutions have the greatest architectural impact. This system is the most cost-effective according to the values obtained, after applying the reinforcement index method (see section 6.4) and after being compared with the other reinforcement solutions.

Reinforcement by means of individual bracing has been shown to be an acceptable technique. However, we concluded that the number and position of the reinforcement elements is key for obtaining high efficiency of the retrofitting.

In terms of cost, the most economical reinforcement techniques are the installation of steel jackets and individual bracing on the columns, with the latter being the most cost-effective (and least architecturally harmful). Steel and reinforced concrete jackets are the least profitable techniques due to their low efficiency values and high cost. Furthermore, it has been shown that it is not necessary to add reinforcement elements to all the columns or openings

SUMARY

of a building. Selecting the most effective positions for the installation of the reinforcement must be done carefully to achieve cost-effective improvements.

6.4. SEISMIC RETROFITTING INDEX

A tool has been developed to classify the various reinforcements within the scope of this project. The seismic retrofitting (SR) index proposed by (Requena-García-Cruz *et al.*, 2019) is based on efficiency, cost and architectural impact. It focuses on the most salient aspects affecting buildings. It is obtained through Eq. (41), and is based on the following parameters: the efficiency index (EI), the cost index (CI) and the architectural impact index (AI).

$$R_I = \alpha_1 \delta E_I + \alpha_2 \beta C_I + \alpha_3 \gamma A_I \qquad \text{Eq. (41)}$$

Coefficients δ, β and γ modify the main indexes according to the unique aspects of each situation. Coefficients α_1, α_2 and α_3 are the important factors.

This method can be applied to any seismic retrofitting scheme. The results obtained in the analysis carried out have shown that this method satisfactorily fulfils the proposed objective. Furthermore, it can be adapted to the reinforcements applied to URM buildings. In this case, the different parameters of efficiency and architectural impact should be modified according to the reinforcement methods applied to this type of building.

SUMARY

SUMARY

Chapter 7. Example of seismic retrofitting

The retrofitting techniques analysed within the research project have been applied in two of the schools that were more vulnerable to earthquakes. These schools present one of the most unfavourable School-score indexes and, therefore, they have greater need for seismic retrofitting compared to the other school buildings. A project for the seismic rehabilitation of a school building in the province of Huelva (Spain) and another in the Algarve region (Portugal) has been carried out. The project carried out at the school in Huelva is briefly described below.

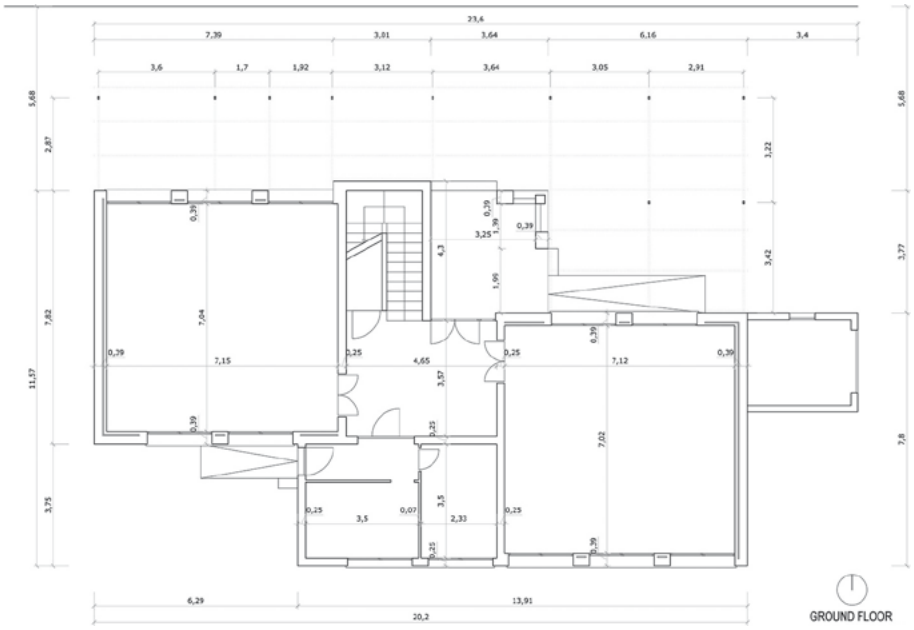

Figure 82. Ground floor. C.E.I.P. Los Llanos, Almonte (Huelva).

SUMARY

The project for the seismic retrofitting of a URM school building in the province of Huelva has been carried out. The school was the C.E.I.P. "Los Llanos" located in Calle Los Llanos, no. 10, in the town of Almonte (Huelva). It should be noted that this URM building presented one of the most unfavourable School-score index. Furthermore, because of its size (figure 82 and figure 83), it adapts to the conditions and scale of intervention proposed in the project. In this project, the seismic retrofitting techniques analysed in the study on the seismic reinforcement of URM school buildings (Segovia-Verjel *et al.*, 2019), carried out in the research project, have been applied.

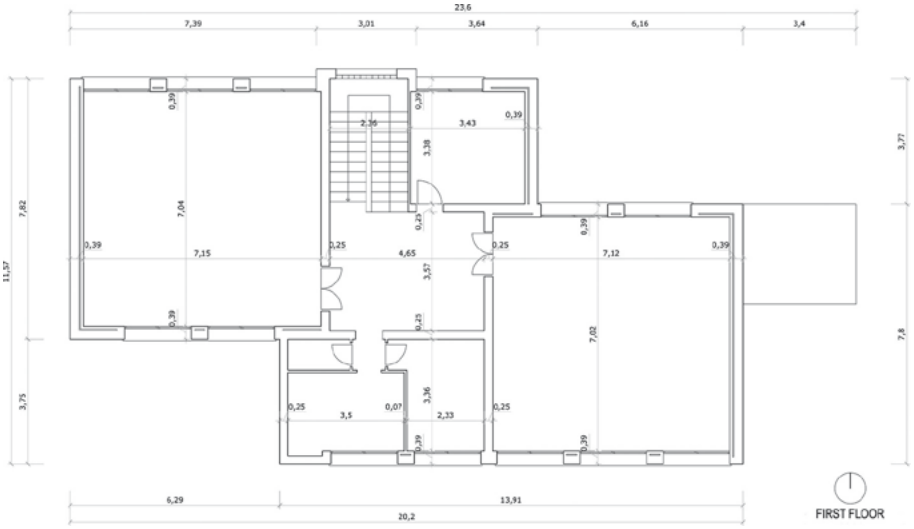

Figure 83. First floor. C.E.I.P. Los Llanos, Almonte (Huelva).

In this case, two retrofitting methods have been applied: the installation of a steel mesh on the outer side of the wall; and the reinforcement of the façade openings by means of a rebar plus an increase in the density of the steel mesh.

SUMARY

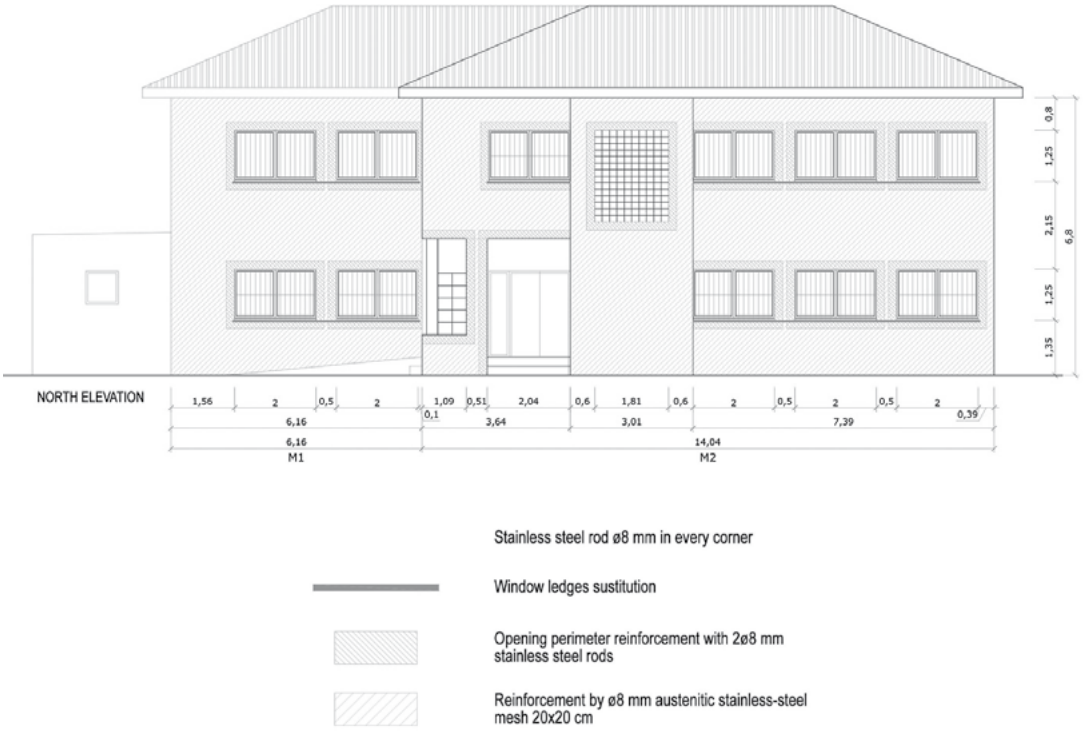

Figure 84. North elevation. C.E.I.P. Los Llanos, Almonte (Huelva).

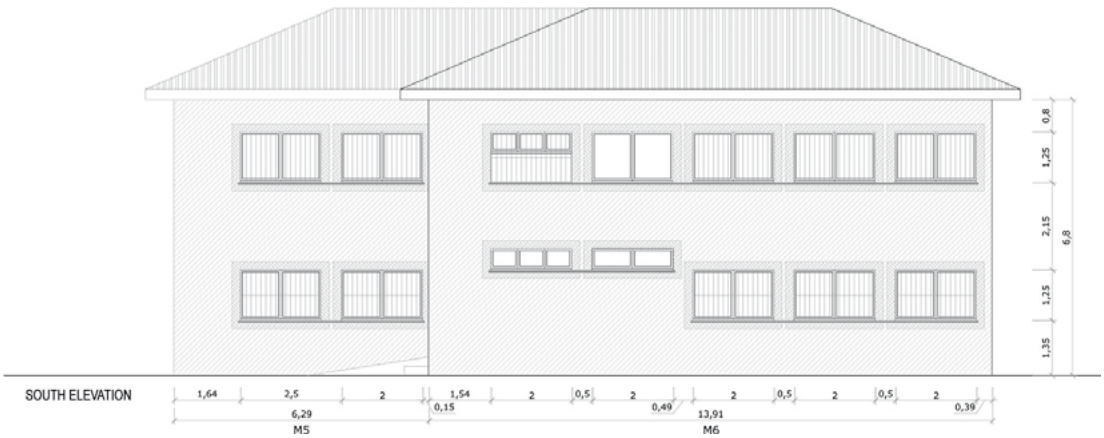

Figure 85. South elevation. C.E.I.P. Los Llanos, Almonte (Huelva).

SUMARY

Figure 86. East elevation. C.E.I.P. Los Llanos, Almonte (Huelva).

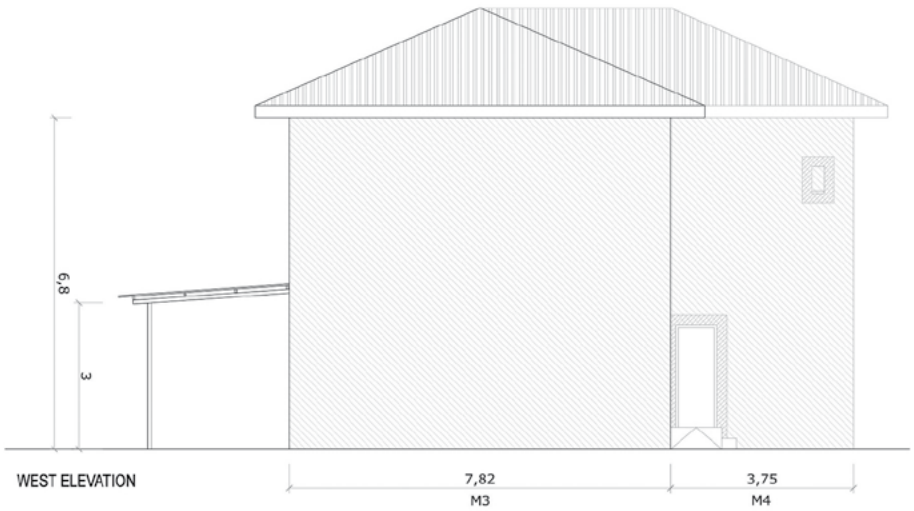

Figure 87. West elevation. C.E.I.P. Los Llanos, Almonte (Huelva).

SUMARY

The retrofitting consisted on the following steps:

- Step 1: Preparation of the external wall surface by sandblasting aluminium silicate particles.
- Step 2: Application of acrylic resin bonding agent on the exposed mortar.
- Step 3: Placing of austenitic stainless-steel mesh of 20 × 20 cm Ø8 mm on the wall by means of mechanical anchoring with zinc-coated screws of Ø8 mm and 120 mm in length.
- Step 4: Application of unrodded cement mortar on the mesh.
- Step 5: Installation of fibreglass mesh covered with PVC.
- Step 6: Application of a screeded and trowelled cement mortar.
- Step 7: Surface finish with cement-based stone paint.

This procedure was applied to the entire surface of the external face of the load-bearing walls, paying special attention to the door and window openings, where additional bars were placed on the perimeter. The perimeter of the openings was also reinforced with steel rods, can be seen in figure 80. This retrofitting scheme produces a similar effect to the rebaring method analysed in the study in section 6.2.

SUMARY

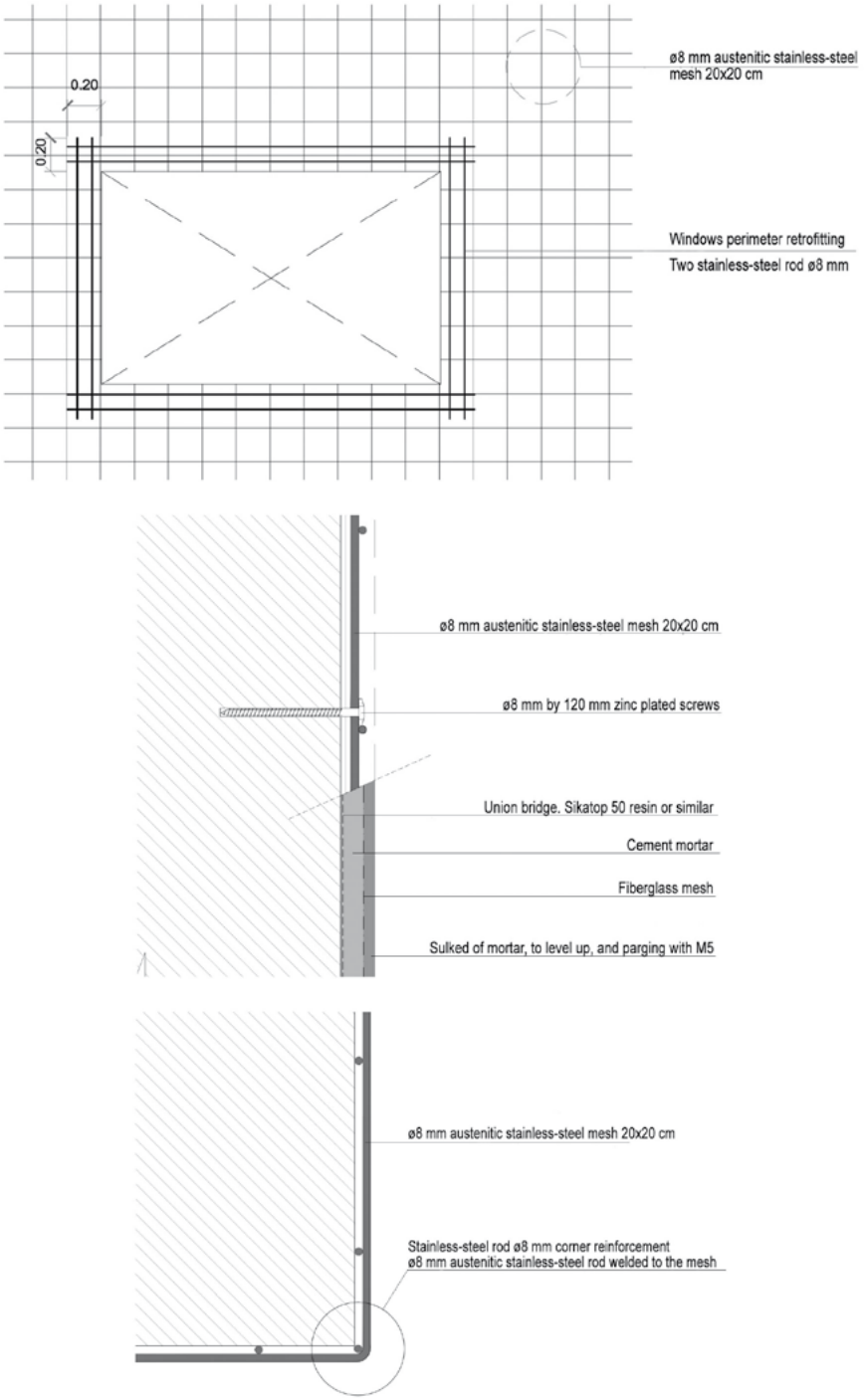

Figure 88. Construction details. Seismic retrofitting project by the C.E.I.P. School Los Llanos, Almonte (Huelva).

SUMARY

References

Abeling, S., Dizhur, D., Ingham, J. (2018). An evaluation of successfully seismically retrofitted URM buildings in New Zealand and their relevance to Australia. Aust. J. Struct. Eng. 19, 234-244. <https://doi.org/10.1080/13287982.2018.1491820>.

AENOR (2018a). Eurocódigo 2: Proyecto de estructuras de hormigón. Parte 1: Reglas generales, acciones sísmicas y reglas para edificación.

—— (2018b). Eurocódigo 8: Proyecto de estructuras sismorresistentes. Parte 3: Evaluación y adecuación sísmica de edificios.

—— (2013). Eurocódigo 6: Proyecto de estructuras de fábrica. Parte 1-1: Reglas generales para estructuras de fábrica armada y sin armar.

—— (1998). Eurocódigo 8: Proyecto de estructuras sismorresistentes. Parte 1: reglas generales, acciones sísmicas y reglas para edificación (EC8-1). Madrid (España).

American Society of Civil Engineers (ASCE) (2000). FEMA-356: prestandard and Commentary for the Seismic Rehabilitation of Building. Estados Unidos.

Andrade, F.O. (1993). Construir en ladrillo dentro de una norma válida. Rev. Edif. 16, 37-50.

Applied Technology Council (ATC) (1996). ATC-40: Seismic evaluation and retrofit of concrete buildings. California.

Augenti, N., Cosenza, E., Dolce, M., Manfredi, G., Masi, A., Samela, L. (2004). Performance of School Buildings during the 2002 Molise, Italy, Earthquake. Earthq. Spectra 20, S257-S270. <https://doi.org/10.1193/1.1769374>.

Autoridade Nacional de Protecção Civi (ANPC) (2010). Estudo do risco sísmico e de isunamis do Algarve. Autoridade Nacional de Protecção Civil, Carnaxide, Portugal.

Barbat, A.H., Pujades, L.G., Lantada, N. (2008). Seismic damage evaluation in urban areas using the capacity spectrum method: Application to Barcelona. Soil Dyn. Earthq. Eng. 28, 851-865. <https://doi.org/10.1016/j.soildyn.2007.10.006>.

Battarra, M., Balcik, B., Xu, H. (2018). Disaster preparedness using risk-assessment methods from earthquake engineering. Eur. J. Oper. Res. 269, 423-435. <https://doi.org/10.1016/J.EJOR.2018.02.014>.

Campos Costa, A., Sousa, M.L., Carvalho, A. (2008). Seismic Zonation for Portuguese National Annex of Eurocode 8, 8-15.

Capozucca, R. (2013). Effects of mortar layers in the delamination of GFRP bonded to historic masonry. Compos. Part B Eng. 44, 639-649. <https://doi.org/10.1016/j.compositesb.2012.02.012>.

SUMARY

Carre, E., Zornoza, V. (2011). Terremotos en la Península Ibérica. Enseñanzas las Ciencias la Tierra 19.3, 289-295.

Colomb, F., Tobbi, H., Ferrier, E., Hamelin, P. (2008). Seismic retrofit of reinforced concrete short columns by CFRP materials. Compos. Struct. 82, 475-487. <https://doi.org/10.1016/j.compstruct.2007.01.028>.

Del Gaudio, C., Ricci, P., Verderame, G.M., Manfredi, G. (2017). Urban-scale seismic fragility assessment of RC buildings subjected to L'Aquila earthquake. Soil Dyn. Earthq. Eng. 96, 49-63. <https://doi.org/10.1016/j.soildyn.2017.02.003>.

Diz, S., Costa, A., Costa, A.A. (2015). Efficiency of strengthening techniques assessed for existing masonry buildings. Eng. Struct. 101, 205-215. <https://doi.org/10.1016/j.engstruct.2015.07.017>.

Dolce, M., Ponzo, F.C., Di Croce, M., Moroni, C., Giordano, F., Nigro, D., Marnetto, R., Mazzolani, F.M. (2009). Experimental assessment of the CAM and DIS-CAM systems for the seismic upgrading of monumental masonry buildings 1021--1027--.

Estêvão, J.M.C. (2020). Computational Strategies for Seismic Assessment and Retrofitting of Existing School Buildings. INCREaSE 2019, 1031-1042. <https://doi.org/10.1007/978-3-030-30938-1_81>.

—— (2019). An integrated computational approach for seismic risk assessment of individual buildings. Appl. Sci. 9. <https://doi.org/10.3390/app9235088>.

—— (2016). Utilização do programa EC8spec na avaliação e reforço sísmico de edifícios do Algarve, in: 10º Congresso Nacional de Sismologia e Engenharia Sísmica. Ponta Delgada, Açores.

Estêvão, J.M.C., Carvalho, A. (2015). The role of source and site effects on structural failures due to Azores earthquakes. Eng. Fail. Anal. 56, 429-440. <https://doi.org/10.1016/j.engfailanal.2014.12.010>.

Estêvão, J.M.C., Ferreira, M.A., Braga, A., Carreira, A., Barreto, V., Requena-García-Cruz, M.V, Segovia-Verjel, M.L., Romero-Sánchez, E., de Miguel, J., Morales-Esteban, A., Fazendeiro Sá, L., Sousa Oliveira, C. (2019). Projetos de escolas resilientes aos sismos no território do Algarve e de Huelva (PERSISTAH), in: 11º Congresso Nacional de Sismologia e Engenharia Sísmica.

Estêvão, J.M.C., Oliveira, C.S. (2012). Point and fault rupture stochastic methods for generating simulated accelerograms considering soil effects for structural analysis. Soil Dyn. Earthq. Eng. 43, 329-341. <https://doi.org/10.1016/j.soildyn.2012.07.019>.

—— (2001). Parâmetros que condicionam os valores da casualidade sísmica. 5º Encontro Nac. sobre Sismol. e Eng. Sísmica 29-41.

Faella, C., Martinelli, E., Nigro, E., Paciello, S. (2010). Shear capacity of masonry walls externally strengthened by a cement-based composite material: An experimental campaign. Constr. Build. Mater. 24, 84-93. <https://doi.org/10.1016/j.conbuildmat.2009.08.019>.

Fathalla, E., Salem, H. (2018). Parametric Study on Seismic Rehabilitation of Masonry Buildings Using FRP Based upon 3D Non-Linear Dynamic Analysis. Buildings 8, 124. <https://doi.org/10.3390/buildings8090124>.

Fazendeiro Sá, L., Morales-Esteban, A., Durand, P. (2016). A Seismic risk simulator for Iberia. Bull. Seismol. Soc. Am. 106, 1198-1209. <https://doi.org/10.1785/0120150195>.

Fiorentino, G., Forte, A., Pagano, E., Sabetta, F., Baggio, C., Lavorato, D., Nuti, C., Santini, S. (2018). Damage patterns in the town of Amatrice after August 24th 2016 Central Italy earthquakes. Bull. Earthq. Eng. 16, 1399-1423. <https://doi.org/10.1007/s10518-017-0254-z>.

Freeman, S.A. (2004). Review of the development of the capacity spectrum method. ISET J. Earthq. Technol. 41, 113.

Fulop, L., Suppola, M. (2011). Steel solutions for the seismic retrofit and upgrade of existing constructions Constructive and performance analysis of the retrofit systems for vertical masonry elements.

García-Mayordomo, J., Faccioli, E., Paolucci, R. (2004). Comparative study of the seismic hazard assessments in European national seismic codes. Bull. Earthq. Eng. 2, 51-73. <https://doi.org/10.1023/B:BEEE.0000039046.42398.9d>.

Gràcia, E., Bartolomé, R., Lo Iacono, C., Moreno, X., Martínez-Loriente, S., Perea, H., Masana, E., Pallàs, R., Diez, S., Dañobeitia, J.J., Terrinha, P., Zitellini, N. (2010). Characterizing active faults and associated mass transport deposits in the South Iberian Margin (Alboran Sean and Gulf of Cadiz): on-fault and off-fault paleoseismic evidence, in: Primera Reunión Ibérica Sobre Fallas Activas y Paleosismología, Volumen de Resúmenes. Sigüenza, España, pp. 163-166.

Imprensa Nacional-Casa da Moeda, E.P. (1983). RSAEEP. Regulamento de segurança e acções para estruturas de edifícios e pontes. Decreto-Lei nº 235/83, de 31 de Maio.

Instituto Geológico y Minero de España (2015). Mapa tectónico de la región del sur de la Península [WWW Document].

Ju, M., Lee, K.S., Sim, J., Kwon, H. (2014). Non-compression X-bracing system using CF anchors for seismic strengthening of RC structures. Mag. Concr. Res. 66, 159-174. <https://doi.org/10.1680/macr.13.00165>.

Lee, M., Lee, J., Kim, J. (2017). Seismic retrofit of structures using steel honeycomb dampers. Int. J. Steel Struct. 17, 215-229. <https://doi.org/10.1007/s13296-015-0101-5>.

Maio, R., Estêvão, J.M.C., Ferreira, T.M., Vicente, R. (2017). The seismic performance of stone masonry buildings in Faial island and the relevance of implementing effective seismic strengthening policies. Eng. Struct. 141, 41-58. <https://doi.org/10.1016/j.engstruct.2017.03.009>.

Martín-Caro Álamo, J.A. (2001). Análisis estructural de puentes arco de fábrica: Criterios de comprobación.

Martinelli, E., Perri, F., Sguazzo, C., Faella, C. (2016). Cyclic shear-compression tests on masonry walls strengthened with alternative contions of CFRP strips. Bull. Earthq. Eng. 14, 1695-1720. <https://doi.org/10.1007/s10518-016-9895-6>.

Martínez, J.L., Martín-Caro, J.A., Leon, J. (2001). Comportamiento mecánico de la obra de fábrica. E.T.S. Ingenieros de Caminos, Canales y Puertos. U.P.M.

Mazzolani, F.M. (2008). Innovative metal systems for seismic upgrading of RC structures. J. Constr. Steel Res. 64, 882-895. <https://doi.org/10.1016/j.jcsr.2007.12.017>.

Mazzoni, S., Eeri, M., Castori, G., Galasso, C., Calvi, P., Dreyer, R., Fischer, E., Fulco, A., Sorrentino, L., Wilson, J., Penna, A., Magenes, G. (2018). 2016-2017 Central Italy Earthquake Sequence: Seismic Retrofit Policy and Effectiveness. Earthq. Spectra 34, 1671-1691. <https://doi.org/10.1193/100717EQS197M>.

SUMARY

Meijninger, B.M.L. (2006). Late-orogenic extension and strike-slip deformation in the Neogene of southeastern Spain. Geol. Ultraiectina. Utrecht University.

Meireles, H.A., Bento, R. (2012). Seismic assessment and retrofitting of Pombalino buildings by fragility curves. 15th World Conf. Earthq. Eng. 1-10. <https://doi.org/10.12989/eas.2014.7.1.057>.

Ministerio de Fomento de España (2012). Actualización de mapas de peligrosidad sísmica de España.

—— (2002). Norma de Construcción Sismorresistente NCSE-02 35898-35967.

Ministerio de la Vivienda de España (1972). Norma MV-201: Muros resistentes de fábrica de ladrillo. España.

Ministerio de Obras Públicas Trasnportes y Medio Ambiente (1994). Norma de Construcción Sismorresistente: Parte General y Efificación (NCSE-94).

—— (1990). Norma básica de la edificación NBE FL-90: Muros resistentes de fábrica de ladrillo.

Ministerio de Planificación del Desarrollo (1974). Norma sismorresistente PDS-1. Parte A.

—— (1968). Norma sismorresistente PGS-1. Parte A. Boletín Of. del Estado.

Morales-Esteban, A., Martínez-Álvarez, F., Scitovski, S., Scitovski, R. (2014). A fast partitioning algorithm using adaptive Mahalanobis clustering with application to seismic zoning. Comput. Geosci. 73, 132-141. <https://doi.org/10.1016/j.cageo.2014.09.003>.

Nacional, I. (1961). RSEP. Regulamento de solicitações em edifícios e pontes. Decreto nº 44 041, de 18 de Novembro de 1961.

—— (1958). RSCCS. Regulamento de segurança das construções contra os sismos. Decreto n. 41 658, de 31 de Maio.

NTC (2008). Decreto Ministeriale 14/1/2008. Norme tecniche per le costruzioni. Ministry of Infrastructures and Transportations. G.U. S.O. n.30 on 4/2/2008; 2008 [in Italian], n.d.

Oh, S.H., Kim, Y.J., Ryu, H.S. (2009). Seismic performance of steel structures with slit dampers. Eng. Struct. 31, 1997-2008. <https://doi.org/10.1016/j.engstruct.2009.03.003>.

Oliveira, C.S. (1977). Sismologia, Sismicidade e Risco Sísmico. Aplicações em Portugal, in: Laboratório Nacional de Engenharia Civil. Lisboa, p. 205.

Oliveira, C.S., Campos-Costa, A., Sousa, M.L. (2000). Definition of seismic action in the context of EC8. Topics for discussion. 12th World Conf. Earthq. Eng. 1-8.

Ozcelik, R., Akpınar, U., Binici, B. (2011). Seismic Retrofit of Deficient RC Structures with Internal Steel Frames. Adv. Struct. Eng. 14, 1205-1222. <https://doi.org/10.1260/1369-4332.14.6.1205>.

Ozcelik, R., Binici, B., Kurç, O. (2012). Pseudo dynamic testing of an RC frame retrofitted with chevron braces. J. Earthq. Eng. 16, 515-539. <https://doi.org/10.1080/13632469.2011.653297>.

Papanicolaou, C., Triantafillou, T., Lekka, M. (2011). Externally bonded grids as strengthening and seismic retrofitting materials of masonry panels. Constr. Build. Mater. 25, 504-514. <https://doi.org/10.1016/j.conbuildmat.2010.07.018>.

Peter Fajfar, M.E. (2000). A Nonlinear Analysis Method for Performance Based Seismic Design. Earthq. Spectra 16, 573-592. <https://doi.org/10.1193/1.1586128>.

Proença, J., Gago, A.S., Cardoso, J., Cóias, V., Paula, R. (2012). Development of an innovative seismic strengthening technique for traditional load-bearing masonry walls. Bull. Earthq. Eng. 10, 113-133. <https://doi.org/10.1007/s10518-010-9210-x>.

Proença, J.M., Gago, A.S., Vilas Boas, A. (2019). Structural window frame for in-plane seismic strengthening of masonry wall buildings. Int. J. Archit. Herit. 13, 98-113. <https://doi.org/10.1080/15583058.2018.1497234>.

Rahimi, A., Maheri, M.R. (2018). The effects of retrofitting RC frames by X-bracing on the seismic performance of columns. Eng. Struct. 173, 813-830. <https://doi.org/10.1016/j.engstruct.2018.07.003>.

Raychowdhury, P., Hutchinson, T.C. (2009). Performance evaluation of a nonlinear Winkler-based shallow foundation 679-698. <https://doi.org/10.1002/eqe>.

Requena-García-Cruz, M.-V., Morales-Esteban, A., Durand-Neyra, P., Estêvão, J.M.C. (2019). An index-based method for evaluating seismic retrofitting techniques. Application to a reinforced concrete primary school in Huelva. PLoS One 14, e0215120. <https://doi.org/10.1371/journal.pone.0215120>.

Reyes, J.C., Yamin, L.E., Hassan, W.M., Sandoval, J.D., Gonzalez, C.D., Galvis, F.A. (2018). Shear behavior of adobe and rammed earth walls of heritage structures. Eng. Struct. 174, 526-537. <https://doi.org/10.1016/j.engstruct.2018.07.061>.

Ruiz-Pinilla, J.G., Adam, J.M., Pérez-Cárcel, R., Yuste, J., Moragues, J.J. (2016). Learning from RC building structures damaged by the earthquake in Lorca, Spain, in 2011. Eng. Fail. Anal. 68, 76-86. <https://doi.org/10.1016/j.engfailanal.2016.05.013>.

Sá, L., Morales-Esteban, A., Durand Neyra, P. (2018). The 1531 earthquake revisited: loss estimation in a historical perspective. Bull. Earthq. Eng. 16, 4533-4559. <https://doi.org/10.1007/s10518-018-0367-z>.

Salgado-Gálvez, M.A., Carreño, M.L., Barbat, A.H., Cardona, O.D. (2016). Evaluación probabilista del riesgo sísmico en Lorca mediante simulaciones de escenarios. Rev. Int. Métodos Numéricos para Cálculo y Diseño en Ing. 32, 70-78. <https://doi.org/10.1016/j.rimni.2014.12.001>.

Sanaz, R., Armen, D.K. (2012). A stochastic ground motion model with separable temporal and spectral nonstationarities. Earthq. Eng. Struct. Dyn. 41, 1549-1568. <https://doi.org/10.1002/eqe>.

Segovia-Verjel, M.L., Requena-García-Cruz, M.V., De-Justo-Moscardó, E., Morales-Esteban, A. (2019). Optimal seismic retrofitting techniques for URM school buildings located in the southwestern Iberian peninsula. PLoS One 14. <https://doi.org/10.1371/journal.pone.0223491>.

Seo, H., Kim, J., Kwon, M. (2018). Optimal seismic retrofitted RC column distribution for an existing school building. Eng. Struct. 168, 399-404. <https://doi.org/10.1016/j.engstruct.2018.04.098>.

Shabdin, M., Attari, N.K.A., Zargaran, M. (2018). Experimental study on seismic behavior of Un-Reinforced Masonry (URM) brick walls strengthened with shotcrete. Bull. Earthq. Eng. 16, 3931-3956. <https://doi.org/10.1007/s10518-018-0340-x>.

Silva, P.G., Rodriguez Pascua, M.A. (2014). Catálogo de los efectos geológicos de los terremotos en España, in: Asociación Española para el Estudio del Cuaternario (ed.), Riesgos Geológicos/Geotecnia Nº 4. Instituto Geológico y Minero de España.

SUMARY

Spinella, N. (2019). Push-over analysis of a rubble full-scale masonry wall reinforced with stainless steel ribbons. Bull. Earthq. Eng. 17, 497-518. <https://doi.org/10.1007/s10518-018-0461-2>.

TahamouliRoudsari, M., Entezari, A., Hadidi, M.H., Gandomian, O. (2017). Experimental Assessment of Retrofitted RC Frames With Different Steel Braces. Structures 11, 206-217. <https://doi.org/10.1016/j.istruc.2017.06.003>.

TahamouliRoudsari, M., Eslamimanesh, M.B., Entezari, A.R., Noori, O., Torkaman, M. (2018). Experimental Assessment of Retrofitting RC Moment Resisting Frames with ADAS and TADAS Yielding Dampers. Structures 14, 75-87. <https://doi.org/10.1016/j.istruc.2018.02.005>.

Terrinha, P., Rocha, R., Rey, J., Cachao, M., Moura, D., Roque, C., Martins, L., Valadares, V., Cabral, J., Azevedo, M.R., Barbero, L., Clavijo, E., Dias, R.P., Gafeira, J., Matias, H., Matias, L., Madeira, J., Marques da Silva, C., Munha, J., Rebelo, L., Ribeiro, C., Vicente, J., Noiva, J., Youbi, N., Bensalah, K. (2013). A Bacia Do Algarve: Estratigrafia, Paleogeografia E Tectonica. Geol. Port. no Context. da Iberia 71.

Teves-Costa, P., Batlló, J., Matias, L., Catita, C., Jiménez, M.J., García-Fernández, M. (2019). Maximum intensity maps (MIM) for Portugal mainland. J. Seismol. 23, 417-440. <https://doi.org/10.1007/s10950-019-09814-5>.

Turco, V., Secondin, S., Morbin, A., Valluzzi, M.R., Modena, C. (2006). Flexural and shear strengthening of un-reinforced masonry with FRP bars. Compos. Sci. Technol. 66, 289-296. <https://doi.org/10.1016/j.compscitech.2005.04.042>.

Udías, A., Mézcua, J. (1986). Fundamentos de geofísica. Alhambra S.L., Madrid.

UNICEF (2011). Para Reconstruir la Vida de los Niños y Niñas: Guía para apoyar intervenciones psicosociales en emergencias y desastres. Fondo de las Naciones Unidas para la Infancia, UNICEF, Santiago de Chile.

Valente, M., Milani, G. (2018). Alternative retrofitting strategies to prevent the failure of an under-designed reinforced concrete frame. Eng. Fail. Anal. 89, 271-285. <https://doi.org/10.1016/j.engfailanal.2018.02.001>.

SUMARY

List of tables

SUMARY

SUMARY

List of figures

SUMARY

SUMARY

SUMARY

SUMARY

SUMARY

This book presents the work carried out within the European research project PERSISTAH (Projetos de Escolas Resilientes aos SISmos no Território do Algarve e de Huelva, in Portuguese), which has been developed jointly by the University of Seville (Spain) and the University of Algarve (Portugal). This research project focuses on the study and assessment of the seismic vulnerability of primary education buildings in the Algarve (Portugal) and Huelva (Spain) territories.

The PERSISTAH project presents a series of essential aspects, which have supported its contribution in the formation of a more seismically resilient society. These aspects are: the singularities of the seismicity of this geographical area, the interest in the typology of school buildings and the analysis of their seismic vulnerability, the development of a seismic retrofitting methodology, which has been applied in two pilot schools of Huelva and the Algarve, the communication of seismic risk to the school community, and finally, the international cooperation for risk reduction.

In the present book, the methodology and seismic regulations applied in the vulnerability analysis and subsequent retrofitting of school buildings is presented. Then, the seismic hazard of the Algarve and Huelva area is explained, as well as the seismic action used in each region for seismic analysis based on the different seismic regulations. Later, the characterization and typological classification of school buildings carried out for subsequent seismic analysis are shown. Finally, several seismic reinforcement techniques proposed by the different regulations are outlined, in greater depth in the case of the solutions studied in the project.

Interreg
España - Portugal
PERSISTAH PROJECT
Fondo Europeo de Desarrollo Regional
Fundo Europeu de Desenvolvimento Regional
UNIÓN EUROPEA
UNIÃO EUROPEIA

Editorial Universidad de Sevilla

BOOK COVER